THE REGULATION AND DYNAMICS OF TYPE IV PILI

THE REGULATION AND DYNAMICS OF TYPE IV PILI IN *PSEUDOMONAS AERUGINOSA*

By KATHERINE JEAN GRAHAM, B.Sc

A Thesis Submitted to the School of Graduate Studies in Partial Fulfillment of the Requirements for the Degree Master of Science

McMaster University MASTER OF SCIENCE (2021)

Hamilton, Ontario (Biochemistry and Biomedical Sciences)

TITLE: The regulation and dynamics of type IV pili in *Pseudomonas aeruginosa*

AUTHOR: Katherine J. Graham, B.Sc. (McMaster University)

PROFESSOR: Dr. Lori L. Burrows

NUMBER OF PAGES: xiii, 106

LAY ABSTRACT

Pseudomonas aeruginosa is a major contributor to hospital-acquired infections and is of particular concern due to its intrinsic resistance to many frontline antibiotics. To aid in infection, *Pseudomonas* encodes an arsenal of virulence factors, including type IV pili (T4P), hair-like adhesins involved in many processes, such as twitching motility and surface attachment. T4P are primarily composed of the major pilin, PilA, whose expression is tightly regulated by the PilS-PilR two-component system. The sensor kinase, PilS, monitors the inner membrane PilA inventory and modifies activity of the response regulator, PilR, to regulate *pilA* transcription. Here, we demonstrate that *P. aeruginosa* virulence in a roundworm infection model is reduced when the amount of T4P expressed at the cell surface increases, regardless of the ability of the bacteria to twitch. We propose that inappropriate increases in surface T4P expression may impair pathogenicity-associated systems which require intimate host-cell contact. New genes in the regulon of the PilS-PilR two-component system were also identified. A tool to fluorescently label and image T4P in real-time using microscopy was established in the lab. This work highlights the consequences of increased surface T4P expression, providing potential new targets for antipseudomonal therapeutics which act on components involved in T4P expression and function.

ABSTRACT

Type IV pili (T4P) are hair-like adhesins involved in many processes, including surface attachment, twitching, DNA uptake, electron transfer, and pathogenesis. These flexible filaments are expressed in various pathogens, including the opportunistic pathogen *Pseudomonas aeruginosa*. The pilus fibre is primarily composed of the major pilin structural subunit, PilA, which is rapidly polymerized or depolymerized during pilus extension or retraction, respectively. The transcription of *pilA* is tightly controlled by the PilS-PilR two-component system, which responds to fluctuating levels of PilA in the inner membrane. In addition to *pilA*, the response regulator, PilR, also regulates a subset of other non-T4P related genes. Here, we used hyperactivating point mutants in the PilS-PilR two-component system, which induce hyperpiliation without loss of pilus function, to assess the effects of increased surface pili expression on virulence against *Caenorhabditis elegans,* and to identify additional non-T4P genes regulated by the PilS-PilR two-component system. We hypothesized that dysregulation of the PilS-PilR two-component system impacts the expression of *pilA* and other genes, which impacts both surface piliation and T4P dynamics, resulting in altered *P. aeruginosa* virulence. *C. elegans* slow killing assays revealed that hyperpiliation, independently of T4P function, reduces virulence of model *P. aeruginosa* strains PAK and PA14. We propose a model whereby a surfeit of pili reduces virulence, potentially

through impeding effective engagement of contact-dependent antagonism systems, such as the type III secretion system. Transcriptomic analysis of the hyperactive PilR point mutant also identified a subset of 26 genes, including those related to phenazine biosynthesis, quorum sensing, and ethanol oxidation, regulated by the PilS-PilR two-component system. Last, a T4P cysteine-labelling system was implemented for *P. aeruginosa*, allowing for the visualization of real-time pilus dynamics. Together, this work provides new insights into the consequences of hyperpiliation and the scope of the PilS-PilR signalling network, as well as novel tools for investigating *P. aeruginosa* T4P dynamics *in vivo*.

ACKNOWLEDGEMENTS

I would like to first and foremost thank my supervisor, Dr. Lori Burrows, for choosing to take me on as a graduate student at the last minute and for her unwavering support throughout this project. Working with Dr. Burrows has been an absolute pleasure and I cannot thank her enough for the supportive feedback and mentorship throughout the past two years. My skills as a writer and presenter grew exponentially thanks to Dr. Burrows, which I will carry on throughout my next chapter and future career.

Thank you to my committee members Dr. Lesley MacNeil and Dr. John Whitney for all their help throughout this project. A special thank you is owed to Dr. MacNeil for providing me access to her lab space to complete endless hours of nematode counting and for being such a friendly face first thing in the morning. Thank you to Dr. Whitney for allowing me to steal any required reagents from his lab at the last second when I would run out in the middle of an experiment. Both of your insightful questions and feedback pushed this project forward and helped me grow as a scientist.

I could not have gotten through the past two years without my wonderful lab mates: Hanjeong, Anne, Luke, Derek, Victoria, Rebecca, and Ikram. Hanjeong, I cannot thank you enough for your invaluable guidance and friendship. To Luke, Derek, and Victoria, who shared this entire experience with me, thank you for all the (very long) chats in the office, as well as our

nights out at the Phoenix (although there were few due to Covid) and our amazing Toy Story costume. I can't wait to see what the future holds for you three.

I would be remiss to exclude Dr. Sara Kilmury from this list of acknowledgements. Although we did not work together in person, this project would not have been possible without her inspiring ideas, experimental design, and conclusions. I feel very grateful that I was able to see this project through.

To my friends and family, none of this would be possible without you. Mom and Dad, thank you for being so supportive, patient, and for always listening to me complaining about my failed worm experiments. Thank you for putting up with me over the past few months while I wrote this thesis. A big thank you is also owed to my siblings, Emma, Adam, and Hayley, for always being so supportive and making me laugh. To my undergraduate school friends, Alia, Elyse, Kyra, and Meghan, thank you for listening to me rant about grad school on the phone and for always providing me with support or a laugh when it was needed. To Mercedes, thank you for being the greatest friend I could've asked for during grad school.

TABLE OF CONTENTS

LAY ABSTRACT ..... **iii**
ABSTRACT ..... **iv**
ACKNOWLEDGEMENTS ..... **vi**
TABLE OF CONTENTS ..... **viii**
LIST OF FIGURES ..... **ix**
LIST OF TABLES ..... **ix**
LIST OF ABBREVIATIONS ..... **x**
DECLARATION OF ACADEMIC ACHIEVEMENT ..... **xii**
CHAPTER 1. INTRODUCTION **1**
1.1 Type IV pili machinery 2
1.2 Type IV pilus functions 9
1.3 Two component systems 13
1.4 Hypothesis and aims 21
CHAPTER 2. MATERIALS AND METHODS **25**
2.1 Bacterial strains and plasmids 25
2.2 Cloning procedures 30
2.3 Mutant generation by allelic exchange 33
2.4 Twitching assay 33
2.5 Transmission electron microscopy 34
2.6 Secretion assay 34
2.7 *Caenorhabditis elegans* slow killing assay 35
2.8 RNA isolation, library preparation, cDNA synthesis, and analysis 36
2.9 Phage plaquing assays 37
2.10 Fluorescently labelling T4P 38
2.11 Fluorescence microscopy 38
CHAPTER 3. RESULTS **39**
3.1 Increased signalling via PilSR causes hyperpiliation without loss of pilus function 39
3.2 Hyperactive PilSR point mutants are less pathogenic towards *C. elegans* 42
3.3 Other hyperpiliated mutants have similarly reduced pathogenicity 44
3.4 Dysregulated type III secretion contributes to the decreased pathogenicity of hyperpiliated mutants 46
3.5 Deletion of the T3SS ruler protein disrupts hyperpiliation and restores pathogenicity 49
3.6 Hyperactivity of PilR dysregulates a subset of genes, including those related to phenazine biosynthesis, quorum sensing, and ethanol oxidation 52
3.7 Cysteine-labelled *P. aeruginosa* T4P can be visualized with fluorescent microscopy 57
CHAPTER 4. DISCUSSION **64**
4.1 Hyperpiliation, not loss of pilus retraction, reduces pathogenicity 64
4.2 Hyperactivation of PilR dysregulates expression of multiple genes, including those involved in phenazine biosynthesis, quorum sensing, and ethanol oxidation 71
4.3 Fluorescent labelling of T4P *in vivo* is a broadly applicable method for studying T4P dynamics 74
CHAPTER 5. CONCLUSIONS AND FUTURE DIRECTIONS **76**
5.1 Future directions 76
5.2 Conclusions 81
CHAPTER 6. REFERENCES **83**

LIST OF FIGURES

Figure 1: Schematic of the T4P machinery in *P. aeruginosa*.

Figure 2: Overview of the PilSR TCS and PilR regulon

Figure 3: PilS N323A and PilR D54E point mutants produce peritrichous T4P, while the *pilT* deletion mutant is hyperpiliated at both poles.

Figure 4: Hyperpiliation, not loss of pilus function, reduces pathogenicity in a pilin-dependent manner.

Figure 5: Hyperpiliated mutants of PA14 have reduced pathogenicity towards *C. elegans.*

Figure 6: Hyperpiliated mutants secrete T3SS exotoxins, while deletion of PscN or PscP abolishes T3SS function.

Figure 7: Impaired T3S contributes to the decreased pathogenicity of hyperpiliated mutants and deletion of the T3SS ruler protein disrupts hyperpiliation and restores pathogenicity.

Figure 8: Deletion of PscP in the PilS N323A background reduces surface pili expression.

Figure 9: Phage susceptibility and twitching of PilA cysteine point mutants.

Figure 10: AF488-labelled T4P in a retraction-deficient PAO1 strain.

Figure 11: AF488-labelled T4P in a PAO1 PilA point mutant.

Figure 12: AF488-labelling of WT PAO1.

Figure 13: AF594-labelling of T4P in PAO1.

Figure 14: Model for integrated regulation of *pilA*, T3S, quorum sensing, phenazine synthesis, and ethanol oxidation.

Figure 15: Hyperpiliation impedes engagement of the T3SS and reduces virulence.

LIST OF TABLES

Table 1: Bacterial strains and plasmids used in this study.

Table 2: Primers used in this study.

Table 3: Genes dysregulated ≥2-fold by PilR D54E.

Table 4: Differential expression profile of “pilin responsive” genes in PAK wt and PilR D54E.

Table 5: Expression of T4P-related genes in PAK WT and PilR D54E.

LIST OF ABBREVIATIONS

AF	AlexaFluor
ATP	adenosine triphosphate
bp	base pairs
c-di-GMP	cyclic-di-guanosine monophosphate
C-terminal	carboxyl-terminal
cAMP	cyclic amp
cDNA	complementary deoxyribonucleic acid
CYP	cytochrome p450
DIC	differential interference contrast
DNA	deoxyribonucleic acid
EGTA	ethylene glycol-bis(β-aminoethyl ether)-n,n,n′,n′-tetraacetic acid
Exo	exotoxin
Gm	gentamicin
h	hour(s)
HK	histidine kinase
IM	inner membrane
kb	kilobase
kDa	kiloDalton
kV	kilovolts
LB	lysogeny broth
MCP	methyl-accepting chemotaxis protein
min	minute(s)
N-terminal	amino-terminal
NA	numerical aperture
NGM	nematode growth medium
OD	optical density
OM	outer membrane
PBS	phosphate buffered saline
PCR	polymerase chain reaction

pH	power of hydrogen
PIA	*Pseudomonas* isolating agar
PQS	*Pseudomonas* quinolone signal
QS	quorum sensing
RNA	ribonucleic acid
RR	response regulator
rRNA	ribosomal ribonucleic acid
SPI1	*Salmonella* pathogenicity island 1
SDS	sodium dodecyl-sulfate
SDS-PAGE	sodium dodecyl-sulfate polyacrylamide gel electrophoresis
SKM	slow killing media
T3SS	type III secretion system
T4aP	type IVa pili
T4bP	type IVb pili
T4P	type IV pili
T6SS	type VI secretion system
TCA	trichloroacetic acid
TCS	two component system
TIRF	total internal reflection fluorescence
TSB	tryptic soy broth
VBMM	Vogel-Bonner minimal medium
VWA	von Willebrand factor A
WT	wild type

DECLARATION OF ACADEMIC ACHIEVEMENT

Sara Kilmury generated the *pilS*, *pilR*, PilS N323A, PilR D54E, PilS N323A *pilA*, PilR D54E *pilA*, PilO M92K *pilA*, *pscN*, PilS N323A *pscN*, PilS N323A *pilA pscN*, *pscP*, and PilS N323A *pscP* mutants in PAK. Sara inspired and designed all experiments, excluding the electron microscopy and secretion assays, within Chapters 3.1-3.5. The conclusions drawn from these results were also inspired by Sara. The first replicate for all the *Caenorhabditis elegans* slow killing assays was completed by Sara, while the additional two or three replicates were completed by Katherine Graham. David Moskal also assisted with *C. elegans* slow killing experiments.

Hanjeong Harvey performed the cloning, phage susceptibility testing, and twitching assays of the PAK PilA cysteine point mutants. Hanjeong also performed the cloning and mating of pEX18Gm-*pilA*$_{T101C}$ to create the PAK PilA T101C strain.

Marcia Reid from the McMaster Electron Microscopy Facility performed the transmission electron microscopy, while Katherine and Hanjeong prepared the samples for imaging.

Katherine performed the remaining work for this thesis unless otherwise stated. She is co-first author of a manuscript on the effects of hyperpiliation on *P. aeruginosa* virulence which is currently in review. She also co-

authored a review published in the Journal of Bacteriology on microscopy approaches to understanding bacterial surface-sensing mechanisms.

CHAPTER 1. INTRODUCTION

The ubiquitous bacterium *Pseudomonas aeruginosa* is a Gram negative, opportunistic pathogen with a broad range of hosts (1). First described in 1872, *P. aeruginosa* most often infects those with severe burns, cystic fibrosis, AIDS, and cancer (2, 3). In 2017, the World Health Organization listed *P. aeruginosa* as a critical pathogen for which new therapeutics are needed due to its high levels of antibiotic resistance (4). To aid in infection, *P. aeruginosa* produces an arsenal of virulence factors, including type IV pili (T4P) (5). T4P are hair-like adhesins that allow for attachment to medical equipment, such as catheters and contact lenses, contributing to widespread nosocomial *P. aeruginosa* infections (6).

Type IV filaments are expressed in a broad range of both Gram negative and positive bacteria, as well as archaea (7–9). Type IV filaments are categorized into type IVa pili (T4aP), type IVb pili (T4bP), the type II secretion system, mannose-sensitive hemagglutinin pili, type IVc tight adherence (Tad) pili, competence pili, and archaeal pili and flagella (10). These filaments are distinguished by structural and functional differences (11–13). This work focuses on T4aP in *P. aeruginosa*, hereby referred to as T4P, which are composed of repeating major pilin subunits plus a set of minor pilins (12, 14). An individual pilus ranges in length from 0.5 to 7 µm and is typically 4-6 nm in diameter (15). Based on differences in pilin structure and post-translational modifications, *P. aeruginosa* major pilins

are classified into five groups (I-V) (16–18). Most *P. aeruginosa* lab strains, such as PAK, are group II strains with no post-translational modifications (17).

1.1 Type IV pili machinery

In *P. aeruginosa*, the T4P machinery is encoded by approximately 20 genes dispersed across several gene clusters. Cryo-electron tomography of the T4P assembly complex in *Myxococcus xanthus* (19) and *Thermus thermophilus* (20) yielded low resolution three-dimensional structural models of this machinery and has given new insight into T4P function. This machinery **(Figure 1)** can be divided into four components: (i) the pilus itself, (ii) the inner membrane (IM) alignment subcomplex, (iii) the outer membrane (OM) secretin complex, and (iv) the motor subcomplex.

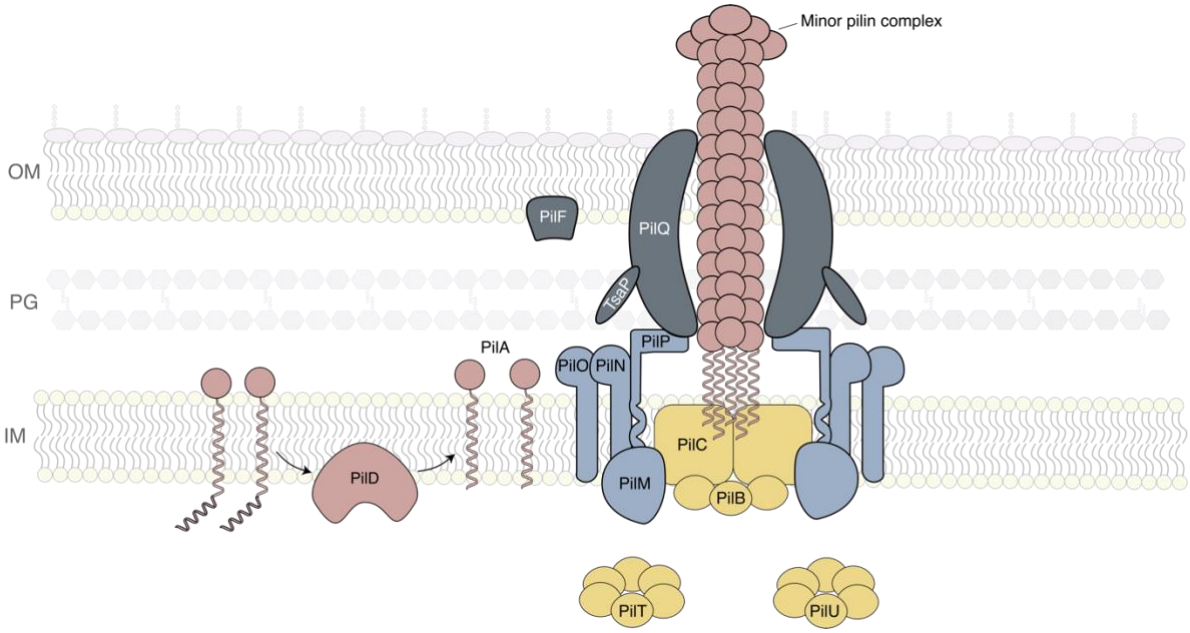

Figure 1. Schematic of the T4P machinery in *P. aeruginosa*. This model displays the four main components of the T4P machinery: (i) the pilus itself (pink), (ii) the IM alignment subcomplex (blue), (iii) the OM secretin complex (grey), and (iv) the motor subcomplex (yellow). Pilins are first translated as pre-pilins which encode an N-terminal secretion signal that is cleaved by the pre-pilin peptidase, PilD. The pilus is composed of repeating major pilin subunits accompanied by a set of minor pilins which form the tip of the fibre. The pilus is polymerized and depolymerized through the action of three hexameric ATPases, PilB, PilT, and PilU, which rotate the platform protein, PilC, and either “scoops up” IM PilA units or recycles pilus-incorporated PilA monomers back into the IM. The IM alignment complex anchors the T4P machinery to the IM and connects the motor complex to the OM secretin complex, which forms a gated pore for pilus extrusion.

Pilus

The pilus is composed of hundreds to thousands of major pilin subunits accompanied by a set of minor pilins which prime pilus assembly and form

the pilus tip (21–25). Pilins are first translated as pre-pilins which contain a unique N-terminal type III secretion signal and are inserted into the IM via the Sec system (26, 27). A specialized pre-pilin peptidase/N methylase, PilD, cleaves the signal peptide on the cytoplasmic side of the membrane and methylates the newly exposed N-terminus to produce assembly-competent mature pilins (28–31). The major pilin, PilA, has a lollipop-shaped structure composed of an extended N-terminal α-helix connected to a four-stranded antiparallel C-terminal β-sheet (25). The PilA N-terminal α-helix can further be divided into two sections: the α1-N and α1-C domains, which are embedded in the IM and globular β-sheet, respectively (25).

The globular C-terminal domain forms the exterior of the pilus and contains a conserved disulfide-bonded loop, known as the D region, which is important for pilin adhesion (12, 32, 33). Recent nanoscale pulling experiments of T4P also revealed adhesive properties along the entire length of the exposed pilus (34, 35). The extended N-terminal α-helix is S-shaped due to proline and glycine/proline residues at positions 22 and 42, respectively, allowing for efficient packing of the pilin subunits (12, 36, 37). Recent cryoelectron microscopy reconstructions of *P. aeruginosa* and *N. gonorrhoeae* pilins revealed differences between individual IM-bound and polymerized pilins. The pilin α1-N domain, flanked by the helix-breaking residues Gly14 and Pro22, becomes unstructured in pilus-incorporated

pilins, while this domain is helical in IM-bound pilins (38). This extended conformation imparts pilus flexibility, contributes to efficient packing of pilin subunits, and may play a role in pilin-mediated surface sensing (38). Force-induced stretching of the *N. meningitidis* major pilin, PilE, exposes key residues at the end of α1-C, which are involved in attachment to the endothelial cell receptor, β2AR (39–41). *N. meningitidis* pili activate β2AR upon attachment, leading to opening of the blood brain barrier (40). Similar force-induced conformational changes have been observed in the mannose-binding adhesin FimH in *E. coli* type I pili, to strengthen catch-bonds and enhance surface attachment (42). The helix-breaking residues in α1-N are conserved across type IVa pilins and type IVb pilins (39, 43), suggesting that force-induced changes in pilin conformation may have an important function in surface sensing.

Inner membrane alignment subcomplex

The IM alignment subcomplex consists of PilM, PilN, PilO, and PilP, which together anchor the T4P machinery to the IM and connect the motor to the OM secretin complex (44). The *pilMNOPQ* gene cluster in *P. aeruginosa* (44, 45), *Neisseria meningitidis* (46), and the homologous *comABCDE* gene cluster in *Haemophilus influenzae* (47) are all essential for T4P function.

PilM is located at the cytoplasmic face of the IM and shares structural similarity to the actin-like cytoskeletal protein, FtsA (11, 48, 49). The N-

terminus of PilN, a mostly periplasmic protein, extends into the cytoplasm to allow for interactions with PilM (48). PilN and the periplasmic protein, PilO, form a tetramer of homo- and heterodimers *in vivo* and the arrangement of this interaction is important for normal T4P function (50, 51). The structure of PilN has yet to be characterized, although it is predicted to resemble PilO, which contains highly conserved, unstructured residues critical for T4P function (52). Despite maintenance of PilO homodimerization, site-directed mutations in these conserved residues disrupt surface piliation and twitching, suggesting that these residues may be involved in critical protein-protein interactions with PilN or PilP (52). The IM lipoprotein, PilP, exclusively interacts with PilN-PilO heterodimers through its unstructured N-terminal region (53), while the C-terminal β-domain of PilP interacts with the secretin monomer, PilQ (54). These interactions form a continuous tetradecameric channel through the periplasm, from PilM in the cytoplasm to PilQ in the OM, supported by structural models of the T4P machinery in *M. xanthus* (19) and *T. thermophilus* (20).

Outer membrane secretin complex

A multimer of PilQ forms the gated OM secretin complex (17, 55). PilF is a lipoprotein that directs PilQ monomers to the OM and is required for T4P biogenesis and function in *P. aeruginosa* (55, 56). A multimer of 14 PilQ

subunits forms a pore in the OM (57, 58). During pilus extrusion, the internal gate is displaced to the interior walls of this pore and no other conformational changes are required to accommodate the pilus (57). The PilQ pore diameter exceeds the 4-6 nm diameter of the pilus, allowing for the pilus to pass (15, 57). Recent cryo-electron tomography of the *P. aeruginosa* secretin (58) revealed a belt-like heptamer of the peptidoglycan-binding protein, TsaP, surrounding the exterior of tetradecameric PilQ barrels. Though the role of TsaP is unclear, its overexpression increases the levels of cyclic-di-GMP (c-di-GMP), the master regulator for biofilm formation, suggesting that TsaP could be involved in T4P-mediated surface sensing (58).

Motor subcomplex

The motor subcomplex translates ATPase conformational changes to insert or extract pilins from the filament. It is composed of the platform protein, PilC, and three ATPase motors, PilB, PilT, and PilU. PilC coordinates the activity of PilB and PilT through interactions with its N- and C-terminal cytoplasmic domains (59). Site-directed mutations in the C-terminal domain of the *Neisseria* PilC homolog, PilG, result in T4P-mediated motility defects due to impairment of platform protein-ATPase interactions (59). In *M. xanthus*, PilC directly interacts with and promotes PilB activity (60).

PilB promotes the polymerization of PilA subunits in the extending pilus (61), while PilT depolymerizes the PilA subunits during retraction (62). During ATP hydrolysis, PilB facilitates clockwise rotation of PilC, while a small cavity in PilC is proposed to “scoop up” PilA from the IM to drive pilus assembly (63). PilT facilitates counterclockwise rotation and downward movement of PilC during pilus disassembly, releasing and recycling PilA subunits into the IM (64, 65).

PilB and PilT are part of the Additional Strand Catalytic ‘E’ superfamily of ATPases, which are phylogenetically related to, but distinct from FtsK-like ATPases and AAA+ ATPases (ATPases associated with diverse cellular activities) (66). These ATPases are capable of binding ATP through their Walker A and B motifs, which stabilize both hexameric complexes (63). Each hexameric ATPase resembles a “molecular scrunchie”, whereby each protomer is elastic and can adopt a given “closed” or “open” conformation. Recent structural analyses of both T4P ATPases revealed several conformations which can affect the ATP-binding capacity of each protomer (63, 65). Interestingly, one of the conformations of *Geobacter metallireducens* PilT showed that this ATPase may have the capacity to switch from counterclockwise to clockwise rotation, allowing for both extension and retraction, respectively (65). This may explain how, in some cases, bacteria can retract pili in the absence of a dedicated ATPase or in a *pilT* background (67–69).

1.2 Type IV pilus functions

T4P are involved in many processes such as adhesion (70), twitching motility (62), bacteriophage defense (71, 72), DNA uptake (68, 73, 74), and electron transfer (75). The adherent properties of T4P enable bacterial attachment to both biotic and abiotic surfaces (70, 76–79). This is important for the establishment of infection and colonization of hosts, contributing to the pathogenesis of many bacteria, including *P. aeruginosa* (80–83), *Kingella kingae* (76), *Acidovorax avenae* subsp. *citrulli* (77), and *Burkholderia pseudomallei* (78).

Twitching motility

T4P mediate a surface-associated form of crawling, known as twitching motility, which occurs in most, but not all, T4P-expressing bacteria (6). First described in *P. aeruginosa*, twitching involves repeated extension, attachment, and retraction of T4P, pulling bacteria along a solid or semi-solid surface (84). PilB and PilT facilitate this movement. PilB, the extension ATPase, incorporates PilA monomers from the IM into the growing pilus. Upon surface attachment, an unknown mechanosensory signal results in swapping of PilB in the motor subcomplex for the retraction ATPase, PilT, which retracts and recycles PilA monomers in the IM at an estimated rate of ~1000 units s^{-1} (64). Similar to a molecular grappling hook, this forceful retraction translocates the cell body towards the direction of pilus

attachment (64). Optical tweezer experiments in *N. gonorrhoeae* revealed that a single T4P retraction event could generate forces up to 100 pN, making PilT the strongest biological motor to be characterized (85). A third PilT-dependent retraction ATPase, PilU, is inessential for twitching but is thought to assist PilT with T4P retraction when twitching along high friction surfaces (86, 87).

The involvement of twitching in pathogenesis has been highlighted in studies using retraction-deficient mutants, which retain T4P but cannot twitch (88–90). In *P. aeruginosa*, the loss of PilT results in less cytotoxicity in a murine model, which corresponded with reduced bacterial adhesion to epithelial cells and liver colonization (88). Retraction-deficient *Neisseria* species had reduced pathogenicity against human epithelial cells due to a partial defect in cortical plaque formation (89). The ovine footrot-causing pathogen, *Dichelobacter nodosus*, was significantly less capable of causing sheep footrot lesions when retraction-deficient, which was directly linked to loss of twitching (90). The reduced pathogenicity in these species could be due to the steric inhibition of other contact-dependent virulence factors (ex. type III secretion system), a loss of host-pathogen stabilizing interactions, or disruption of signalling pathways which rely on stimuli produced by mechanical forces generated during T4P retraction (6).

Surface sensing

For many pathogens, virulence is directly related to surface association, as host colonization is contact-dependent (91). A clear example of this is enterohemorrhagic *E. coli*, a foodborne pathogen that upregulates the expression of type III secreted effector proteins, adhesins, and Shiga toxins in response to shear forces from direct contact with a host (92). In *P. aeruginosa*, the T4P adhesin, PilY1, is implicated in surface sensing and activation of virulence. This sensing is independent of surface type or host, allowing *P. aeruginosa* to infect a broad range of hosts, although the exact mechanosensory signal leading to virulence is unknown (93, 94). A 200 amino acid segment at the N-terminus of PilY1 shares weak sequence similarity with a von Willebrand factor A (VWA) domain, a conformationally flexible structure commonly found in eukaryotic extracellular and cellular adhesion proteins (95, 96). A similar domain was identified in the *Streptococcus agalactiae* PilY1 homolog, PilA, and is essential for adhesion to epithelial cells, the first to be functionally characterized in prokaryotes (97). In *P. aeruginosa*, deletion of the VWFa domain is thought to “activate” PilY1 and increases the virulence of planktonic cells against amoebae (93). The shear force from surface attachment is hypothesized to partly unfold this region of PilY1. This signal is then propagated along the length of the pilus in an unknown manner to a periplasmic or membrane sensor protein, leading to downstream upregulation of virulence factor expression (93). Signaling could occur via activation of the diguanylate cyclase, SadC, to

increase c-di-GMP levels (98–101) or via the minor pilin-regulated TCS FimS-AlgR (83, 102). The consequences of specific mutations must be considered when evaluating phenotypes, as *pilY1* deletion strains are nonpiliated, making it difficult to dissociate phenotypes associated with loss of T4P assembly and function from those related specifically to loss of PilY1 (93). Complementation of *pilY1* mutants using multicopy plasmids has additional consequences, as PilY1 and its partners PilVWX negatively control their own expression via the FimS-AlgR TCS. Overexpression of these components *in trans* represses expression of genes in the broader AlgR regulon, while deletion of minor pilins or PilY1 leads to AlgR activation (83).

Association of bacteria with surfaces is implicated in the regulation of virulence factor expression and quorum sensing via changes in levels of c-di-GMP (93, 100, 103, 104). Upon surface association, c-di-GMP, a secondary messenger that controls expression of biofilm-forming genes, is upregulated through yet uncharacterized signalling mechanisms (100, 105). The mechanical signal from T4P retraction is potentially involved in c-di-GMP upregulation, as knockout mutants of the retraction ATPase, PilT, are deficient in a c-di-GMP response (100). Kuchma et. al (2010) also showed that PilY1 is involved in the regulation of swarming motility through c-di-GMP signalling via the T4P alignment complex and diguanylate cyclase, SadC (96, 99). Expression of the cyclic-AMP-dependent virulence factor

regulator (Vfr) cascade is also regulated by PilY1 in a contact-dependent manner (99, 106). More recently, the sensitization of surface-associated *P. aeruginosa* to quorum sensing was identified. Unlike other surface-associated behaviours, the upregulation of the quorum sensing regulator, *lasR*, was independent of PilA expression and instead, relied on the retraction ATPases (PilT/U) and several minor pilins (PilW, PilE, and PilX) (104).

1.3 Two component systems

Signal transduction pathways in eukaryotes have been widely studied, however, the ability of prokaryotes to sense and respond to specific stimuli in their environment is less understood. In eukaryotes, protein kinases regulate protein expression by phosphorylating themselves or another protein at a serine, threonine, or tyrosine residue (107). Prokaryotes use two-component systems (TCS) to respond to environmental stimuli and regulate the expression of housekeeping genes, toxins, and virulence factors (108). TCSs are present in Gram negative and Gram positive pathogenic bacteria and involve a phospho-relay between two central proteins: a histidine kinase (HK) and response regulator (RR) (107, 108). HKs are membrane-bound, homodimeric proteins typically composed of a highly variable, periplasmic N-terminal sensing domain coupled to a highly conserved, cytoplasmic C-terminal kinase domain (107, 109). One HK

subunit phosphorylates a given His residue on its partner subunit, though some HK subunits can self-phosphorylate. The phosphate is then transferred to an Asp residue on the RR (107). Some HKs also have phosphatase activity against their RR for fine-tuning regulation (110). RRs act as transcriptional switches by regulating the transcription of certain genes in response to their cognate HK (107). A highly conserved N-terminal regulatory domain on the RR interacts with the phosphorylated HK subunit and catalyzes the transfer of the phosphate to itself (107). The RR variable C-terminal effector domain(s) then activates or represses the activities of effectors, usually DNA at a promoter element, in a phosphorylated-dependent manner (107).

P. aeruginosa has a significantly higher number of TCSs encoded in its genome compared to other bacterial species (111). They include the GacS TCS for switching between acute and chronic infection, the Cup TCS for surface adhesive components, and most notably for this work, the PilS-PilR TCS, hereby referred to as the PilSR TCS, which regulates expression of the major pilin, *pilA* (112–114).

The PilSR TCS

The expression of T4P on the surface of bacteria is energetically costly, as it requires the conversion of chemical energy from ATP binding and hydrolysis to mechanical energy for pilus extension and retraction (66, 115).

Hundreds to thousands of PilA subunits are incorporated into a single pilus and recycled in the IM upon retraction to be used in subsequent pilus assembly events (66, 116). Two ATP molecules appear to be required for the insertion or extraction of each PilA monomer into the filament (65, 66). PilA contains a high percentage of metabolically-inexpensive amino acids, with glycine, alanine, serine, and threonine accounting for ~38-47% of residues (117). This reduces the synthetic cost of this highly abundant protein without sacrificing the stability of PilA (118). *P. aeruginosa* also conserves energy by tightly regulating the expression of *pilA* through the PilSR TCS **(Figure 2)** (119).

The *P. aeruginosa* PilSR TCS acts to regulate PilA inventory through a phospho-relay between the IM HK, PilS, and cytoplasmic RR, PilR (120, 121). In the absence of intramembrane PilA, PilS autophosphorylates its conserved, cytoplasmic His 319 residue, which is then transferred to Asp 54 on PilR (116, 121, 122). Phosphorylated PilR coordinately binds to cis elements upstream of the *pilA* protomer region along with RNA polymerase containing the alternative σ factor, RpoN (σ^{54}) (123, 124). RpoN enables RNA polymerase to access specific promotor regions and is a common sigma factor associated with bacterial TCSs (123, 125, 126). Both unphosphorylated and phosphorylated PilR bind DNA with similar specificity, however, phosphorylation of D54 is thought to increase the affinity of the PilR-RNA polymerase-RpoN complex for the pilin promoter

region, as seen in the *E. coli* OmpR transcriptional activator (124, 127, 128). Adjacent to the His 319 phosphorylation site at residues 320-323, PilS has an ExxN phosphatase motif which is essential for PilA autoregulation (116). High levels of PilA in the IM promote the phosphatase state of PilS, dephosphorylating PilR, and suppressing *pilA* expression (116).

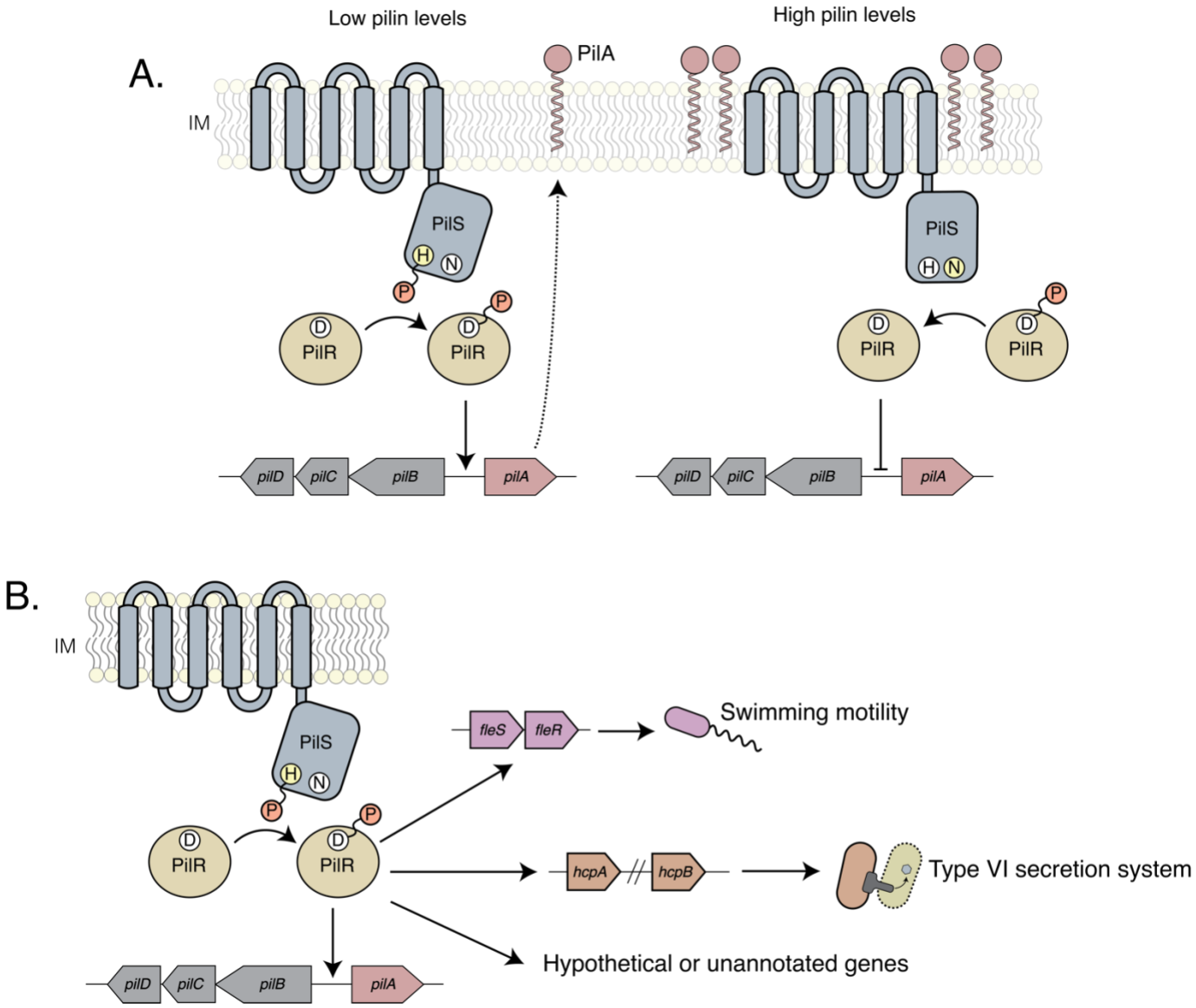

Figure 2. Overview of the PilSR TCS and PilR regulon. A. When the IM pilin inventory is low, the IM sensor kinase, PilS, autophosphorylates and relays this phosphate to the cytoplasmic response regulator, PilR. Activated PilR then binds to the *pilA* promoter and upregulates *pilA* transcription. Inversely, high IM pilin levels promote the phosphatase state of PilS, which dephosphorylates and deactivates PilR, resulting in downregulation of *pilA* transcription. **B.** In addition to *pilA*, the PilSR TCS regulates the expression of the *fleSR* TCS and components of the *fleSR* regulon which control flagella

biosynthesis, genes (*hcpA* and *hcpB*) encoding secreted proteins associated with the type VI secretion system, and eight hypothetical or unannotated genes.

Other T4P-expressing bacteria, including *D. nodosus* (129), *K. kingae* (130), *M. xanthus* (131), *G. sulfurreducens* (132), and *Neisseria* species (133, 134), also tightly regulate T4P expression with TCSs, although their regulatory mechanisms vary. For example, in contrast to the *P. aeruginosa* PilSR TCS, unphosphorylated PilR in *G. sulfurreducens* activates *pilA* transcription.

PilS and PilR

PilS is a 37 kDa protein spanning the IM of *P. aeruginosa* (120, 135). This protein is localized to the cell poles by its transmembrane domains and interactions with PilO (136–138). PilS topology is atypical, composed of six transmembrane domains connected by short periplasmic and cytoplasmic loops (135). Unlike most HKs, the sensing domain of PilS is located in transmembrane segments which interact directly with the N-terminal segment of PilA (116, 135). In addition to PilA, PilE and FimU also interact with PilS, although only PilA and PilE regulate the transcription of *pilA* (116). PilS also phosphorylates SagS and GcbA (139). SagS is involved in motility and biofilm formation, while GcbA promotes initial surface attachment through motility regulation, suggesting that the PilSR TCS may play a role in surface sensing (140, 141).

The 50 kDa cytoplasmic protein, PilR, shares significant overall similarity (62.2%) with the NtrC family of response regulators, which activate the transcription of RpoN-dependent promoters (121, 142). The 40 bp PilR-DNA binding region has four essential binding sites located 120-80 bp upstream from the *pilA* transcriptional start site, including direct repeats of 5'$(N)_{4-6}$(C/G)TGTC-3' (124). NtrC-family response regulators have a phosphorylation-dependent ATPase activity, which can help to form an open complex at the transcriptional start site to initiate transcription (143, 144). As both phosphorylated and unphosphorylated PilR bind to the pilin promoter region, the potential phosphorylation-dependent ATPase activity of PilR could explain why only the phosphorylated form activates *pilA* expression (124).

The PilR regulon

In *G. sulfurreducens* (145, 146), *D. nodosus* (129), and *Lysobacter enzymogenes* (147), PilR regulates several pathways. PilR in *G. sulfurreducens* is essential for soluble and insoluble Fe (III) reduction, which acts as a terminal electron transfer for the protein nanowires in this species (145). Genome-wide analysis of *G. sulfurreducens* also revealed genes related to pili, flagella, chemotaxis, and cell wall synthesis whose promoter regions contain PilR recognition sites and, thus, may be coordinately regulated by PilR (146). Transcriptional profiling of *D. nodosus* identified

several surface-exposed proteins with unknown function that are regulated by PilR in addition to the major pilin (129). The production of antifungal compounds in the ubiquitous soil bacterium *L. enzymogenes* is also regulated by PilR via a c-di-GMP-dependent pathway (147). Recently, a transcriptomic analysis of *P. aeruginosa* uncovered both characterized and uncharacterized genes regulated by PilR, including those related to twitching, swimming, and virulence (148).

Both pilin-dependent and -independent PilR regulons were recently identified in *P. aeruginosa* (148). A comparative analysis of the transcriptomes of T4P-deficient *pilA* and *pilR* mutants was performed to identify genes regulated exclusively by PilR (148). Loss of PilA results in downregulation of cAMP, an important signalling molecule for the expression of over 200 *P. aeruginosa* genes, including those associated with virulence (149). Thus, genes with altered expression in both *pilA* and *pilR* mutants were excluded, as transcriptional changes may have been due to loss of T4P (148). Expression of 24 genes was ≥3-fold altered in *pilR* but unaffected in the *pilA* background, 12 of which were flagellar-related (148). Flagellum biosynthesis and function are regulated by the FleSR-TCS (150). *fleS*, *fleR*, and eight additional flagellar biosynthetic genes were downregulated in the *pilR* mutant, along with PA1967 and PA4326, two hypothetical FleR-regulated proteins (148, 151). Transcription of *fleSR* is controlled predominantly by FleQ (151, 152), although *fleQ* was not

differentially expressed in *pilR* mutants, suggesting that PilSR directly promotes *fleSR* transcription (148). Swimming motility in *pilS* and *pilR* mutants was also significantly impaired, consistent with the idea that the PilSR TCS is involved in regulating flagellar expression and motility (148). Loss of the FleSR TCS was also shown to modestly impact twitching and *pilA* expression (148).

Interestingly, a subset of ten genes with an expression pattern similar to *pilA* were identified, suggesting that their transcription is responsive to pilin levels in the membrane (148). RNAseq analysis revealed genes with ≥5-fold increased expression in a *pilA* mutant and ≥5-fold decreased expression in a *pilR* mutant (148). These included two characterized genes (*hcpA* and *hcpB*, part of the type VI secretion system, T6SS) and eight uncharacterized genes (148). A subset of transposon mutants with insertions in *hcpA*, *hcpB*, and the eight uncharacterized genes had motility defects, substantial increases in biofilm formation, and a reduction of virulence in a *C. elegans* model, while others had wild-type phenotypes in these assays (148, 153).

1.4 Hypothesis and aims

Although the contributions of T4P to host cell attachment and twitching during *P. aeruginosa* infection are well documented (64, 88), the underlying regulatory mechanisms controlling T4P expression and dynamics during

infection remain poorly understood. Recent studies in *P. aeruginosa* have identified the signal to which PilS responds (*pilA*), as well as additional genes regulated by PilR (116, 148). However, the potential impacts of PilSR dysregulation on both *P. aeruginosa* virulence and the expression of genes within the PilSR signalling network have yet to be assessed. The overarching hypothesis guiding this work was that dysregulation of PilSR signalling impacts the expression of *pilA*, as well as a subset of other genes, disrupting both surface piliation and T4P dynamics, thus resulting in altered *P. aeruginosa* virulence.

This hypothesis was tested through three research aims:

1. **To determine the effects of hyperactivity of PilSR on pathogenicity in a *C. elegans* infection model.**

Several studies have described the importance of retractile T4P for *P. aeruginosa* infection across a broad range of hosts (154–157). The virulence of retraction-deficient *P. aeruginosa pilT* mutants is significantly reduced in murine and human infection models (88, 158), which was attributed to a loss of twitching and pilus dynamics. However, the effects of pilin overproduction on virulence are unclear. We used a *C. elegans* slow killing model to show that hyperpiliation, not loss of pilus retraction, reduces virulence of *P. aeruginosa* strains PAK and PA14. Hyperactivating point mutations in the PilSR TCS increased levels of surface pili to the same

extent as deleting *pilT*, without impairing twitching. Taken together with data from other hyperpiliated mutants outside of the known PilSR regulatory network, we propose a model whereby a surfeit of surface pili reduces virulence, potentially through the prevention of effective engagement of contact-dependent virulence factors.

2. **To characterize the PilR regulon and investigate how these PilR-regulated genes alter virulence.**

Recent RNAseq studies of *pilA* versus *pilR* deletion mutants identified PilR-regulated genes, including a subset of ten “pilin-responsive” genes inversely dysregulated ≥5-fold by *pilA* and *pilR* (148). Transposon insertions in some of these genes revealed pathogenicity-associated phenotypes, including those related to biofilm formation, motility, and interbacterial competition (148). This finding poses the question as to whether PilR activation connects T4P dynamics and upregulation of *P. aeruginosa* pathogenicity-associated genes. We aimed to validate the expression patterns of these genes in a hyperactive PilR point mutant via transcriptomics, as well as to identify novel genes in the PilSR regulon.

3. **To visualize T4P in *P. aeruginosa* through cysteine-labelling of PilA.**

With their average diameter of 6 nm (15), live imaging of T4P *in vivo* is challenging, as their size is below the diffraction limit of standard light microscopy. Studies of T4P have thus relied on comparisons of piliated cells with nonpiliated or genetically modified systems, or on static imaging methods (19, 34, 85, 159). While these studies provide insight into T4P structure, the dynamics of T4P expression *in vivo* are lost. We applied a cysteine-labelling system originally developed to visualize T4P in *C. crescentus* (67) to *P. aeruginosa*, allowing for the fluorescent labelling and subsequent visualization of T4P *in vivo*.

CHAPTER 2. MATERIALS AND METHODS

2.1 Bacterial strains and plasmids

Strains and plasmids used in this work are listed in **Table 1**. Bacteria were grown overnight at 37°C in 5 ml lysogeny broth (LB) Lennox, or on 1.5% agar LB plates, unless otherwise specified. When required, gentamicin (Gm) was added at 30 µg/mL for *P. aeruginosa* or 15 µg/mL for *E. coli*, and L-arabinose was added at 0.02% to induce pBADGr expression. For expression of the T3SS, *P. aeruginosa* strains of interest were transformed with the plasmid pBADGr containing the *exsA* gene and grown at 37°C in tryptic soy broth (TSB) supplemented with 2 mM EGTA.

Table 1. Bacterial strains and plasmids used in this study.

Strain	Characteristics	Source
E. coli strains		
E. coli DH5α	F- φ80*lac*ZΔM15 Δ(*lac*ZYA-*arg*F)U169 *rec*A1 *end*A1 *hsd*R17(rk-, mk+) *pho*A *sup*E44 *thi*-1 *gyr*A96 *rel*A1 λ	Invitrogen
E. coli SM10	*thi-1 thr leu tonA lacY supE recA*::RP4-2- Tc::Mu (KmR)	(160)
E. coli OP50		(L.T. MacNeil)
P. aeruginosa strains		
PAK WT	WT, Group II T4P	(J. Boyd)
PAK WT + pBADGr-*exsA*	WT with pBADGr containing *exsA*	(This work)
PAK WT + pBADGr	WT with pBADGr	(This work)
PA14 WT	WT, Group III T4P	(G.A. O'Toole)
PAK *pilA*	Chromosomal deletion of *pilA*	(This work)
PAK *pilA* + pBADGr-*exsA*	Chromosomal deletion of *pilA* with pBADGr containing *exsA*	(This work)

PAK *pilA* + pBADGr	Chromosomal deletion of *pilA* with pBADGr	(This work)
PAK *pilS*	Chromosomal deletion of *pilS*	(This work)
PAK *pilR*	Chromosomal deletion of *pilR*	(This work)
PAK *pilT*	Chromosomal deletion of *pilT*	(This work)
PAK *pilT* + pBADGr-*exsA*	Chromosomal deletion of *pilT* with pBADGr containing *exsA*	(This work)
PAK *pilT* + pBADGr	Chromosomal deletion of *pilT* with pBADGr	(This work)
PAK PilS N323A	Chromosomal substitution of PilS phosphatase motif residue N323 to alanine	(116)
PAK PilS N323A + pBADGr-*exsA*	Chromosomal substitution of PilS phosphatase motif residue N323 to alanine with pBADGr containing *exsA*	(This work)
PAK PilS N323A + pBADGr	Chromosomal substitution of PilS phosphatase motif residue N323 to alanine with pBADGr	(This work)
PAK PilR D54E	Chromosomal substitution of PilR phosphorylation site D54 to glutamic acid	(This work)
PAK PilR D54E + pBADGr-*exsA*	PAK with a chromosomal substitution of PilR phosphorylation site D54 to glutamic acid with pBADGr containing *exsA*	(This work)
PAK PilR D54E + pBADGr	Chromosomal substitution of PilR phosphorylation site D54 to glutamic acid with pBADGr	(This work)
PAK PilO M92A	Chromosomal substitution of residue M92 to alanine in PilO	(51)
PAK PilO M92K	Chromosomal substitution of residue M92 to lysine in PilO	(51)
PAK PilO M92K/*pilA*	PilO M92K strain with chromosomal *pilA* deletion	(This work)
PAK *pilA*::FRT/*pilT*::FRT	FRT scar in *pilA* and FRT scar at position 540 in *pilT*	(116)

PAK *pilA*::FRT/*pilT*::FRT + pBADGr-*exsA*	FRT scar in *pilA* and FRT scar at position 540 in *pilT* with pBADGr containing *exsA*	(This work)
PAK *pilA*::FRT/*pilT*::FRT + pBADGr	FRT scar in *pilA* and FRT scar at position 540 in *pilT* with pBADGr	(This work)
PAK PilS N323A/*pilA*	Disrupted PilS phosphatase motif and clean *pilA* deletion	(This work)
PilR D54E/*pilA*	Altered PilR phosphorylation site and *pilA* deletion	(This work)
PAK *pscN*	Chromosomal deletion of the Type III secretion ATPase *pscN*	(This work)
PAK *pscN* + pBADGr-*exsA*	Chromosomal deletion of the Type III secretion ATPase *pscN* with pBADGr containing *exsA*	(This work)
PAK *pscN* + pBADGr	Chromosomal deletion of the Type III secretion ATPase *pscN* with pBADGr	(This work)
PAK *pscN*/PilS N323A	Chromosomal deletion of Type III secretion ATPase and chromosomal substitution of PilS residue N323 to alanine	(This work)
PAK *pscN*/PilS N323A + pBADGr-*exsA*	Chromosomal deletion of Type III secretion ATPase and chromosomal substitution of PilS residue N323 to alanine with pBADGr containing *exsA*	(This work)
PAK *pscN*/PilS N323A + pBADGr	Chromosomal deletion of Type III secretion ATPase and chromosomal substitution of PilS residue N323 to alanine with pBADGr	(This work)
PAK *pscN*/PilS N323A/*pilA*	Chromosomal deletion of *pscN* and *pilA* combined with PilS N323A substitution	(This work)
PAK *pscN*/PilS N323A/*pilA*+ pBADGr-*exsA*	Chromosomal deletion of *pscN* and *pilA* combined with PilS N323A substitution and pBADGr containing *exsA*	(This work)
PAK *pscN*/PilS N323A/*pilA* + pBADGr	Chromosomal deletion of *pscN* and *pilA* combined with PilS N323A substitution and pBADGr	(This work)

PAK *pscP*	Chromosomal deletion of *pscP*	(This work)
PAK *pscP* + pBADGr-*exsA*	Chromosomal deletion of *pscP* with pBADGr containing *exsA*	(This work)
PAK *pscP* + pBADGr	Chromosomal deletion of *pscP* with pBADGr	(This work)
PAK *pscP*/PilS N323A	Chromosomal deletion of *pscP* combined with PilS N323A substitution	(This work)
PAK *pscP*/PilS N323A + pBADGr-*exsA*	Chromosomal deletion of *pscP* combined with PilS N323A substitution and pBADGr containing *exsA*	(This work)
PAK *pscP*/PilS N323A	Chromosomal deletion of *pscP* combined with PilS N323A substitution and pBADGr	(This work)
PAK *pilT/pscP*	Chromosomal deletion of *pilT* and *pscP*	(This work)
PAK *pilT/pscP* + pBADGr-*exsA*	Chromosomal deletion of pilT and pscP with pBADGr containing exsA	(This work)
PAK *pilT/pscP* + pBADGr	Chromosomal deletion of pilT and pscP with pBADGr	(This work)
PAK PilA T101C	Chromosomal substitution of PilA residue T101 to cysteine	(116)
PA14 *pilA*	Chromosomal deletion of *pilA*	(This work)
PA14 *pilS*	Chromosomal deletion of *pilS*	(This work)
PA14 *pilR*	Chromosomal deletion of *pilR*	(This work)
PA14 PilS N323A	Chromosomal substitution of PilS residue N323 to alanine	(This work)
PA14 PilR D54E	Chromosomal substitution of PilR residue D54 to glutamic acid	(This work)
PAO1 *fliC pilA* + pBADGr-*exsA*	Chromosomal deletion of *fliC* and *pilA* with pBADGr containing PAK *exsA*	(This work)
PAO1 *fliC pilA* + pBADGr	Chromosomal deletion of *fliC* and *pilA* with pBADGr	(This work)

PAO1 *pilA* + pBADGr-*pilA*$_{A76C}$	Chromosomal deletion of *pilA* with pBADGr containing PAK *pilA* with a cysteine substitution at residue A76	(This work)
PAO1 *pilA* + pBADGr-*pilA*$_{A77C}$	Chromosomal deletion of *pilA* with pBADGr containing PAK *pilA* with a cysteine substitution at residue A77	(This work)
PAO1 *pilA* + pBADGr-*pilA*$_{D78C}$	Chromosomal deletion of *pilA* with pBADGr containing PAK *pilA* with a cysteine substitution at residue D78	(This work)
PAO1 *pilA* + pBADGr-*pilA*$_{K81C}$	Chromosomal deletion of *pilA* with pBADGr containing PAK *pilA* with a cysteine substitution at residue K81	(This work)
PAO1 *pilA* + pBADGr-*pilA*$_{T84C}$	Chromosomal deletion of *pilA* with pBADGr containing PAK *pilA* with a cysteine substitution at residue T84	(This work)
PAO1 *pilA* + pBADGr-*pilA*$_{A86C}$	Chromosomal deletion of *pilA* with pBADGr containing PAK *pilA* with a cysteine substitution at residue A86	(This work)
PAO1 *pilA* + pBADGr-*pilA*$_{T101C}$	Chromosomal deletion of *pilA* with pBADGr containing PAK *pilA* with a cysteine substitution at residue T101	(This work)
PAO1 *pilA pilT* + pBADGr-*pilA*$_{T101C}$	Chromosomal deletions of *pilA* and *pilT* with pBADGr containing PAK *pilA* with a cysteine substitution at residue T101	(This work)
PAO1 *pilA* + pBADGr-*pilA*	Chromosomal deletion of *pilA* with pBADGr containing PAK *pilA*	(This work)
C. elegans species		
C. elegans N2	WT Bristol strain	(L.T. MacNeil)
Bacteriophage		
JBD26		(161)
DMS3		(162)
JBD26 chimera	JBD26 with gp58-59-60 replaced by gp48-49-50-51 from DMS3	(71)
JBD68		(161)
MP22		(163)

Vector	Characteristics	Source
pEX18Gm	Suicide vector used for gene replacement	(116)
pBADGr	Broad host range arabinose inducible vector used for complementation; ori *araC-PBAD* Gm^r mob^+	(164)
pBADGr+*pilA*	pBADGr expressing PAK PilA	(16)
pBADGr+ *exsA*	pBADGr expressing PAK ExsA	(This work)
pBADGr+$pilA_{A76C}$	pBADGr expressing PAK PilA with cysteine substitution of residue A76	(This work)
pBADGr+$pilA_{A77C}$	pBADGr expressing PAK PilA with cysteine substitution of residue A77	(This work)
pBADGr+$pilA_{D78C}$	pBADGr expressing PAK PilA with cysteine substitution of residue D78	(This work)
pBADGr+$pilA_{K81C}$	pBADGr expressing PAK PilA with cysteine substitution of residue K81	(This work)
pBADGr+$pilA_{T84C}$	pBADGr expressing PAK PilA with cysteine substitution of residue T84	(This work)
pBADGr+$pilA_{A86C}$	pBADGr expressing PAK PilA with cysteine substitution of residue A86	(This work)
pBADGr-$pilA_{T101C}$	pBADGr expressing PAK PilA with cysteine substitution of residue T101	(This work)

2.2 Cloning procedures

Primers used for cloning are listed in **Table 2**. Deletion constructs were generated by amplifying 500-1000 bp upstream and downstream of the gene. These flanking regions were restriction digested and ligated into the pEX18Gm suicide vector. Site-directed mutagenesis was performed using

overlap extension polymerase chain reaction (PCR) (165). Overlap extension products were digested and ligated into the pEX18Gm suicide vector. Constructs were verified with Sanger Sequencing (Mobix, McMaster Genomics Facility, Hamilton).

Table 2. Primers used in this study[a,b].

Primer Name	Sequence (5'→3')
pilA F1	GCG GAA TTC GTG TTG GCG GAC CAG CTT
pilA R1	GCA CCC GGG GCC TTT TTG AGC TTT CAT
pilA F2	GCA CCC GGG CCG AAA GGT TGC TCT AAG TAA
pilA R2	ATT GCA TGC ATT GCC GAG GCC CGG
pilS F1	GTT GAA TTC GCC GGA AAA CCA GGA TC
pilS R1	GTT GGA TCC CAG ACG GAG GAT GCG TTG
pilS F2	GTT GGA TCC GGA AGG CGG CGG CTG C
pilS R2	GTT AAG CTT ACT GAT GTA GAC CGG CGC
pilR F1	GTC AGA ATT CCT CCC GTC GCC GCC AGG C
pilR R1	TGA CGG ATC CGA CGA TCA GGG CTT TTT G
pilR F2	GTC AGG ATC CCG CCT GAA AAA GCT GGG C
pilR R2	TGA CAA GCT TGG CCT GGA ACT GCC CGT G
pilT F1	CTT AGA ATT CGA TGA ACG CTA TGC G
pilT R1	CTT AGG ATC CGT TCA TGA TGT CGT AG
pilT F2	CTT AGT CGA CCA CGA GAT CAT GAT C
pilT R2	CTT AAA GCT TCA GGG TGT TCT TCA G
pilB F1	ATA GAG CTC CCA CGA GAA AGC GC
pilB R1	ATA GGA TCC CAG GCC GCT CAG T
pilB F2	ATA GGA TCC GGA GGA AGT CAA CCG
pilB R2	ACT AAG CTT GCC AGA CTG TTC CCC
PilR D54E F	GAC CTG TGC CTC ACC GAG ATG CGC CTG CCG GAC
PilR D54E R	GTC CGG CAG GCG CAT CTC GGT GAG GCA CAG GTC
PilS N323A F	GCC CAT GAG ATC CGC GCC CGC CTG GGC GCG ATC
PilS N323A R	GAT CGC GCC CAG CGG GGC GCG GAT CTC ATG GGC
pscN F1	ATT GAA TTC GGT GGG CGA TCA GCG CCT
pscN R1	ATT GGA TCC CGA TGG CGT GGC GCA TCC
pscN F2	ATT GGA TCC AGC GAT TAC GCA CAG GCC
pscN R2	GGC AAG CTT TTC CAG TTC GCC TTC CTC
pscP F1	GTC AGA GCT CCG CAC AGG CCT GCG CGC A

pscP R1	GCT AGG ATC CGT CGG ACG ACA CGA GCG
pscP F2	GCT AGG ATC CCG CTC GCG GCA ACG TCG C
pscP R2	GCT AAA GCT TCA GGC CGG GCC ATT GCA G
exsA F	ATT AGA ATT CGT TCT TAT AAT ATG CAA GGA GCC
exsA R	ATT AAA GCT TTC AGT TAT TTT TAG CCC GGC ATT C
0507 F1	ATT AGA GCT CAA GAA AGC CGC CGA CTC
0507 R1	ATT AGG TAC CAA GTC GAA TAC CTC ATC G
0507 F2	ATT AGG ATT CTT CTA CGA AGC CAA GCT G
0507 R2	ATT AAA GCT TAT CTT GTA GGA GCC GTC
0951a F1	ATT AGA ATT CAT TGT TGC TGG GGG CC
0951a R1	ATT AGA GCT CTA ATC CGG TTC AAA CGC TC
0951a F2	ATT AGG ATC CTG AGA AAG CGC GGG AC
0951a R2	ATT ACT GCA GAA TCT CGG TCC GGC AG
0952 F1	ATT AGA ATT CAG GTT TCG CAC CCA ACC
0952 R1	ATT AGA GCT CAA TGT TGT AGT CCG CGA C
0952 F2	ATT AGG ATC CAG GAG TTC TTC GTA CAA G
0952 R2	ATT AGT CGA CCG AAA ACC CTG TTC GGG
4027 F1	ATT AGA GCT CAT CAA TCC TGC CAC CGA
4027 R1	ATT AGG TAC CAT GGT CGA AGG GCA G
4027 F2	ATT ACT GCA GTA TCG CAA CTG CAT CTC
4027 R2	ATT AAA GCT TAA CAC CAG TTC GGC GC
4683 F1	ATT AGA ATT CTG TTC GCC GAG CAG G
4683 R1	ATT AGA GCT CTT TGA GGA AGG CGA TCG
4683 F2	ATT AGG ATT CAT CAA CCC CGC CCG C
4683 R2	ATT AAA GCT TAT GAT GGT GCT GTC GTG
5228 F1	ATT AGA ATT CAA GAT GGT TAT CCT AGC AC
5228 R1	ATT AGA GCT CAG TTG TCG ATA GAG GGC
5228 F2	ATT ACT GCA GTC ACA AAC CGA CGC TG
5228 R2	ATT AAA GCT TTT CTT CTT CGG CGC GC
hcpB F1	ATT AGA GCT CAG TTG TTC GCC CTG ATG
hcpB R1	ATT AGG TAC CAC TTC GTG GTT GAA GCC
hcpB F2	ATT AGG ATC CAC TTC ACC TAC CGC AAG
hcpB R2	ATT AAA GCT TTT TCT CGA AGT CGT AGT C
hcpC F1	ATT AGA ATT CAA CTA CCA GCA GGC TTC
hcpC R1	ATT AGA GCT CAA TCC TCG GTG AAG GC
hcpC F2	ATT AGG ATC CAA GAC GTG CAC TTC ACC
hcpC R2	ATT AAA GCT TCT TTC GGT GAA AGG CCG
PilA T101C F	ATT AAC C**G**G ATC CTG CTG ATG GT**T** **G**TG C
PilA T101C R	ATT AGC A**CA** ACC ATC AGC AGG ATC **C**GG T

[a] – Restriction sites are underlined.

[b] – Mismatched bases for site-directed mutagenesis are bolded.

2.3 Mutant generation by allelic exchange

Allelic exchange was used to delete or generate site-directed mutations in *P. aeruginosa* genes (166). Deletion constructs or point mutations were introduced into *E. coli* SM10 using heat shock transformation and conjugated into the PAK parent strain. Mating mixtures were plated on *Pseudomonas* isolation agar (PIA) supplemented with 100 µg/mL Gm and grown overnight at 37°C for selection of colonies with pEX18Gm integrated onto the chromosome. Colonies were streaked onto 5% LB sucrose-no salt plates and incubated overnight at 37°C to select against merodiploids. Bacterial colonies were then patched onto LB or PIA supplemented with 100 µg/mL Gm and grown overnight at 37°C to select for resistant colonies. Constructs were amplified using PCR and confirmed with Sanger sequencing (Mobix, McMaster Genomics Facility, Hamilton).

2.4 Twitching assay

Twitching assays were performed as described previously (167). Briefly, a single colony of each strain of interest was stab-inoculated to the agar-plastic interface of an LB 1% (w/v) agar plate. Plates were incubated at 37°C for 24-48 h. Following incubation, the agar was carefully removed from the plate and discarded, and twitching zones were visualized by staining the plastic plate with 1% (w/v) crystal violet for 20 min. Plates were washed with water and imaged using a flatbed scanner. Twitching zones were measured

using ImageJ (http://imagej.nih.gov/ij/, NIH, Bethesda, MD). Three independent replicates were performed.

2.5 Transmission electron microscopy

Strains of interest were grown overnight in TSB supplemented with 2 mM EGTA, arabinose, and Gm. Overnight cultures were diluted 1:50 in 1X PBS or 1X VBMM and 100 µL was applied on glow-discharged carbon grids. Cultures were incubated on the grids for 30 min to allow for bacterial binding, followed by a 1.5-3 h incubation in fresh 1X PBS or 1X VBMM at 37°C. The grids were washed four times with 1X PBS or 1X VBMM. The cells were negatively stained with aqueous 1% uranyl acetate and then viewed with a JEOL JEM 1200 EX TEMSCAN transmission electron microscope (JEOL, Peabody, MA) operating at an accelerating voltage of 80 kV. Images were acquired with an AMT 4-megapixel digital camera (Advanced Microscopy Techniques, Woburn, MA). Images were analyzed using AMT Image Capture Engine (Version 7.0.0.264) software and higher magnification insets were generated using Adobe Illustrator (Version 25.2.3).

2.6 Secretion assay

Overnight bacterial cultures were diluted to OD=0.1 in TSB with 2 mM EGTA and grown at 37°C. At an OD = 0.4-0.5, 1 mL of culture was pelleted at

maximum speed for 4 min. The supernatant was transferred to a fresh 1.5 mL tube containing 350 µL of 50% trichloroacetic acid (TCA), mixed by inversion, and incubated overnight at 4°C for protein precipitation. The precipitated proteins were collected at maximum speed (~12,000 g; Eppendorf Centrifuge 5415D) for 15 min and the supernatant discarded without disturbing the pellet. The pellet was resuspended in 1 mL of acetone and collected at maximum speed for 5 min. Once the supernatant was discarded, the protein was collected at maximum speed for 1 min and any residual liquid was removed by micropipette. To dry the pellet, the 1.5 mL tube was left open on benchtop for 10 min. Fifteen µL of SDS-PAGE sample buffer (125 mM Tris [pH 6.8], 2% β-mercaptoethanol, 20% glycerol, 4% SDS, 0.001% bromophenol blue) and 1 µL 1M Tris (pH=8.0) were added to the dried pellet. Twelve µL of each sample was separated on 12.5% SDS-PAGE and proteins visualized by staining with Coomassie brilliant blue (0.1% Coomassie brilliant blue R-250, 50% methanol, 10% glacial acetic acid). Densitometry of ExoS/T or PilA was performed using ImageJ (http://imagej.nih.gov/ij/, NIH, Bethesda, MD). Three independent replicates were performed.

2.7 *Caenorhabditis elegans* slow killing assay

C. elegans slow killing assays with *P. aeruginosa* strains were completed as described in (168). *C. elegans* populations were propagated on NGM

plates supplemented with *E. coli* OP50. To obtain a synchronized *C. elegans* population, eggs were collected from the NGM *E. coli* OP50 plates in M9 buffer. The suspension was bleached (20% NaClO, 10% 5N NaOH) for 5-7 min to degrade all nematodes, leaving only intact eggs. Eggs were washed in M9 and hatched overnight on a shaker at 20°C in M9 buffer. Hatched worms (L1) were plated onto NGM *E. coli* OP50 for 45 h to develop into early adult (L4) worms. During nematode development, slow killing media (SKM; 0.35% peptone, 50 mM NaCl, 2% agar, 1 mM $CaCl_2$, 5 µg/ml cholesterol, 1 mM $MgSO_4$, 20 mM KH_2PO_4, 5 mM K_2HPO_4, 100 µM FUDR) plates seeded with 100 µL of a *P. aeruginosa* strain grown overnight at 37°C in LB were prepared. Seeded SKM plates were incubated at 37°C for 16-18 h. L4 worms were resuspended and washed with M9 buffer prior to plating on SKM plates. At least 30-40 L4 worms were transferred to each assay plate. Plates were incubated at 25°C and scored for live worms daily using a dissecting microscope. Worms that were unresponsive to touch with a platinum worm picker were considered dead and removed each day. Survival curves were generated using Prism 8.3.1 (GraphPad, La Jolla, CA) and statistically significant differences in pathogenicity between strains were calculated using Gehan-Breslow-Wilcoxon analysis.

2.8 RNA isolation, library preparation, cDNA synthesis, and analysis

RNA isolation, library preparation, cDNA synthesis, and analysis were performed as previously described in (148). To isolate RNA, bacterial strains of interest were streaked in triplicate onto half of a 1.5% LB agar plate and incubated overnight at 37°C. Cells were scraped off the plates and immediately resuspended in 1.5 mL RNAprotect Bacteria Reagent (Qiagen) to maintain RNA integrity. The RNeasy Mini Kit (Qiagen) was used to lyse cells and isolate bacterial RNA, as per the Qiagen protocol. Two DNAse on-column treatments were performed following isolation to deplete excess DNA. RNA was then eluted with 50 µL of RNAse-free water.

Library preparation and cDNA synthesis were completed by the Farncombe Metagenomics Facility (McMaster University, Hamilton, Ontario). rRNA was depleted from the samples using the Ribo-zero rRNA depletion kit (Illumina), and cDNA libraries were prepared with the NEBnext Ultra Directional library kit. RNAseq was then performed using paired-ends 75 bp reads on the MiSeq system (Illumina). Reads were mapped back to the PAO1 reference genome and alterations in gene expression quantified by Rockhopper software (169).

2.9 Phage plaquing assays

Phage plaque assays were performed as described previously in (71). Bacteria were grown overnight at 37°C with shaking and subcultured 1:100 for 3 h at 37°C with shaking in LB supplemented with 8 mM $MgSO_4$. The

subculture was standardized to an OD = 0.3 and 100 µL was mixed with 8 ml top agar (0.6% LB agar plus 8 mM $MgSO_4$) which was overlaid on a pre-poured rectangular 1.5% LB agar plus 8 mM $MgSO_4$ plate supplemented with Gm and arabinose. Phage stocks were standardized to a plaque-forming unit per ml of 10^8. 5 µl of tenfold serially diluted phage stocks suspended in LB plus 8 mM $MgSO_4$ were spotted on prepared plates. After drying the spots for ~10 min, the plates were incubated for 18 h at 37°C inverted. Phage plaques were then imaged on an Epson scanner. Three independent replicates were performed.

2.10 Fluorescently labelling T4P

Labelling of T4P was completed as described in (170). PAK strains were grown overnight at 37°C in 5 mL of LB Lennox. Overnight cultures were diluted 1:1000 in LB and grown for 4 h at 37°C in the shaker. 100 µL of the culture was pelleted and resuspended in phosphate buffer solution (PBS). The suspension was stained with 0.5 µL of 5 mg/mL AlexaFluor (AF)-488/AF-594 C_5 maleimide dye (ThermoFisher Scientific) for 30-60 min, washed with PBS, and then transferred to a 1% LB agarose pad.

2.11 Fluorescence microscopy

LB 1% agarose pads were prepared by transferring 80 µL of melted 1% LB agarose to a microscope slide and mounting with a coverslip. Agarose pads

were dried for ~30 min at room temperature and the cover slip was then removed. Bacterial strains to be imaged were incubated overnight in a shaker at 37°C, sub-cultured 1:1000, stained with AF-488/AF-594 C_5 maleimide dye (ThermoFisher Scientific), and 1 µL of labelled bacteria was transferred onto the agarose pad. Cultures were dried for ~5 min on the agarose pad and bacteria were then mounted with a glass coverslip directly prior to imaging. Differential interference contrast (DIC) and fluorescence microscopy were used to image bacteria on a Nikon A1 confocal microscope through a Plan Apo 60X (NA=1.40) oil objective. All confocal image acquisition was done using Nikon NIS-Elements Advanced Research (Version 5.11.01 64-bit) software and images were adjusted using ImageJ software (1.52K). Deconvolution was performed using the Nikon Denoise.ai software.

CHAPTER 3. RESULTS

3.1 Increased signalling via PilSR causes hyperpiliation without loss of pilus function

The PilSR two-component system controls the transcription of the major pilin gene, *pilA* (120–122). We showed previously that the system can be constitutively activated using a specific point mutation in the conserved phosphatase motif of PilS, N323A, preventing deactivation of phospho-PilR (116, 171). To test if hyperactivation of PilR also led to increased surface

piliation, we generated a point mutant, D54E, which mimics the active, phosphorylated state of the response regulator (172, 173). Both point mutations were introduced at the native *pilSR* loci on the chromosome to ensure WT expression levels. Similar to PilS N323A, the PilR D54E mutant expressed more PilA compared to WT**.** Electron microscopy revealed that PilS N323A and PilR D54E strains are hyperpiliated **(Figure 3EF)**. This phenotype resembled that of mutants lacking the retraction ATPase, *pilT* (174), or with an M92K mutation in the alignment subcomplex protein, PilO (175). In contrast to the retraction-deficient *pilT* mutant that fails to twitch or the PilO M92K mutant which has reduced twitching, the PilS and PilR point mutants retain WT levels of twitching, suggesting that their pili are fully functional **(Figure 3I)**. This set of hyperpiliated mutants, representing a range of pilus functionality, was used in further studies.

Surface pili expression was further characterized in a subset of the mutants used in this study using transmission electron microscopy **(Figure 3)**. Deletion of *pilT* **(Figure 3C)** or constitutive activation of PilS or PilR via the N323A **(Figure 3D)** or D54E **(Figure 3E)** point mutations, respectively, resulted in increased surface piliation at both poles compared to WT **(Figure 3A)** and non-piliated *pilA* mutants **(Figure 3B)**, which expressed several or no pili at one pole. Interestingly, the PilS N323A and PilR D54E hyperpiliated mutants, but not the retraction-deficient *pilT* mutant, also

produced peritrichous T4P, similar to those recently observed in *Acinetobacter baylyi* (176).

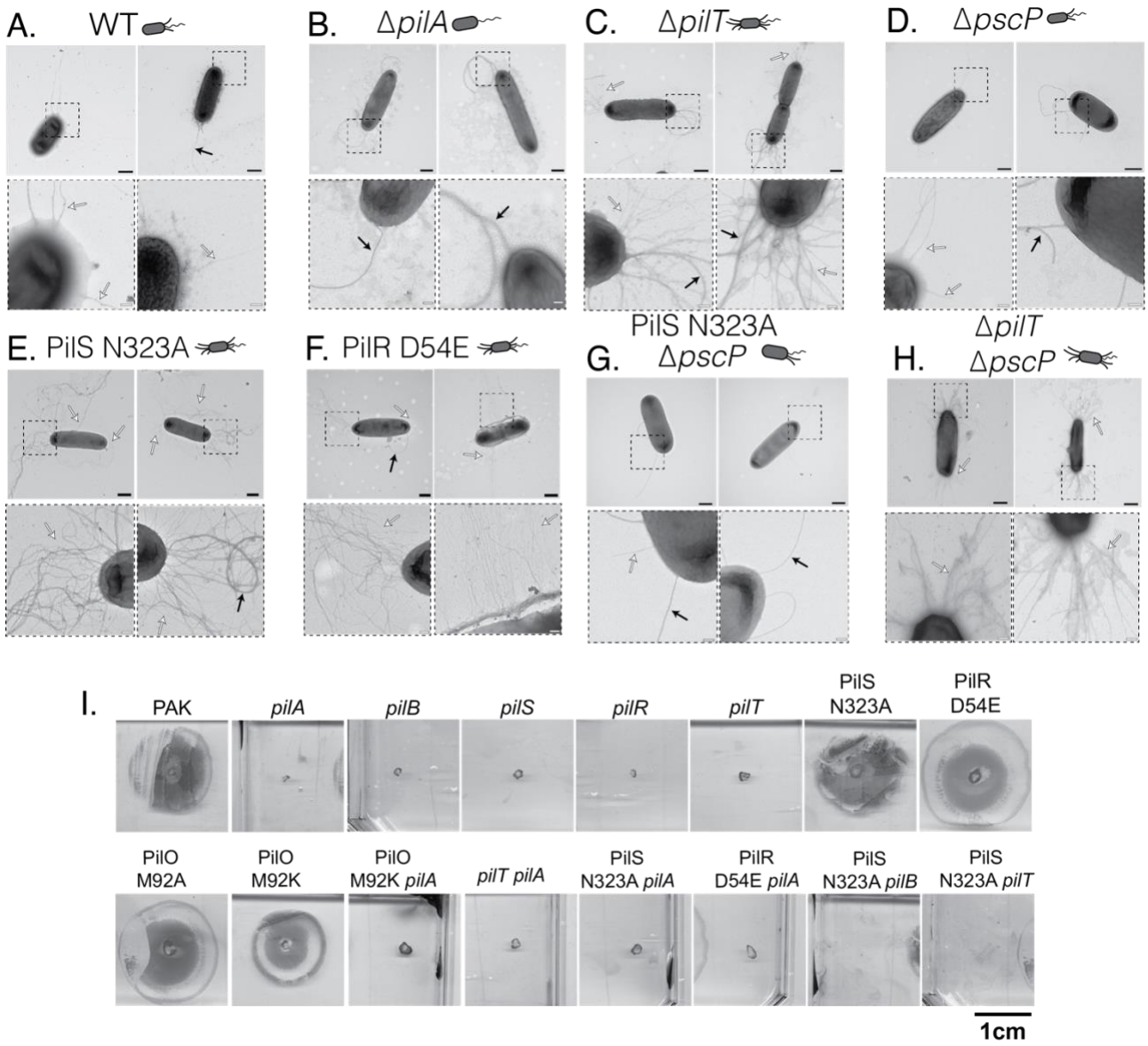

Figure 3. PilS N323A and PilR D54E point mutants produce functional, peritrichous T4P, while the *pilT* deletion mutant is hyperpiliated at both poles. A. WT produces pili and flagella at one pole. **B.** Deletion of PilA results in a non-piliated strain with a single polar flagellum. **C.** PilT deletion results in a hyperpiliated phenotype with an abundance of pili expressed at

both poles and a flagellum expressed at one pole. **D. and E.** PilS N323A and PilR D54E point mutants are hyperpiliated, but express polar and peritrichous T4P. **F.** Type III secretion system (T3SS) needles were not observed in the *pscP* strain under T3S-inducing conditions. **G. and H.** Deletion of PscP in the PilS N323A background resulted in a loss of hyperpiliation, while loss of *pscP* in the *pilT* background had no effect on hyperpiliation. White and black arrows denote T4P and flagella, respectively. **I.** Representative twitching phenotypes of a subset of the mutants used in this study. The PilS N323A and PilR D54E mutants have levels of surface pili similar to a *pilT* mutant, but their twitching is similar to WT. In addition to being hyperpiliated, the PilO M92K mutant has reduced twitching, consistent with a retraction defect (175).

3.2 Hyperactive PilSR point mutants are less pathogenic towards *C. elegans*

To clarify the roles of piliation versus twitching in *P. aeruginosa* pathogenicity, we used a *C. elegans* slow killing infection model, where worms propagated on solid media feed on the bacterial strains of interest. As in previous studies (78, 81), non-piliated mutants including *pilA, pilS,* and *pilR* had slightly decreased pathogenicity compared to WT. In contrast, hyperactivation of PilS or PilR via the N323A or D54E point mutations, respectively, significantly decreased pathogenicity, with 50% killing that took on average 4 days longer than WT **(Figure 4A)**. To confirm that this was not a strain-specific phenotype, we also tested the pathogenicity of PilS N323A and PilR D54E point mutants of the PA14 strain, which kills *C.*

elegans more rapidly than PAK (168). We saw similar reductions in pathogenicity for the PA14 point mutants **(Figure 5)**. To clarify whether this phenotype was dependent on increased pilin expression, versus changes in expression of other members of the PilSR regulon (148), *pilA* was deleted in the PilS N323A and PilR D54E backgrounds. In both cases, the pathogenicity of the double mutants was comparable to that of PAK, suggesting that reduced pathogenicity in the PilSR mutants was PilA-dependent **(Figure 4B)**.

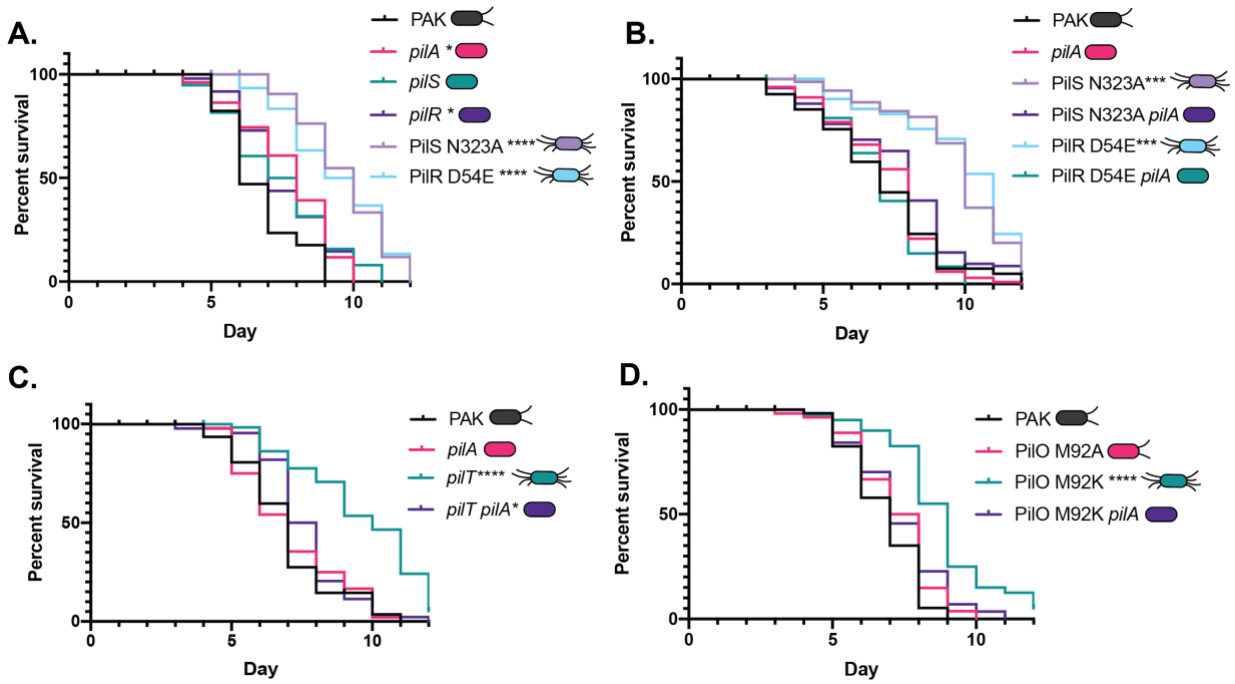

Figure 4. Hyperpiliation, not loss of pilus function, reduces pathogenicity in a pilin-dependent manner. A. The hyperpiliated PilS N323A and PilR D54E mutants are significantly less pathogenic in slow killing assays than the PAK parent strain or its isogenic *pilA*, *pilS*, or *pilR* mutants; all of which lack surface pili. **B.** Deletion of *pilA* in the PilS N323A or PilR D54E backgrounds restores pathogenicity to levels similar to PAK

and the *pilA* control. **C.** Loss of *pilA* in the *pilT* background, which is significantly less pathogenic than WT, restores pathogenicity to levels similar to WT and the *pilA* control. **D.** The hyperpiliated PilO M92K mutant is less pathogenic than PAK or an isogenic PilO M92A mutant, and pathogenicity is restored by deletion of *pilA* in the M92K background. *p<0.05, *** p<0.001, **** p<0.0001. Shown are representative datasets from triplicate or quadruplicate experiments.

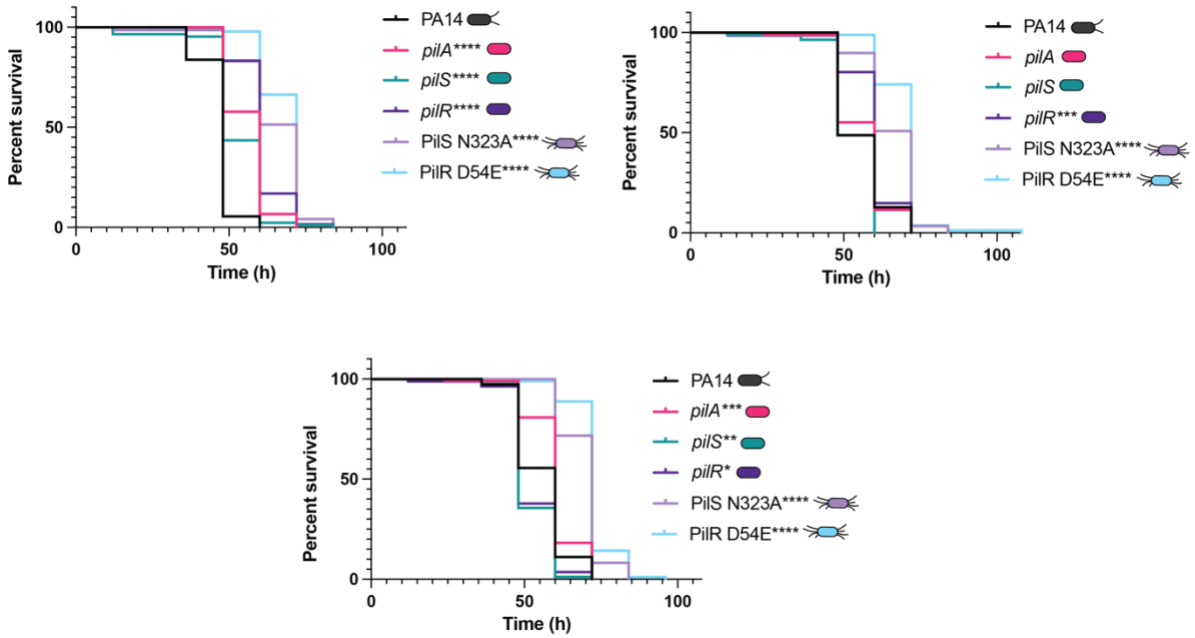

Figure 5. Hyperpiliated mutants of PA14 have reduced pathogenicity towards *C. elegans*. Hyperpiliated PilS N323A and PilR D54E point mutants of the highly virulent *P. aeruginosa* PA14 strain are less pathogenic than wild type or its isogenic non-piliated *pilA*, *pilS*, or *pilR* mutants. These data show that loss of pathogenicity in those mutant backgrounds is not strain-specific. * p<0.05, ** p<0.01, *** p<0.001, **** p<0.0001. Three biological replicates are shown.

3.3 Other hyperpiliated mutants have similarly reduced pathogenicity

To understand how the level of surface piliation influences pathogenicity in *C. elegans*, we compared the pathogenicity of a *pilT* deletion mutant with a double mutant lacking both *pilT* and *pilA*. As expected, the *pilT* mutant was hyperpiliated and unable to twitch **(Figures 3B and 3I)**. In the slow killing assay, loss of *pilT* significantly reduced pathogenicity, but pathogenicity was restored to WT levels by deletion of both *pilA* and *pilT* **(Figure 4C)**. As neither of these mutants can twitch, loss of pilus-mediated motility is not correlated with reduced pathogenicity in this infection model.

Each of the single mutations above has the potential to directly or indirectly modulate transcription of the pilin gene because of their effects on levels of pilin inventories in the IM (121, 122, 177). For example, a *pilT* mutant has low levels of PilA in the IM due to its inability to disassemble extended pili, while a *pilA* mutant has none. While both these mutations activate the PilSR system, the *pilT* and *pilA* mutants have different virulence phenotypes in *C. elegans*. To further separate the contributions to pathogenicity of changes in the levels of surface pili versus regulation of *pilA* transcription, we examined the pathogenicity of strains that were hyperpiliated due to mutations in genes outside of the known PilSR regulatory network (148). We previously identified two point mutations in the T4P alignment subcomplex protein, PilO, that differently affected surface piliation even though intracellular levels of PilA are similar (175). PilO M92A has no detectable impact on surface piliation or motility, while a charged residue at

the same position, M92K, causes a hyperpiliated phenotype coupled with reduced motility **(Figure 3I)**. Consistent with the results above, the hyperpiliated PilO M92K mutant, but not the M92A mutant, was significantly impaired in its ability to kill *C. elegans,* with the time to 50% mortality increased by an average of 2 days **(Figure 4D)**. Deletion of *pilA* in the PilO M92K background restored WT killing kinetics, further supporting our hypothesis that hyperpiliation is detrimental to pathogenicity in *C. elegans*.

3.4 Dysregulated type III secretion contributes to the decreased pathogenicity of hyperpiliated mutants

To explain the decreased pathogenicity in hyperpiliated *P. aeruginosa* strains, we considered potential changes in the interaction between the bacteria and *C. elegans*. Efficient T3S relies on intimate cell-cell contact between bacteria and host, and T3S is important for virulence in many infection models (178). The role of T3S in *P. aeruginosa* killing of nematodes has been controversial and may depend on the specific *P. aeruginosa* strain tested. For example, studies using highly-virulent strain PA14 suggested that T3S has a negligible role in *C. elegans* slow killing (179), whereas others using the less-pathogenic PAO1 strain indicated that loss of T3S diminishes pathogenicity (180).

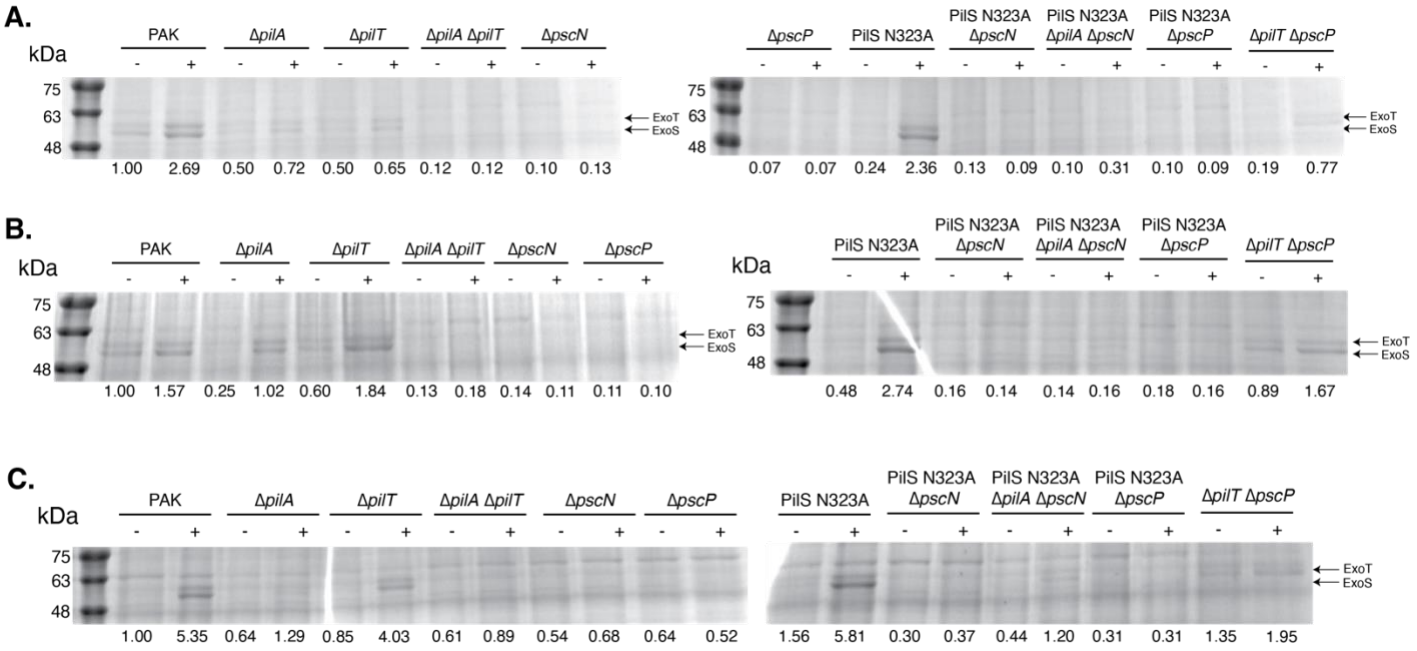

Figure 6. Hyperpiliated mutants secrete T3SS exotoxins, while deletion of PscN or PscP abolishes T3SS function. Strains were grown in T3S-inducing conditions and supplemented with either pBADGr (-) or pBADGr-*exsA* (+). WT PAK, *pilT,* and PilS N323A strains had comparable secretion of ExoS/T, while *pilA*, *pilA pilT*, and *pilT pscP* strains had less ExoS/T in culture supernatants. Excluding the *pilT pscP* strain, strains harbouring a deletion in PscN or PscP had no detectable ExoS/ExoT in culture supernatants. Three biological replicates are shown. Pixel density of ExoS/T relative to WT (-) are displayed in each lane.

We tested the contribution of T3S to slow killing of *C. elegans* by strain PAK by generating a *pscN* deletion mutant lacking the T3SS ATPase, which prevents the secretion of toxic effectors as shown for *Yersinia enterocolitica* (181) and a number of other T3SS-expressing pathogens (182–185). As expected, deletion of *pscN* resulted in a loss of ExoS/T secretion **(Figure 6)** and significantly reduced the pathogenicity of PAK in the slow killing assay

(Figure 7A). In contrast, when the *pscN* mutation was introduced into the less pathogenic PilS N323A mutant, it did not further reduce pathogenicity. However, deleting *pscN* in the PilS N323A *pilA* double mutant – which has WT levels of virulence – decreased its pathogenicity. Together, these data suggest that T3S is important for *C. elegans* slow killing by PAK, and that hyperpiliation of *P. aeruginosa* may impair injection of T3SS exotoxins into host cells.

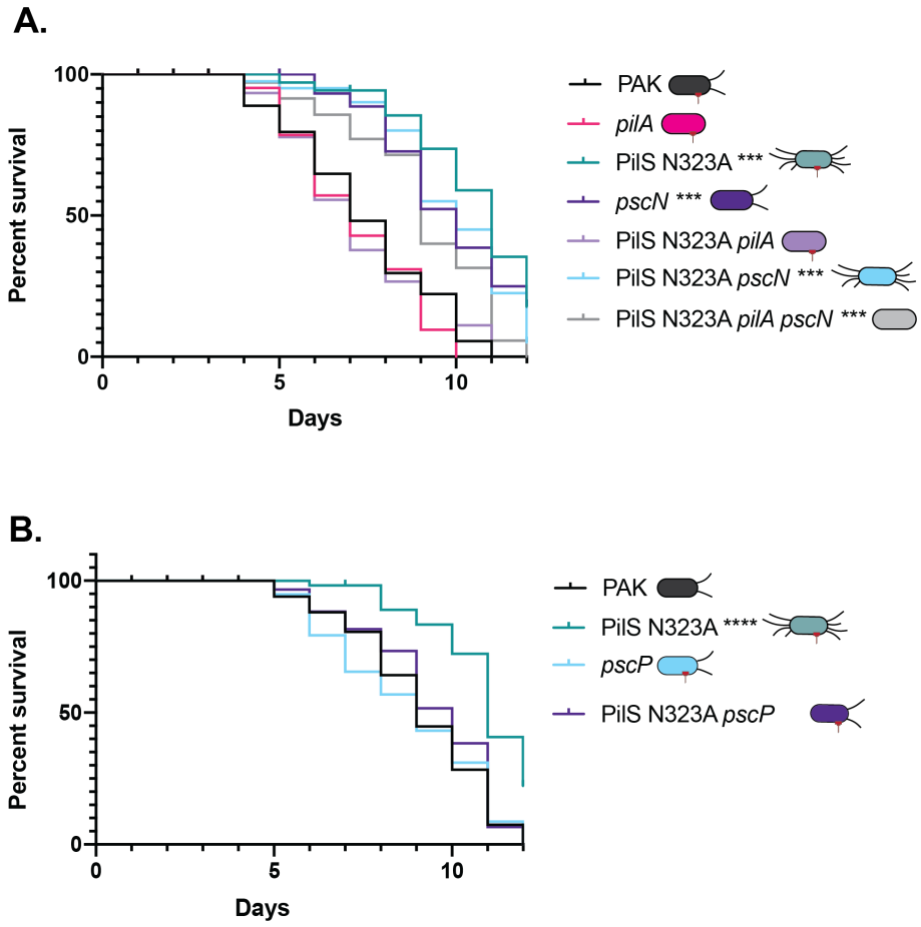

Figure 7. Impaired T3S contributes to the decreased pathogenicity of hyperpiliated mutants and deletion of the T3SS ruler protein disrupts hyperpiliation and restores pathogenicity. A. Deletion of *pscN*, encoding

the T3SS ATPase, reduces pathogenicity of PAK towards *C. elegans*, showing that virulence of this strain is T3SS-dependent. Combining the *pscN* and PilS N323A mutations does not further decrease virulence. While loss of *pilA* in the N323A background increases pathogenicity, further deletion of *pscN* in the N323A *pilA* background reduces pathogenicity, confirming that virulence is T3SS-dependent. **B.** While deletion of *pscP*, encoding the T3SS ruler protein that controls needle length does not impair virulence of PAK towards *C. elegans*, deletion of this gene in the hyperpiliated N323A background increases pathogenicity. *** $p<0.001$, **** $p<0.0001$. These are representative datasets from triplicate experiments.

3.5 Deletion of the T3SS ruler protein disrupts hyperpiliation and restores pathogenicity

Secretion of ExoS/T by the *pilT* and PilS N323A hyperpiliated strains was comparable to WT **(Figure 6)** despite the reduced virulence of these mutants in the slow killing model **(Figure 7)**. This result suggested that while exotoxin secretion was not impaired in these strains, efficient T3S into host cells may be impaired by hyperpiliation. We reasoned that hyperpiliated *P. aeruginosa* strains might be able to overcome the potential impairment of T3SS engagement, even in mutants with an overabundance of surface pili, if we extended the length of T3SS needles. *pscP* encodes the T3S ruler protein, and *Pseudomonas* mutants lacking PscP were reported to produce longer needle structures that can reach up to 1µm in length (186). In *Y. enterocolitica*, deletion of the PscP homolog, YscP, produces longer yet functional T3S needles (187). However, we could not detect ExoS/T in the

supernatants of *pscP* or PilS N323A *pscP* mutants, though the *pilT pscP* strain secreted ExoS/T **(Figure 6)**.

While deletion of *pscP* in a strain with WT piliation had no significant effect on pathogenicity against *C. elegans*, deleting *pscP* in the hyperpiliated PilS N323A strain restored pathogenicity to near-WT levels **(Figure 7B)**. Despite repeated attempts, we could not see longer (>50 nm) T3SS needles in the *pscP*, PilS N323A *pscP*, and *pilT pscP* mutants under T3SS-inducing conditions **(Figure 3)**, though this phenotype was previously reported in a *P. aeruginosa* H103 *fliC pscP* mutant (186).

Deletion of *pscP* in the PilS N323A background unexpectedly reduced surface pili expression **(Figures 3G and 8)**, while the *pilT pscP* strain remained hyperpiliated **(Figures 3H and 8)**. Deletion of *pscN* only slightly reduced surface pilin expression in the PilS N323A background **(Figure 8)**, suggesting that the loss of hyperpiliation in the PilS N323A *pscP* strain is PscP-dependent. Our original hypothesis was that deletion of PscP would increase the length of T3S needles enough to contact host cells, even in mutants with an overabundance of surface pili. The lack of appreciable ExoS/T secretion and loss of hyperpiliation in the PilS N323A *pscP* strain instead suggests that deletion of *pscP* in this genetic background disrupts both T3S function and surface pili expression.

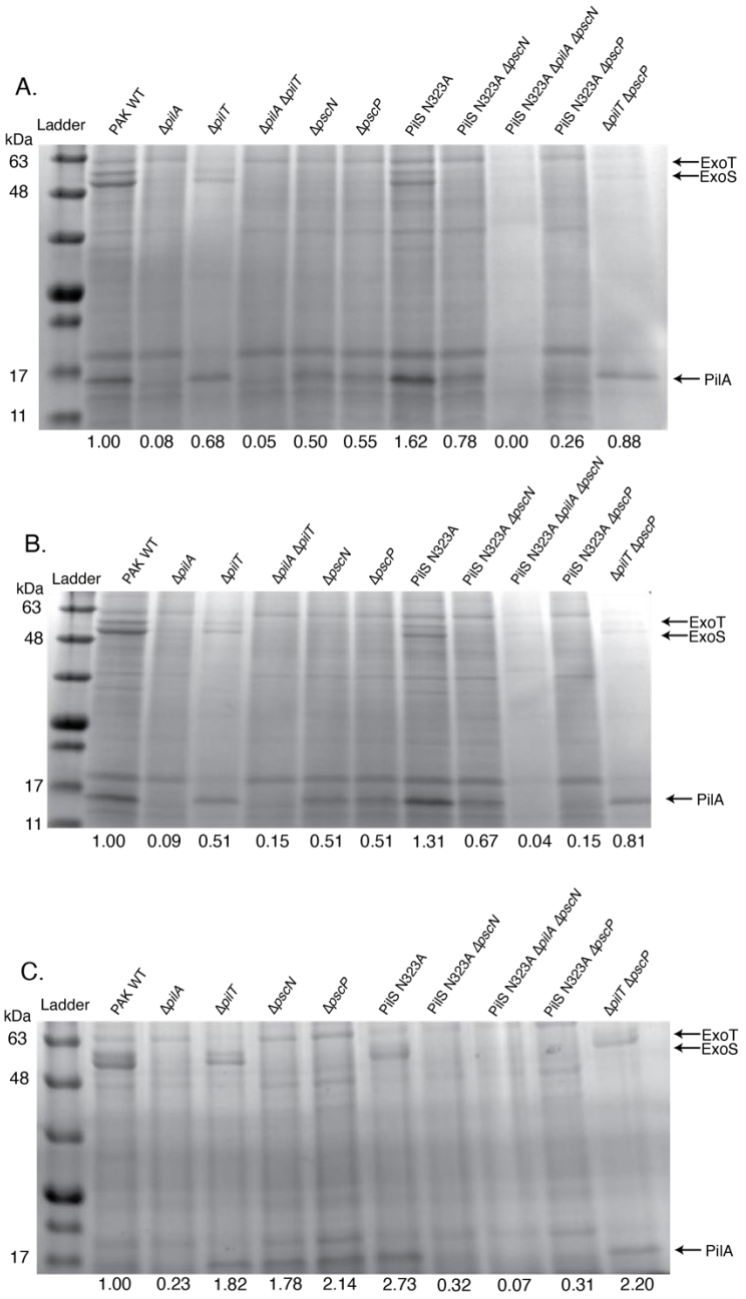

Figure 8. Deletion of PscP in the PilS N323A background reduces surface pili expression. Strains were grown in T3SS-inducing conditions and supplemented with pBADGr-*exsA*. While WT, *pilT*, *pscN*, *pscP*, PilS N323A, PilS N323A *pscN*, and *pilT pscP* strains had detectable PilA (15.5 kDa), PilA was undetected in strains harbouring a genetic lesion in *pilA* and

the PilS N323A *pscP* mutant. Pixel density of PilA relative to WT are displayed in each lane.

3.6 Hyperactivity of PilR dysregulates a subset of genes, including those related to phenazine biosynthesis, quorum sensing, and ethanol oxidation

Given that hyperactivation of PilSR reduces *P. aeruginosa* virulence, we next wanted to rule out that this reduction in virulence was not the result of significant dysregulation of virulence-associated genes in the PilR D54E hyperpiliated point mutant. RNAseq was performed on the WT and PilR D54E strains, revealing twenty-six genes that were dysregulated ≥2-fold by PilR D54E **(Table 3)**.

Table 3. Genes dysregulated ≥2-fold by PilR D54E.

PA Gene	WT PAK Count	PilR D54E Count	log2Fold Change	p Value	Function
PA4210	0	31	-7.809	0.002	pHZA1 - phenazine synthesis
PA3330	16	285	-4.483	NA	Hypothetical operon - cytochrome P450
PA3332	11	192	-4.444	NA	
PA3334	10	131	-4.134	0.008	
PA3331	36	415	-3.918	NA	
PA3328	23	244	-3.753	NA	
PA3333	33	322	-3.693	NA	
PA3329	29	281	-3.641	NA	
PA3335	30	219	-3.244	NA	
PA3327	221	1615	-3.240	NA	
PA4213	3	23	-3.138	0.001	PhzD - phenazine biosynthesis protein
PA1905	7	37	-2.692	0.002	PhzG2 - probable pyridoxamine 5'-phosphate oxidase
PA4211	15	73	-2.635	NA	PhzB1 - probable phenazine biosynthesis protein
PA1904	7	32	-2.428	0.003	PhzF2 - probable phenazine biosynthesis protein
PA1901	13	54	-2.413	0.003	PhzC2 - phenazine biosynthesis protein
PA3326	466	1878	-2.361	0.046	ClpP2 - Clp protease proteolytic subunit
PA3479	26	96	-2.231	0.001	RhlA - rhamnosyltransferase chain A
PA4212	19	70	-2.224	0.069	PhzC1 - phenazine biosynthesis protein PhzC
PA3476	307	1070	-2.143	0.046	RhlI - autoinducer synthesis protein RhlI
PA2591	41	137	-2.076	0.045	VqsR - positive regulation of secondary metabolite biosynthetic process
PA1891	3	12	-2.057	0.012	Hypothetical protein

PA Gene	WT PAK Count	PilR D54E Count	log2Fold Change	p Value	Function
PA1219	9	3	1.434	0.081	hypothetical protein
PA1980	39	11	1.607	0.108	response regulator EraR (ethanol oxidation)
PA3866	24	7	1.610	0.009	pyocin S4
PA1982	236	55	1.989	0.141	ExaA - quinoprotein ethanol dehydrogenase
PA1983	85	17	2.205	NA	ExaB - cytochrome c550

Of the 21 genes upregulated ≥2-fold by PilR D54E, seven were related to phenazine synthesis. Phenazines are produced by fluorescent *Pseudomonas* species and contribute to several virulence pathways, including redox cycling, biofilm formation, and lung damage in cystic fibrosis patients (188). 1-hydroxyphenazine, phenazine-1-carboxylic acid, and pyocyanin are essential for *C. elegans* fast killing by *P. aeruginosa* PA14 (189). Two seven-gene biosynthetic loci are involved in phenazine synthesis, *phzA1B1C1D1E1F1G1* and *phzA2B2C2D2E2F2G2*. Biosynthetic genes from both operons were upregulated in PilR D54E (*pHZA1B1C1D1, pHZC2F2G2*).

Nine (PA3327, PA3328, PA3329, PA3330, PA3331, PA3332, PA3333, PA3334, PA3335) of the twenty-seven genes upregulated ≥2-fold by PilR D54E are located within a hypothetical cytochrome P450 operon. Cytochrome P450s (CYPs) are heme-thiolates that function as iron-dependent monooxygenases and are found in both eukaryotes and prokaryotes (190).

The remaining five genes upregulated ≥2-fold by PilR D54E included one gene encoding a hypothetical protein (PA1891), as well as genes involved in rhamnolipid production (*rhlA*, *rhlI*) (191, 192), protein cleavage (*clpP2*) (193), and quorum sensing (*vqsR*) (194).

Five genes were downregulated ≥2-fold by PilR D54E **(Table 3)**. Three of the downregulated genes are involved in ethanol oxidation, including the quinoprotein ethanol dehydrogenase *exaA* gene (195), the cytochrome c550 *exaB* gene (196), and the transcriptional regulator *eraR* (197). *P. aeruginosa* produces two soluble (S) pyocins, pyocin S2 and pyocin S4, which are bacteriocins that enter non-immune *P. aeruginosa* cells by hijacking siderophore receptors (198). The remaining gene (PA1219) downregulated ≥2-fold by PilR D54E encodes a hypothetical protein.

The expression of the ten “pilin responsive” genes previously identified by Kilmury and Burrows (148) was assessed **(Table 4)**. We expected to see similar gene expression profiles in the *pilA* and PilR D54E strains, since PilR

is continuously active in both strains, promoting the transcription of both *pilA* and the PilR regulon (148). Unexpectedly, none of the ten genes were dysregulated ≥2-fold in the PilR D54E background. Even more unexpectedly, the expression of *pilA* was not significantly upregulated by PilR D54E **(Table 5)**. Both WT PAK and PilR D54E strains were validated with Sanger sequencing prior to RNAseq analysis. Previous RT-PCR by Kilmury and Burrows (148) demonstrated that PilR D54E strains have a ~4-fold increase in *pilA* expression compared to WT PAK. It is unclear why the expression of both PilR-regulated genes and pilin genes are not consistent between *pilA* and PilR D54E strains.

Table 4. Differential expression profile of "pilin responsive" genes in PAK wt and PilR D54E.

Gene Name	PA Gene	PAK wt Count	PilR D54E Count	log2 Fold Change	p Value	Function
	PA0951a	4434	4459	-0.249	0.223	Unannotated
	PA0952a	3250	3142	-0.178	0.208	Unannotated
	PA0952	3250	3142	-0.178	0.208	Unannotated
hcpB	PA5267	122	115	-0.150	0.600	Secreted protein (T6S)
	PA5228	852	764	-0.067	-0.418	Hypothetical protein
	PA5228a	852	764	-0.067	-0.418	Hypothetical protein
	PA0507	141	114	0.091	0.639	Acyl-CoA dehydrogenase
	PA4027	518	365	0.256	0.350	Hypothetical protein
hcpA	PA1512	210	139	0.356	0.191	Secreted protein (T6S)
	PA4683	1575	1020	0.385	1.774	Hypothetical protein

Table 5. Expression of T4P-related genes in PAK WT and PilR D54E.

Gene Name	PA Gene	PAK wt Count	PilR D54E Count	log2 Fold Change	p Value	Function
pilX	PA4553	1264	1351	-0.316	0.085	Type 4 fimbrial biogenesis protein PilX
pilW	PA4552	2072	2198	-0.303	0.094	type 4 fimbrial biogenesis protein PilW
pilY1	PA4554	6979	7386	-0.297	0.082	Type 4 fimbrial biogenesis protein PilY1
pilY2	PA4555	890	935	-0.285	0.039	Type 4 fimbrial biogenesis protein PilY2
pilQ	PA5040	24093	25055	-0.272	0.053	Type 4 fimbrial biogenesis outer membrane protein PilQ
pilP	PA5041	4743	4875	-0.252	0.032	Type 4 fimbrial biogenesis protein PilP
fimU	PA4550	2082	2121	-0.247	0.108	Type 4 fimbrial biogenesis protein FimU
pilE	PA4556	1822	1845	-0.241	0.098	Type 4 fimbrial biogenesis protein PilE
pilN	PA5043	4490	4532	-0.229	0.063	Type 4 fimbrial biogenesis protein PilN
pilT	PA0395	4997	5030	-0.226	0.036	Retraction ATPase PilT
pilU	PA0396	4848	4858	-0.225	0.072	Probable retraction ATPase PilU
-	predicted RNA	3321	3314	-0.216	0.070	Antisense: fimX PA4958
vfr	PA0652	7559	7495	-0.215	0.117	cAMP-regulatory protein
pilM	PA5044	11504	11419	-0.208	0.077	Type 4 fimbrial biogenesis protein PilM
algZ	PA5262	815	802	-0.207	0.230	Alginate biosynthesis protein AlgZ/FimS
pilZ	PA2960	1456	1438	-0.206	0.130	Type 4 fimbrial biogenesis protein PilZ
pilR	PA4547	1422	1400	-0.199	0.142	Two-component response regulator PilR
pilO	PA5042	4538	4484	-0.196	0.069	Type 4 fimbrial biogenesis protein PilO
pilH	PA0409	3433	3396	-0.195	0.063	Twitching motility protein PilH
pilV	PA4551	1321	1301	-0.194	0.156	Type 4 fimbrial biogenesis protein PilV
pilJ	PA0411	13158	12969	-0.190	0.102	Twitching motility protein PilJ
pilG	PA0408	4935	4786	-0.171	0.079	Twitching motility protein PilG
pilA	PA4525	54176	51725	-0.164	0.272	Type 4 fimbrial PilA
pilS	PA4546	1270	1219	-0.157	0.195	Two-component sensor PilS
fimX	PA4959	5402	5191	-0.154	0.134	Protein FimX
pilD	PA4528	3403	3253	-0.151	0.186	Type 4 prepilin peptidase PilD
pilF	PA3805	1609	1517	-0.127	0.317	Type 4 fimbrial biogenesis protein PilF
pilI	PA0410	2721	2554	-0.120	0.264	Twitching motility protein PilI
pilK	PA0412	2673	2478	-0.108	0.376	Methyltransferase PilK
algR	PA5261	1053	954	-0.099	0.622	Alginate biosynthesis regulatory protein AlgR
fimT	PA4549	21	19	-0.075	0.879	Type 4 fimbrial biogenesis protein FimT
fimV	PA3115	20690	18800	-0.075	0.505	Motility protein FimV
fimL	PA1822	3637	3304	-0.070	0.505	Hypothetical protein
-	predicted RNA	2419	2174	-0.062	0.522	Antisense: PA1821 fimL
pilB	PA4526	9496	8336	-0.020	0.866	Type 4 fimbrial biogenesis protein PilB
-	PA0499	19	16	-0.016	0.972	Probable pili assembly chaperone
-	predicted RNA	5964	5203	-0.010	0.934	Antisense: PA3806 pilF

3.7 Cysteine-labelled *P. aeruginosa* T4P can be visualized with fluorescent microscopy

The dynamics of type IV filaments in *Caulobacter crescentus* and *Vibrio cholerae* were recently visualized using a pilus labelling system (67, 68). A cysteine point mutation in the major pilin allows for staining of PilA subunits with a fluorescent maleimide dye, allowing for direct visualization of pili dynamics (170). With their average diameter of ~6 nm (15), live imaging of T4P *in vivo* is challenging, as their size falls below the diffraction limit of standard light microscopy. Studies of T4P have thus relied on comparisons of piliated cells with non-piliated or genetically-modified systems, or static methods, such as indirect force spectroscopy (34, 85, 159) and electron microscopy (19). While these studies provide insight into T4P structure, the dynamics of T4P expression *in vivo* are lost.

This labelling method involves introduction of site-directed cysteine substitutions at solvent-exposed positions in the globular C-terminal domain of pilins (170). The modified T4P can then be fluorescently labeled with a thiol-reactive maleimide dye (67, 170). The contributions of single amino acid residues to pilin structure and function, as well as the relative surface accessibility of residues (199), must be considered, as mutations of nonconserved, solvent-exposed residues are more likely to produce functional labeled T4P (170). Although many type IV pilins contain a

disulfide bond critical for their folding and polymerization, addition of a third Cys residue does not impact function if the site is carefully selected. Cysteine point mutations at residues A76, A77, D78, K81, T84, A86, and T101 within the globular C-terminal of PAK PilA were generated, with varying effects on phage susceptibility and twitching **(Figure 9)**. The PilA T101C mutant had near WT twitching and was susceptible to T4P-specific phage, so this mutant was used for imaging to maximize our chances of observing a T4P extension and retraction event. Using the methods described by Ellison et. al (170), strains were stained with AF-conjugated, thiol-reactive maleimide dyes.

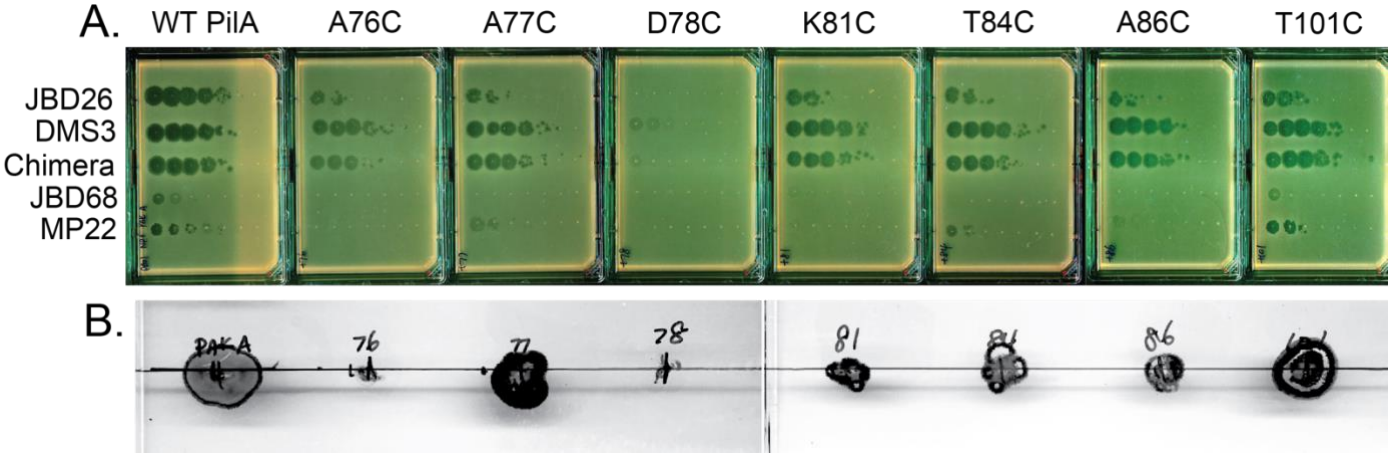

Figure 9. Phage susceptibility and twitching of PilA cysteine point mutants. A. Plaque assays using 5 µl of serial tenfold dilutions of the phages indicated on the left (JBD26, DMS3, chimera, JBD68, MP22) against the PAO1 *pilA* strains expressing either WT PAK PilA or PilA cysteine point mutants. **B.** Twitching phenotypes of the PAK PilA cysteine point mutants. PilA A77C and PilA T101C have twitching similar to WT, while PilA A76C/D78C/K81C/T84C/A86C mutants have reduced or no twitching.

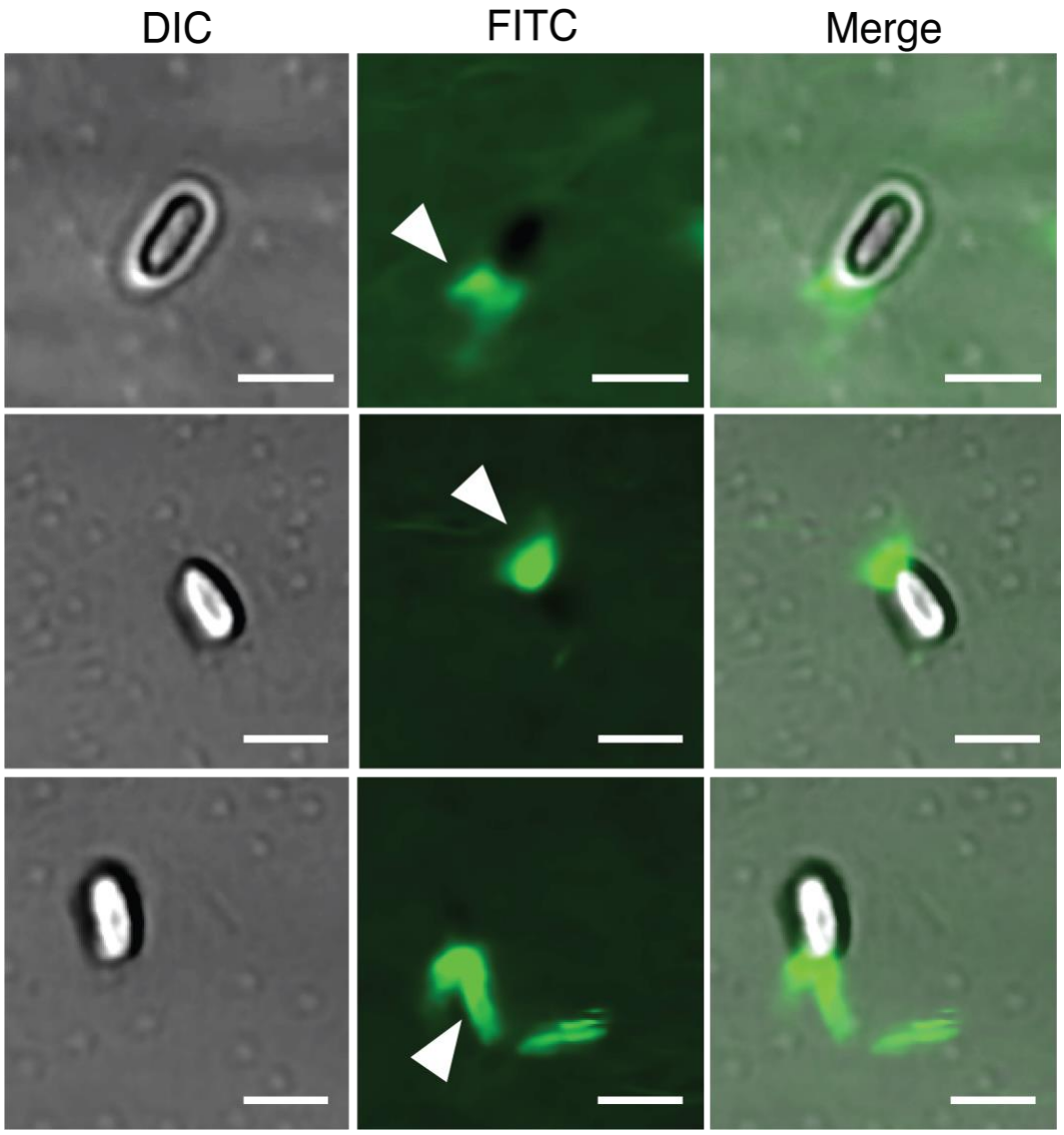

Figure 10. AF488-labelled T4P in a retraction-deficient *P. aeruginosa* PAO1 strain. PAO1 *pilA pilT* + pBADGr PAK PilA T101C was stained with AF488-maleimide dye for 45 min and imaged on a Nikon A1 confocal microscope with a 60X Plan Apo oil objective (numerical aperture (NA) =1.40) and an FITC filter set. White arrows denote labelled T4P.

The PilA T101C construct was electroporated into the retraction-deficient PAO1 *pilA pilT* strain **(Figure 10)**. Multiple T4P were primarily observed at

one cell pole in the AF-488-stained PAO1 *pilA pilT* + pBADGr PAK PilA T101C, though the middle panel shows T4P expressed at both poles. This confirmed labeling of the mutant *P. aeruginosa* pilin.

Labelled T4P were also observed in the PAO1 *pilA* + pBADGr PAK PilA T101C strain at 60X magnification **(Figure 11)**. Interestingly, AF-488-stained pili were only visualized in dividing cells; single cells with cysteine labelled T4P were not observed.

As a negative control, a PAO1 *pilA* + pBADGr PAK PilA strain expressing wild-type PilA was labelled with maleimide dye and imaged **(Figure 12)**. PilA has no surface-exposed cysteines, so minimal labelling with the thiol-reactive maleimide dye was expected. Minimal periplasmic labelling was observed for all bacteria, which could be due to the maleimide dye reacting with surface-exposed cysteines in other membrane proteins.

To expand our applications of the T4P cysteine-labelling system, the PilA T101C mutant was also stained with the AF-594 maleimide dye. Ellison et. al (170) noted that the brightness of labelled pili can vary across different dyes for certain cysteine substitutions. Multiple T4P were observed in the AF-594-stained PAO1 *pilA pilT* + pBADGr PAK PilA T101C at one bacterial cell pole **(Figure 13A)**, while the PAO1 *pilA* + pBADGr PAK PilA strain had no visible staining with the AF-594 dye **(Figure 13B)**. This confirms that the PilA T101C substitution is compatible with both AF-488 and AF-594

conjugated maleimide dyes, providing more flexibility for imaging T4P alongside other fluorescent proteins.

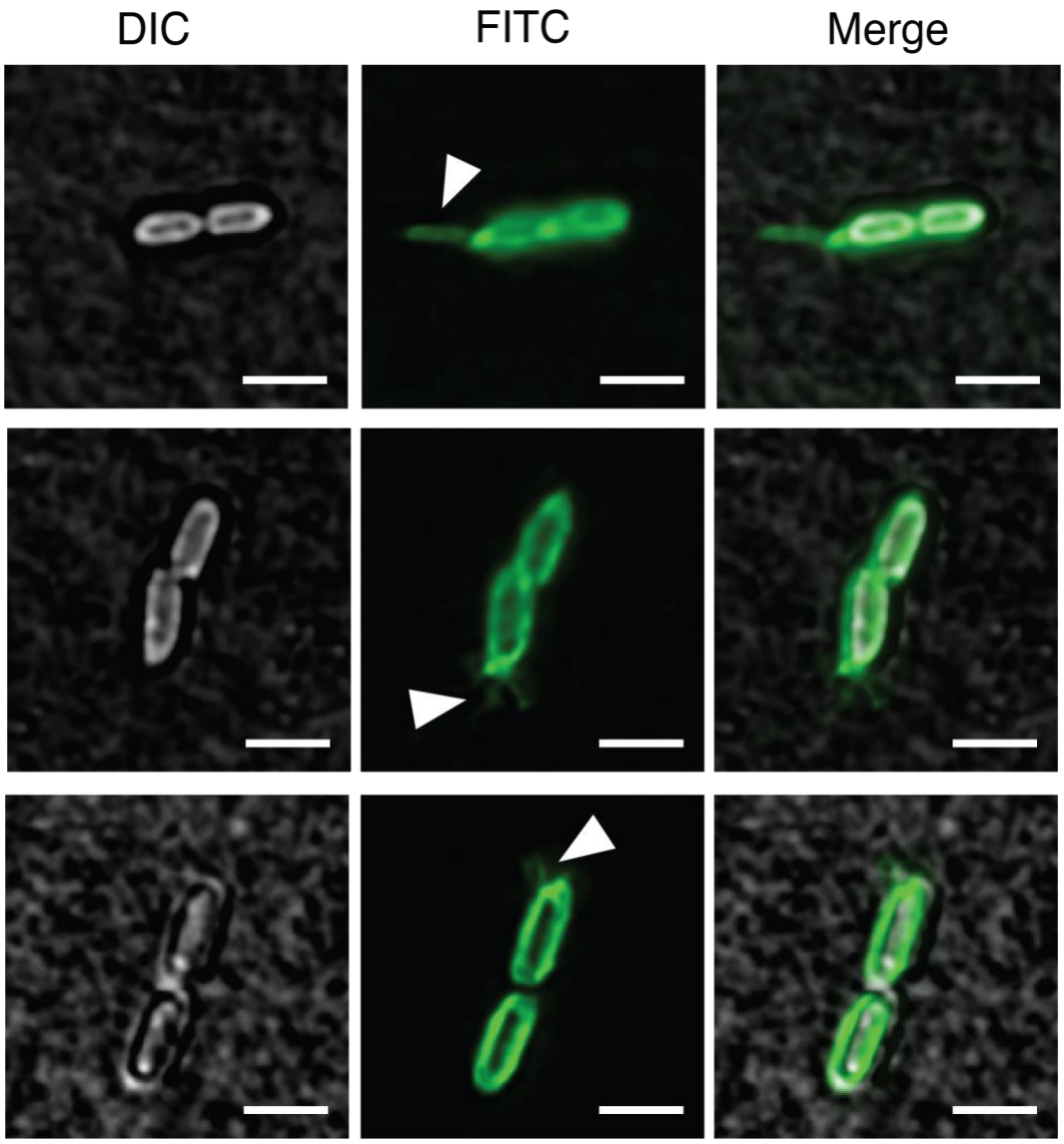

Figure 11. AF488-labelled T4P in a *P. aeruginosa* PAO1 PilA point mutant. PAO1 *pilA* + pBADGr PAK PilA T101C was stained with AF488-maleimide dye for 45 minutes and imaged on the Nikon A1 confocal microscope with a 60X Plan Apo oil objective (NA=1.40) and an FITC filter set. White arrows denote labelled T4P.

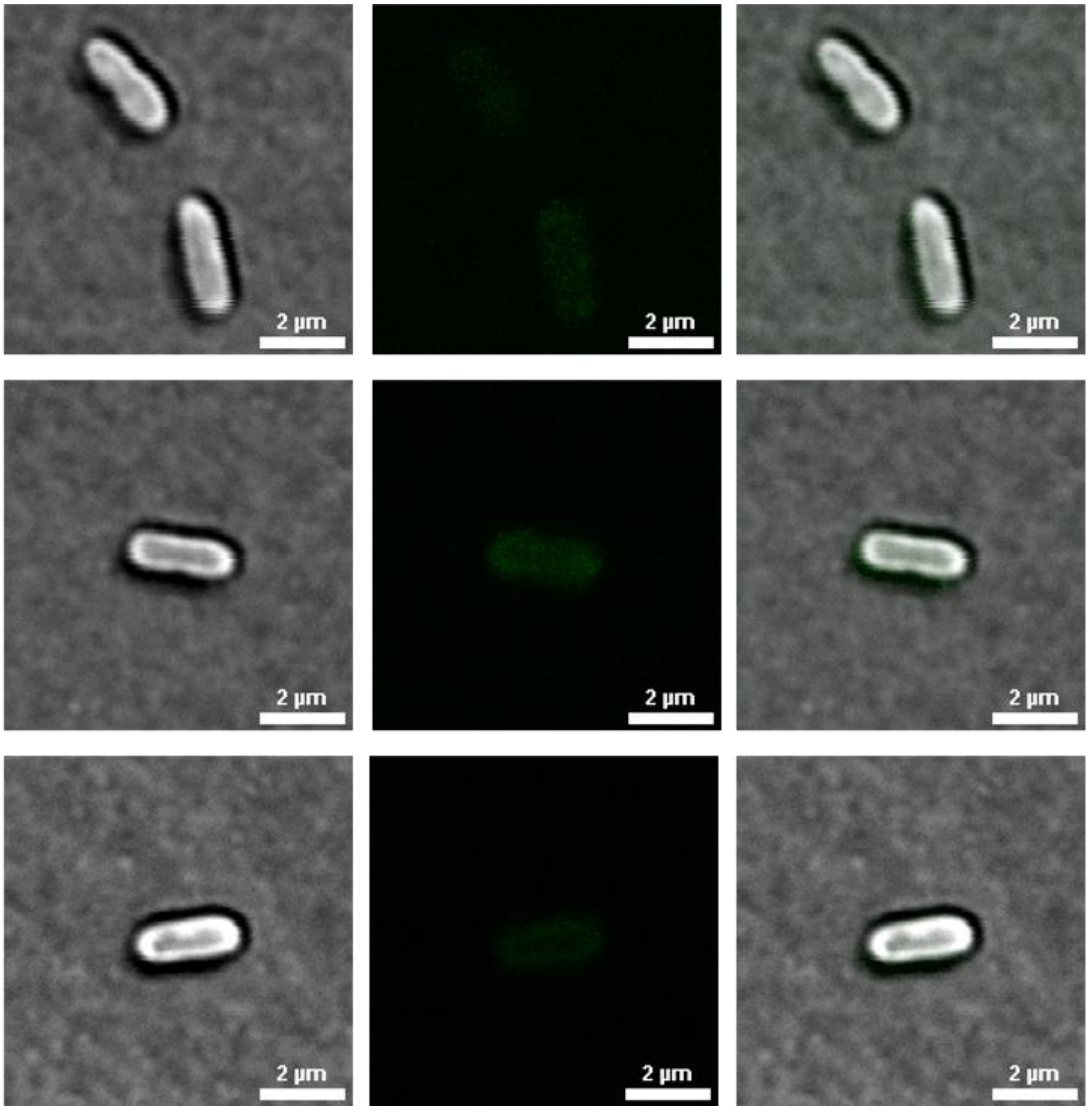

Figure 12. AF488-labelling of WT *P. aeruginosa* PAO1. PAO1 *pilA* + pBADGr PAK PilA was stained with AF488-maleimide dye for 45 minutes and imaged on the Nikon A1 confocal microscope with a 60X Plan Apo oil objective (NA=1.40) and an FITC filter set.

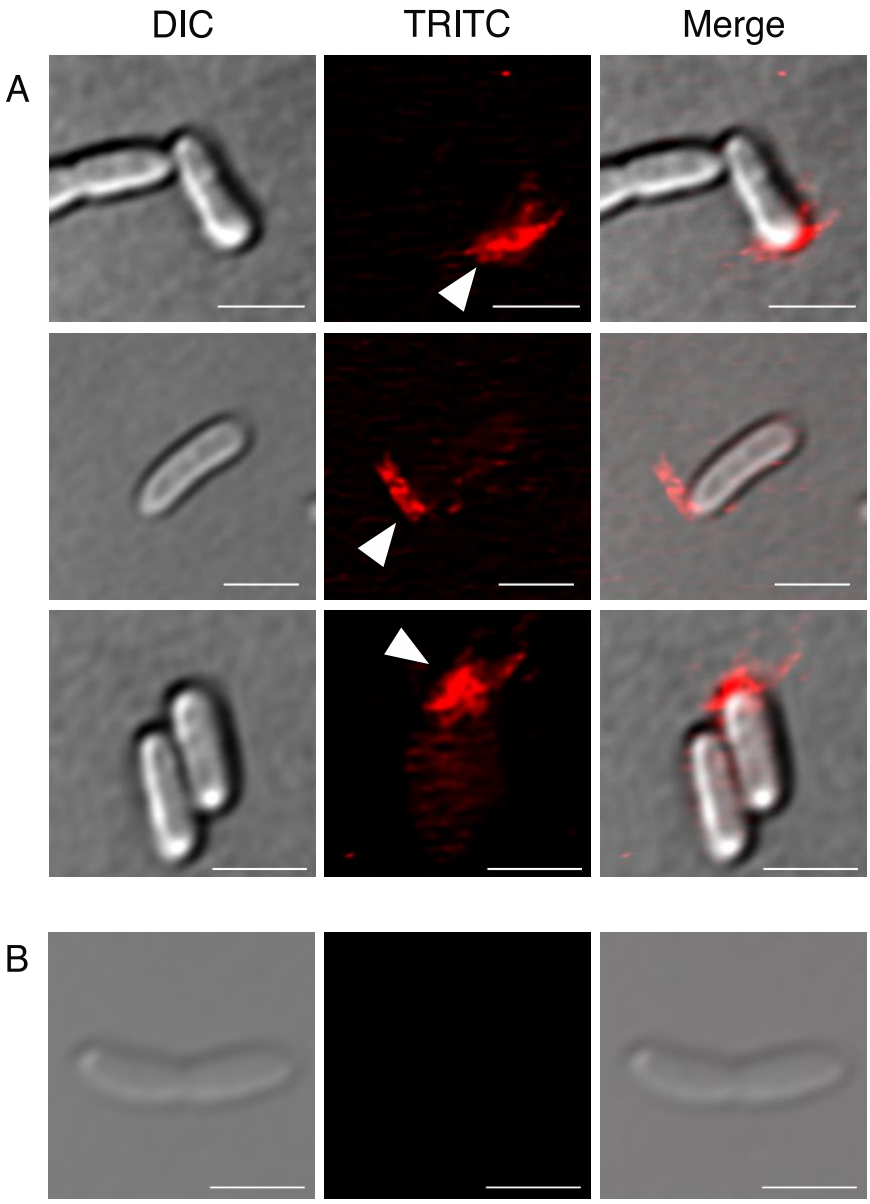

Figure 13: AF594-labelling of T4P in PAO1. (A) PAO1 *pilA pilT* + pBADGr PAK PilA T101C and **(B)** PAO1 *pilA* + pBADGr PAK PilA were stained with AF594-maleimide dye for 45 minutes and imaged on the Nikon A1 confocal microscope with a 60X Plan Apo oil objective (NA=1.40) and an TRITC filter set. White arrows denote labelled T4P. Scale, 2 µm.

CHAPTER 4. DISCUSSION

4.1 Hyperpiliation, not loss of pilus retraction, reduces pathogenicity

T4P are important virulence factors for *P. aeruginosa* and other bacterial pathogens (12, 62, 76, 80, 81, 154–156, 200–203). Most studies compare the pathogenicity-associated phenotypes of piliated strains to isogenic non-piliated mutants. While these studies highlight the importance of T4P expression during infection, uncovering the dynamics and signalling pathways involved in T4P-mediated surface attachment and subsequent upregulation of virulence-related genes proves difficult. A loss of T4P dynamics via deletion of *pilT* reduces virulence or surface attachment of *D. nodosus* in sheep (90), *Pantoea ananatis* in onion seedlings (204), *P. aeruginosa* in murine and human infection models (88, 158), *Acidovorax avenae* in seed transmission assays (77), and *N. meningitidis* in mice (205). These studies attributed a loss of virulence to loss of pilus dynamics and twitching, though the contributions of increased surface piliation to virulence were not assessed.

Use of a set of hyperpiliated mutant strains with a range of twitching phenotypes enabled us to separate the contributions of surface piliation levels and motility to pathogenicity. Although *pilT*, PilS N323A, PilR D54E, and PilO M92K mutants are all hyperpiliated compared to WT**,** only *pilT* is completely deficient in twitching.

PilS N323A and PilR D54E mutants produced peritrichous T4P, similar to T4P expression patterns recently observed in *A. baylyi* (176). The functional consequences of T4P localization along the long axis of the cell were not confirmed in *A. baylyi* (176), though PilS N323A and PilR D54E mutants have fully functional pili and WT twitching. The localization of T4P in the hyperpiliated point mutants could be connected to the PilA-interacting protein, PilJ (164). Components of the Pil-Chp chemosensory system and T4P machinery are proposed to co-localize at cell poles in a FimV-dependent manner (206). A previous study showed that, under native expression levels, PilJ localizes to both cell poles, whereas *pilJ* overexpression results in peritrichous PilJ localization (207). It is plausible that constitutive upregulation of PilA in the PilSR hyperactive mutants results in increased PilJ signalling and expression, leading to peritrichous PilJ expression and co-localization of T4P-components.

Conversely, the hyperpiliated PilO M92K mutant has partial twitching, suggesting a role for this protein in modulating extension and retraction dynamics (175). Regardless of their twitching phenotypes, all hyperpiliated mutants had PilA-dependent defects in pathogenicity in *C. elegans*. These results help to explain the important role of PilSR in the regulation of *pilA* expression and modulation of the levels of surface piliation (116). If too many pili are produced, it can negatively impact virulence.

Prior studies showed that injection of the T3S effector, ExoS, requires T4P (208) and the retraction ATPase, PilT (209). Both *pilA* and *pilT* single mutants secreted less ExoS/T compared to WT, while T3SS-related exotoxins were undetectable in the *pilA pilT* double mutant, suggesting that PilA and PilT play an important role together in exotoxin secretion. Interactions between PilA and the methyl-accepting chemotaxis protein (MCP)-like chemosensory receptor, PilJ, require contact with a surface and subsequent retraction (116, 164). When bound to surface-attached pilins, PilJ promotes CyaB activity via ChpA, leading to subsequent cAMP-Vfr signalling (164). Here, a loss of T4P-mediated surface attachment and retraction upon deletion of *pilA* and *pilT*, respectively, reduces PilJ and Vfr-mediated signalling, leading to downregulation of the Vfr regulon, including pilus biogenesis genes and the T3SS activator, *exsA* (210). The ExsA regulon contains *exoS/T* (211), so reduced expression of these exotoxins in the *pilA*, *pilT*, and *pilA pilT* mutants is likely due to reduced signalling via PilJ and Vfr.

Studies in PA14 indicated that while the T3SS is expressed during infection of *C. elegans,* it is not required for full pathogenicity (179), but also suggested that loss of the effector ExoU impaired PA14 virulence (212). In PAO1, the T3SS plays a major role, as loss of function significantly reduces pathogenicity (180). PAK is more closely related to PAO1 than to PA14, with PAK and PAO1 expressing the T3SS effectors ExoSTY, while PA14

expresses ExoSTU (213, 214). Consistent with the PAO1 data, a PAK *pscN* mutant had significantly reduced virulence towards *C. elegans.* Given the increased virulence of PA14 towards *C. elegans* relative to PAK and PAO1, it is possible that T3SS contributes to PA14 pathogenicity, but that more potent virulence factors produced by that strain kill *C. elegans* rapidly before the contributions of T3SS effectors become obvious. Even so, our data show that hyperpiliated strains of PA14 are less pathogenic than WT.

The PilS N323A *pscN* double mutant had levels of pathogenicity similar to single PilS N323A and *pscN* mutants, and a PilS N323A *pscN pilA* triple mutant had decreased virulence compared to the PilS N323A *pilA* strain. These data refute previous conclusions that a functional T4P system is required for T3SS engagement (208, 209), as the non-piliated PilS N323A *pilA* mutant lacks pili but was more pathogenic than the triple mutant that lacks PscN. Deletion of *pscP* in the PilS N323A background reduced surface pili expression and restored pathogenicity to near-WT levels.

While PscP expression is independent of PilSR (148) and its deletion did not affect pathogenicity in an otherwise WT background, our data suggests that PscP may play a role in regulating surface pili expression, potentially through the cAMP-Vfr signalling system. Inappropriate increases in functional surface pili increase signalling via the Pil-Chp chemosensory system, a complex signalling transduction pathway that controls both

twitching and cAMP production through the activation of the adenylate cyclase, CyaB (99, 149, 215, 216). Increases in intracellular cAMP activate Vfr, which controls the expression of more than 100 pathogenicity-associated genes, including the T3SS activator *exsA* and components of the T4P machinery **(Figure 14)** (99, 217).

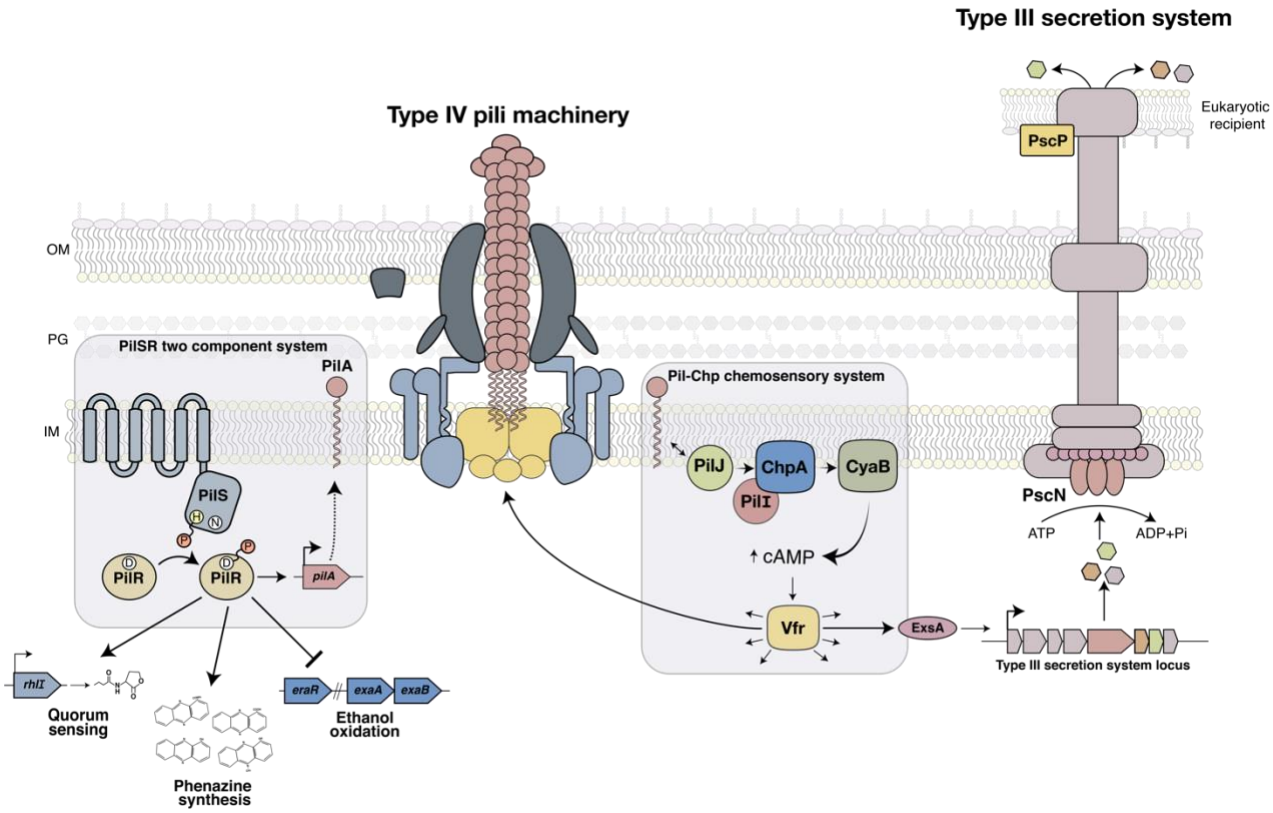

Figure 14. Model for integrated regulation of *pilA*, T3S, quorum sensing, phenazine synthesis, and ethanol oxidation. The PilSR TCS regulates the IM PilA inventory. PilA interacts with PilJ, an MCP-like chemosensory receptor, which undergoes a conformational change that promotes autophosphorylation of the kinase ChpA. ChpA, in complex with PilI, promotes CyaB activity, leading to upregulation of cAMP and subsequent activation of Vfr and its regulon (164), which includes both *pilA*

and the T3SS activator *exsA*. The T3SS needle length regulator, PscP, disrupts hyperpiliation in the PilSR hyperactive point mutants, although the signaling mechanism is unclear. In addition to *pilA*, PilR dysregulates a subset of genes, including those related to quorum sensing, phenazine synthesis, and ethanol oxidation.

Taken together, these data challenge the idea that loss of twitching reduces *P. aeruginosa* pathogenicity in *C. elegans* and other eukaryotic models. Instead, we suggest that inappropriate increases in the amount of surface pili, even if they are functional, reduce *Pseudomonas* virulence through disruption of intimate attachment with host cells. This has previously been observed in TEM of retraction-deficient *N. meningitidis*, whereby *pilT* strains could make direct contact with epithelial cells but were unable to intimately attach to these cells to cause destruction to microvilli (218). We propose that disruption of intimate host cell contact via hyperpiliation interferes with the function of contact-dependent antagonism systems, like the T3SS **(Figure 15)**.

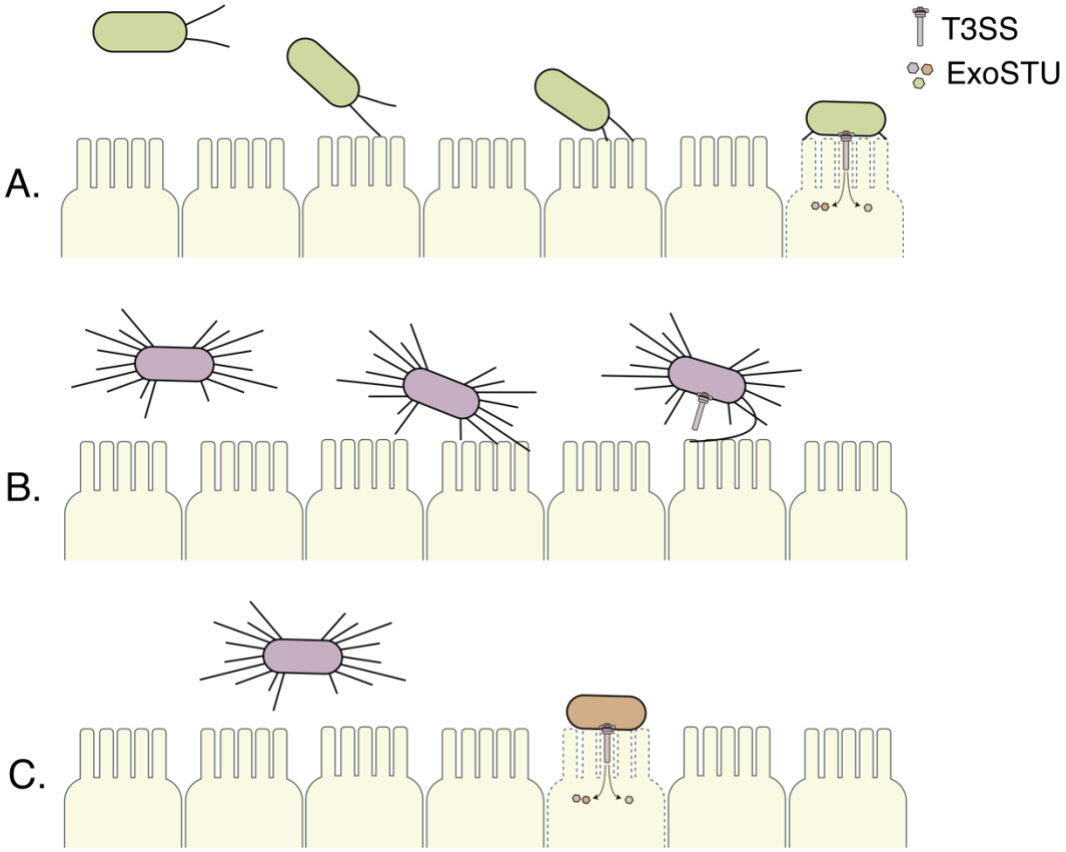

Figure 15. Hyperpiliation impedes intimate host cell contact and reduces virulence. A. *P. aeruginosa* can retract its T4P upon contact with the epithelial cells lining the gut of the worms, leading to intimate engagement of contact-dependent antagonism systems, such as the T3SS. **B.** The T3SS of hyperpiliated mutants (lacking the retraction ATPase PilT, or with specific point mutations in PilO, PilR, or PilS) are unable to effectively engage with host cells to inject effectors, and thus, are less pathogenic. **C.** In those hyperpiliated backgrounds, removing surface pili – which are not critical for pathogenicity in the slow killing model of *C. elegans* (83) – via *pilA* mutations or through disruption of hyperpiliation via deletion of the T3SS ruler protein gene *pscP* restores virulence.

4.2 Hyperactivation of PilR dysregulates expression of multiple genes, including those involved in phenazine biosynthesis, quorum sensing, and ethanol oxidation

We performed comparative RNAseq between the WT strain and PilR D54E mutant to identify genes dysregulated in the hyperpiliated point mutant. A previous study by Kilmury and Burrows (148) identified ten genes, consisting of *hcpA*, *hcpB*, and eight unannotated genes, upregulated in a *pilA* mutant and downregulated in a *pilR* mutant, which were deemed “pilin responsive” (148). As the PilR D54E mutant has constitutively activated PilR, we expected that the 10 genes of interest would be upregulated in this context, similar to the *pilA* background. Given that this mutant can twitch, we also expected to uncover previously unidentified genes, including genes related to surface sensing. Surprisingly, none of the ten “pilin responsive” genes were dysregulated ≥2-fold in the PilR D54E background. Even more unexpectedly, the expression of *pilA* was not significantly upregulated by PilR D54E. However, we identified twenty-six genes dysregulated ≥2-fold by PilR D54E, most notably those related to phenazine synthesis, quorum sensing, and ethanol oxidation **(Figure 14)**.

Genes from two phenazine biosynthesis operons were upregulated by PilR D54E (*pHZA1B1C1D1, pHZC2F2G2*). Phenazine biosynthesis is dependent on 2-heptyl-3-hydroxy-4-quinolone, the *Pseudomonas*

Quinolone Signal (PQS) quorum sensing (QS) molecule, and occurs as part of the *Pseudomonas* stress response, including under conditions of high cell density and nutrient limitation (219, 220). Another quorum sensing-associated gene, *rhlI*, also was upregulated ≥2-fold by PilR D54E.

In addition to the phenazine biosynthetic genes, nine genes located within a hypothetical CYP operon were upregulated ≥2-fold by PilR D54E. The function of cytochromes in *P. aeruginosa* are not well understood, although a subset of cytochromes drive biofilm formation and matrix production for uropathogenic *E. coli* infection (221). With the exception of PA3327, the genes in this operon were previously shown to be regulated by the quorum sensing-associated proteins, LasR and RhlI, as well as the virulence and quorum sensing regulator (VqsR) (194, 222, 223). The altered expression of the hypothetical cytochrome P450 is likely due to downstream signalling via VqsR and Rhll, as the expression of both *vqsR* and *rhlI* were increased ≥2-fold by PilR D54E.

P. aeruginosa encodes two caseinolytic peptidases (ClpP) isoforms, ClpP1 and ClpP2, which through unknown mechanisms play roles in motility, pigment production, iron scavenging, and biofilm production (193). Surprisingly, both ClpP1 and ClpP2 were not upregulated by PilR D54E, as the ClpP2 functions characterized to date are reliant on ClpP1 expression (193).

Three of the eight genes downregulated ≥2-fold by PilR D54E are involved in ethanol oxidation, including the quinoprotein ethanol dehydrogenase *exaA* gene (195), the cytochrome c550 *exaB* gene (196), and the transcriptional regulator *eraR* (197). The remaining two genes downregulated ≥2-fold by PilR D54E, PA3866 and PA1219, encode pyocin S4 and a hypothetical protein, respectively. Pyocins S2 and S4 both use the siderophore pyoverdine receptor FpvAI to enter competing cells (198). A possible connection between PilR signalling and pyocin S4 production is unclear. The hypothetical protein may be subject to future studies.

Based on the low numbers of genes dysregulated by PilR D54E identified by RNAseq and discordance with previous data (116, 148), this transcriptomic analysis will need to be repeated. RNA quality is critical for accurate quantification of transcripts, and degradation of RNA leads to significant loss of transcript library complexity (224). Here, the RNA sample collection may have yielded low quality samples due to technical error, which significantly reduced the number of transcripts identified. Further, transcript degradation is not uniform within a sample, with different transcripts degrading at different rates (224). The twenty-six genes dysregulated ≥2-fold by PilR D54E may have more stable RNA transcripts compared to previously identified PilR-regulated genes or T4P-associated genes, contributing to our conflicting transcriptomic data.

4.3 Fluorescent labelling of T4P *in vivo* is a broadly applicable method for studying T4P dynamics

To complement the genetic manipulations of the PilSR TCS, this work also applied a newly developed T4P-labelling method to *P. aeruginosa* to investigate T4P dynamics *in vivo*. We identified a functional, labelable cysteine point mutant, PilA T101C, in PAK which was expressed on pBADGr in both the single *pilA* mutant and retraction-deficient *pilA pilT* double mutant. AF488- and AF594-labelled T4P were directly observed using static microscopy, which revealed polar T4P localization in several cells in both the *pilA* and *pilA pilT* mutants expressing pBADGr-*pilA*$_{T101C}$. In contrast to our TEM data, fluorescently labelled T4P were primarily expressed at one pole in the retraction-deficient mutant. This discrepancy could be a consequence of PilA overexpression, as plasmid-based overexpression of PilA reduces native PilA levels in the cell through PilSR-mediated negative feedback regulation on *pilA* transcription (116).

We were unable to observe real-time T4P dynamics using our experimental setup. Ideally, we would use total internal reflection fluorescence (TIRF) microscope to resolve individual T4P (64) and charge-coupled device camera to resolve individual T4P (170). Our laser scanning confocal microscope cannot provide a rate fast enough or at a high enough resolution to capture T4P extension and retraction. Nonetheless, the development and

optimization of a reproducible T4P labelling system in *P. aeruginosa* that is compatible with multiple fluorescently conjugated maleimide dyes will foster future studies to uncover the mechanisms driving twitching and T4P-mediated surface attachment.

CHAPTER 5. CONCLUSIONS AND FUTURE DIRECTIONS

5.1 Future directions

Identify other contact-dependent virulence factors affected by hyperpiliation

P. aeruginosa encodes an arsenal of virulence factors that contribute to acute infection across a variety of hosts (5), including contact-dependent antagonism systems for both interbacterial competition and virulence against eukaryotic hosts, such as the T6SS and T3SS, respectively (225, 226). This work identified three potential connections between the T3SS and surface pili expression; (i) hyperpiliation may sterically hinder T3SS function, (ii) deletion of *pilA* and/or *pilT* reduces the secretion of T3SS effectors, and (ii) deletion of the needle length regulator, PscP, reduces surface pili expression in some hyperpiliated strains. This suggests that not only does hyperpiliation affect contact dependent killing via the T3SS, but also that there are signalling pathways connecting *pilA* expression and T3S that have yet to be characterized. This poses the question of whether other contact-dependent antagonism systems are affected by hyperpiliation, including CdiA-associated contact-dependent growth inhibition (CDI) systems and the T6SS. CDI systems secrete the CdiA toxin into the periplasm of target bacterial cells (227) and have been implicated in biofilm formation and cell-to-cell adhesion (228, 229). CDI systems and T3SS needles extend ~33 nm and ~60-80 nm, respectively, from the bacterial cell

surface (227, 230), so we predict that hyperpiliation may also impede effective secretion of the CdiA toxin. Interestingly, Kilmury and Burrows (148) identified *hcpA* and *hcpB*, which encode the primary structural components of the T6SS (231), as “pilin-responsive”, which may represent a previously unknown connection between T4P expression and the T6SS. Preliminary data (not shown) also indicates that Hcp expression is upregulated in the PAK PilR D54E and PilS N323A mutants. Future work should assess whether interbacterial antagonism is affected in these strains. If so, this would further our hypothesis that hyperpiliation reduces virulence through disruption of the intimate host cell contact required for effective engagement of contact-dependent antagonism systems.

How does deletion of the T3S needle length regulator reduce surface pili expression?

Our electron microscopy and secretion assay data revealed a potential regulatory connection between PilSR and the T3SS needle length regulator, PscP. Upon deletion of PscP in the PilS N323A hyperpiliated background, surface pili expression was reduced, while the *pilT pscP* strain remained hyperpiliated. Deletion of *pscN* only slightly reduced surface pilin expression in the PilS N323A background, suggesting that the loss of hyperpiliation in the PilS N323A *pscP* strain is PscP-dependent. To validate this phenotype, secretion assays, sheared surface protein preparations, and TEM should

be performed on the PilS N323A *pscP* mutant complemented with *pscP in trans* to assess whether hyperpiliation is restored in this background. Deletion of *pscP* in the hyperpiliated mutants could result in Vfr-mediated downregulation of T4P assembly and expression due to reduced PilA-PilJ interactions (99, 164, 217), although it is unclear why surface PilA expression is not reduced in the single *pscP* mutant. The strains harbouring a deletion in *pscP* have been validated with Sanger sequencing, so the phenotypes observed in these strains is likely due to loss of *pscP* and not polar effects from disruptions to expression of neighbouring genes.

In *Salmonella enterica*, the *Salmonella* pathogenicity island 1 (SPI1)-encoded T3SS is negatively regulated by the PhoPQ TCS through repression of the T3SS activators, HilD, HilC, and RtsA (232). While the genetically distinct PhoPQ TCS encoded by *P. aeruginosa* plays a critical role in virulence against epithelial cells, there is no evidence that it controls T3SS expression in this species (233). We questioned whether deletion of *pscP* dysregulates T3SS-mediated secretion of a negative regulator, leading to downregulation of both the T3SS and T4P expression. *P. aeruginosa* secretes the negative regulator, ExsE, which is involved in a regulatory cascade controlling the transcriptional activity of ExsA (234, 235), though connections between ExsE- and ExsA-mediated regulation and T4P expression have yet to be characterized. ExoS and several domains of ExoT also contribute to feedback inhibition of T3SS-mediated effector

secretion in *P. aeruginosa* (236), though this likely does not contribute to loss of hyperpiliation in the PilS N323A *pscP* mutant, as we did not observe appreciable ExoS/T secretion in this strain.

To confirm that this finding applies to both PilS and PilR, the *pscP* mutation will also be introduced into the PilR D54E hyperpiliated mutant and surface PilA expression will be quantified. As deletion of *pscP* in the retraction-deficient *pilT* background does not alter surface T4P expression, it will also be important to assess whether PilA expression is altered in the PilO M92K hyperpiliated background when PscP is deleted, as this will help to distinguish whether this phenotype is PilSR-specific.

Repeat the RNAseq analysis to validate genes dysregulated by PilR D54E

Transcriptomics revealed twenty-six genes dysregulated ≥2-fold by PilR D54E, including a subset related to phenazine synthesis, quorum sensing, and ethanol oxidation. These genes did not align with previous RNAseq data of *pilA* and *pilR* mutants from Kilmury and Burrows (148), though we expected the *pilA* and PilR D54E strains to have comparable transcriptomes as both strains have constitutive signalling via PilSR. Unexpectedly, *pilA* was not dysregulated by PilR D54E. Due to the low number of genes identified and discordance with previous data (116, 148), this RNAseq analysis should be repeated. The low complexity of the transcript library could be a result of RNA degradation during sample preparation (224), so

future work should ensure that the RNA concentration and purity are of high enough quality prior to transcriptomic analysis.

If the genes identified in this follow-up RNAseq analysis align with the twenty-six genes identified here, their expression, along with any newly identified genes, will be confirmed with real-time reverse transcription PCR (RT-PCR). We are also currently generating in-frame deletions of the ten "pilin-responsive" genes inversely dysregulated ≥5-fold by *pilA* and *pilR*, including *hcpA*, *hcpB*, and eight uncharacterized genes (148). Pathogenicity-associated phenotypes in these deletion constructs, including biofilm formation, *C. elegans* virulence, motility, and interbacterial competition, will be tested to characterize the function of the eight unannotated genes. Other assays may be required to assess novel phenotypes.

Expand the T4P labelling system to other P. aeruginosa genetic backgrounds

We expressed cysteine point mutants of PilA on the pBADGr expression vector to fluorescently label and visualize T4P in retraction-deficient and functional backgrounds. For PilA point mutants expressed from pBADGr, both Gm and arabinose are required for selection and induction of expression, respectively (164). Now that a functional and labelable PilA point mutant (PilA T101C) has been identified, we want to express other

fluorescently tagged T4P-associated proteins (ex. PilU, PilT, PilB) alongside cysteine-labelled T4P to assess pilus dynamics in real time. We generated a PilA T101C chromosomal knock-in and are working on obtaining real-time videos of T4P dynamics using a high-resolution TIRF microscope. Introducing the PilA T101C mutation into the PilS N323A and PilR D54E strains will also be the subject of future work, as this will confirm the peritrichous localization of T4P and help to determine whether T4P expressed along the long axis of the cell are functional. Previously developed mCherry fusions to PilO and PilQ will also be transformed into the hyperpiliated mutants to confirm the peritrichous localization of the T4P machinery. *Neisseria* species express peritrichous T4P yet exhibit directional twitching (237), which is proposed to be a result of directional memory (238). Marathe et al. (238) used theoretical and experimental methods to demonstrate that *N. gonorrhoeae* persist in one direction by re-elongation of T4P from membrane-standing complexes that are stable for several seconds following retraction, as well as through small pilus bundle formation at the leading pole. Directional memory could explain the normal twitching phenotype observed in the PilSR hyperpiliated point mutants despite their peritrichous T4P localization.

5.2 Conclusions

The establishment of *P. aeruginosa* infection is a complex process involving the coordinated regulation of multiple virulence factors, including T4P. T4P facilitate initial contact and attachment to host cells, twitching, and biofilm formation. The expression of T4P is tightly regulated at the transcriptional level by the PilSR TCS, which regulates *pilA* expression. Here, we challenged the paradigm that loss of twitching reduces *P. aeruginosa* virulence. We instead show that inappropriate increases in T4P expression, even if they are functional in terms of motility, reduces virulence by potentially impacting the expression and/or function of contact dependent virulence systems, such as the T3SS. Additional genes dysregulated by hyperactivity of the PilSR TCS were also identified, including those related to phenazine synthesis, quorum sensing, and ethanol oxidation. A T4P cysteine labelling system was also implemented for *P. aeruginosa*, allowing for further characterization of the dynamics involved in T4P extension and retraction. With recent calls for anti-*Pseudomonas* treatments (239), a greater understanding of how T4P regulation and dynamics alter virulence may aid in the targeted development of novel antipseudomonal therapies.

CHAPTER 6. REFERENCES

1. He J, Baldini RL, Déziel E, Saucier M, Zhang Q, Liberati NT, Lee D, Urbach J, Goodman HM, Rahme LG. 2004. The broad host range pathogen *Pseudomonas aeruginosa* strain PA14 carries two pathogenicity islands harboring plant and animal virulence genes. Proc Natl Acad Sci U S A 101:2530–2535.

2. Skerman VBD, McGowan V, Sneath PHA. 1980. Approved lists of bacterial names. Int J Syst Bacteriol 30:225–420.

3. Govan JR, Deretic V. 1996. Microbial pathogenesis in cystic fibrosis: mucoid *Pseudomonas aeruginosa* and *Burkholderia cepacia*. Microbiol Mol Biol Rev 60.

4. World Health Organization. 2017. Prioritization of pathogens to guide discovery, research and development of new antibiotics for drug resistant bacterial infections, including tuberculosis.

5. Giltner CL, Nguyen Y, Burrows LL. 2012. Type IV Pilin Proteins: Versatile Molecular Modules. Microbiol Mol Biol Rev 76:740–772.

6. Burrows LL. 2012. *Pseudomonas aeruginosa* Twitching Motility: Type IV Pili in Action. Annu Rev Microbiol 66:493–520.

7. Giltner CL, Rana N, Lunardo MN, Hussain AQ, Burrows LL. 2011. Evolutionary and functional diversity of the *Pseudomonas* type IVa pilin island. Environ Microbiol 13:250–264.

8. Imam S, Chen Z, Roos DS, Pohlschröder M. 2011. Identification of surprisingly diverse type IV Pili, across a broad range of gram-positive bacteria. PLoS One 6.

9. Ng SYM, Wu J, Nair DB, Logan SM, Robotham A, Tessier L, Kelly JF, Uchida K, Aizawa S-I, Jarrell KF. 2011. Genetic and Mass Spectrometry Analyses of the Unusual Type IV-Like Pili of the Archaeon *Methanococcus maripaludis*. J Bacteriol 193:804–814.

10. Denise R, Abby SS, Rocha EPC. 2019. Diversification of the type IV filament superfamily into machines for adhesion, protein secretion, DNA uptake, and motility. PLoS Biol 17.

11. Ayers M, Howell PL, Burrows LL. 2010. Architecture of the type II secretion and type IV pilus machineries. Future Microbiol 5:1203–1218.

12. Craig L, Pique ME, Tainer JA. 2004. Type IV pilus structure and bacterial pathogenicity. Nat Rev Microbiol.

13. Pelicic V. 2008. Type IV pili: *e pluribus unum*? Mol Microbiol.

14. Paranchych W, Sastry PA, Frost LS, Carpenter M, Armstrong GD, Watts TH. 1979. Biochemical studies on pili isolated from *Pseudomonas aeruginosa* strain PAO. Can J Microbiol 25:1175–1181.

15. Touhami A, Jericho MH, Boyd JM, Beveridge TJ. 2006. Nanoscale characterization and determination of adhesion forces of *Pseudomonas aeruginosa* pili by using atomic force microscopy. J Bacteriol 188:370–377.

16. Harvey H, Kus J V., Tessier L, Kelly J, Burrows LL. 2011. *Pseudomonas aeruginosa* D-arabinofuranose biosynthetic pathway and its role in type IV pilus assembly. J Biol Chem 286:28128–28137.

17. Nguyen Y, Jackson SG, Aidoo F, Junop M, Burrows LL. 2010. Structural Characterization of Novel *Pseudomonas aeruginosa* Type IV Pilins. J Mol Biol 395:491–503.

18. Giltner CL, Rana N, Lunardo MN, Hussain AQ, Burrows LL. 2011. Evolutionary and functional diversity of the *Pseudomonas* type IVa pilin island. Environ Microbiol 13:250–264.

19. Chang YW, Rettberg LA, Treuner-Lange A, Iwasa J, Søgaard-Andersen L, Jensen GJ. 2016. Architecture of the type IVa pilus machine. Science (80-) 351.

20. Gold VA, Salzer R, Averhoff B, Kühlbrandt W. 2015. Structure of a type IV pilus machinery in the open and closed state. Elife 4.

21. Nguyen Y, Sugiman-Marangos S, Harvey H, Bell SD, Charlton CL, Junop MS, Burrows LL. 2015. *Pseudomonas aeruginosa* minor pilins prime type IVa pilus assembly and promote surface display of the PilY1 adhesin. J Biol Chem 290:601–611.

22. Winther-Larsen HC, Wolfgang M, Dunham S, Van Putten JPM, Dorward D, Løvold C, Aas FE, Koomey M. 2005. A conserved set of pilin-like molecules controls type IV pilus dynamics and organelle-associated functions in *Neisseria gonorrhoeae*. Mol Microbiol 56:903–917.

23. Hélaine S, Carbonnelle E, Prouvensier L, Beretti JL, Nassif X, Pelicic V. 2005. PilX, a pilus-associated protein essential for bacterial aggregation, is a key to pilus-facilitated attachment of *Neisseria meningitidis* to human cells. Mol Microbiol 55:65–77.

24. Giltner CL, Habash M, Burrows LL. 2010. *Pseudomonas aeruginosa* minor pilins are incorporated into type IV Pili. J Mol Biol 398:444–461.

25. Craig L, Li J. 2008. Type IV pili: paradoxes in form and function. Curr Opin Struct Biol.

26. MS S, S L. 1992. Kinetics and sequence specificity of processing of prepilin by PilD, the type IV leader peptidase of *Pseudomonas aeruginosa*. J Bacteriol 174:7345–7351.

27. Nunn D. 1999. Bacterial Type II protein export and pilus biogenesis: more than just homologies? Trends Cell Biol 9:402–408.

28. Szabó Z, Stahl AO, Albers S V., Kissinger JC, Driessen AJM, Pohlschröder M. 2007. Identification of diverse archaeal proteins with class III signal peptides cleaved by distinct archaeal prepilin peptidases. J Bacteriol 189:772–778.

29. Sastry PA, Finlay BB, Pasloske BL, Paranchych W, Pearlstone JR, Smillie LB. 1985. Comparative studies of the amino acid and nucleotide sequences of pilin derived from *Pseudomonas aeruginosa* PAK and PAO. J Bacteriol 164:571–577.

30. Strom MS, Nunn DN, Lory S. 1993. A single bifunctional enzyme, PilD, catalyzes cleavage and N-methylation of proteins belonging to the type IV pilin family. Proc Natl Acad Sci U S A 90:2404–2408.

31. Strom MS, Lory S. 1991. Amino acid substitutions in pilin of *Pseudomonas aeruginosa*. Effect on leader peptide cleavage, amino-terminal methylation, and pilus assembly. J Biol Chem 266:1656–1664.

32. Harvey H, Habash M, Aidoo F, Burrows LL. 2009. Single-residue changes in the C-terminal disulfide-bonded loop of the *Pseudomonas aeruginosa* type IV pilin influence pilus assembly and twitching motility. J Bacteriol 191:6513–6524.

33. Strom MS, Lory S. 1993. Structure-Function and Biogenesis of the Type Iv Pili. Annu Rev Microbiol 47:565–596.

34. Beaussart A, Baker AE, Kuchma SL, El-Kirat-Chatel S, Otoole GA, Dufrêne YF. 2014. Nanoscale adhesion forces of *Pseudomonas aeruginosa* type IV pili. ACS Nano 8:10723–10733.

35. Lu S, Giuliani M, Harvey H, Burrows LL, Wickham RA, Dutcher JR. 2015. Nanoscale Pulling of Type IV Pili Reveals Their Flexibility and Adhesion to Surfaces over Extended Lengths of the Pili. Biophys J 108:2865–2875.

36. Parge HE, Forest KT, Hickey MJ, Christensen DA, Getzoff ED, Tainer JA. 1995. Structure of the fibre-forming protein pilin at 2.6 Å resolution. Nature 378:32–38.

37. Keizer DW, Slupsky CM, Kalisiak M, Campbell AP, Crump MP, Sastry PA, Hazes B, Irvin RT, Sykes BD. 2001. Structure of a pilin monomer from *Pseudomonas aeruginosa*: Implications for the assembly of pili. J Biol Chem 276:24186–24193.

38. Wang F, Coureuil M, Osinski T, Orlova A, Altindal T, Gesbert G, Nassif X, Egelman EH, Craig L. 2017. Cryoelectron Microscopy Reconstructions of the *Pseudomonas aeruginosa* and *Neisseria gonorrhoeae* Type IV Pili at Sub-nanometer Resolution. Structure 25:1423-1435.e4.

39. Kolappan S, Coureuil M, Yu X, Nassif X, Egelman EH, Craig L. 2016. Structure of the *Neisseria meningitidis* Type IV Pilus. Nat Commun 7.

40. Coureuil M, Lécuyer H, Scott MGH, Boularan C, Enslen H, Soyer M, Mikaty G, Bourdoulous S, Nassif X, Marullo S. 2010. Meningococcus Hijacks a β2-Adrenoceptor/β-Arrestin Pathway to Cross Brain Microvasculature Endothelium. Cell 143:1149–1160.

41. Miller F, Phan G, Brissac T, Bouchiat C, Lioux G, Nassif X, Coureuil M. 2014. The hypervariable region of meningococcal major pilin PilE controls the host cell response via antigenic variation. MBio 5.

42. Thomas WE, Vogel V, Sokurenko E. 2008. Biophysics of Catch Bonds. http://dx.doi.org/101146/annurev.biophys37032807125804 37:399–416.

43. Bardiaux B, de Amorim GC, Luna Rico A, Zheng W, Guilvout I, Jollivet C, Nilges M, Egelman EH, Izadi-Pruneyre N, Francetic O. 2019. Structure and Assembly of the Enterohemorrhagic *Escherichia coli* Type 4 Pilus. Structure 27:1082-1093.e5.

44. Ayers M, Sampaleanu LM, Tammam S, Koo J, Harvey H, Howell PL, Burrows LL. 2009. PilM/N/O/P Proteins Form an Inner Membrane Complex That Affects the Stability of the *Pseudomonas aeruginosa* Type IV Pilus Secretin. J Mol Biol 394:128–142.

45. Martin PR, Watson AA, McCaul TF, Mattick JS. 1995. Characterization of a five-cluster required for the biogenesis of type 4 fimbriae in *Pseudomonas aeruginosa*. Mol Microbiol 16:497–508.

46. Carbonnelle E, Helaine S, Nassif X, Pelicic V. 2006. A systematic genetic analysis in *Neisseria meningitidis* defines the Pil proteins required for assembly, functionality, stabilization and export of type IV pili. Mol Microbiol 61:1510–1522.

47. Bakaletz LO, Baker BD, Jurcisek JA, Harrison A, Novotny LA, Bookwalter JE, Mungur R, Munson RS. 2005. Demonstration of type IV pilus expression and a twitching phenotype by *Haemophilus influenzae*. Infect Immun 73:1635–1643.

48. Karuppiah V, Derrick JP. 2011. Structure of the PilM-PilN inner membrane type IV pilus biogenesis complex from *Thermus thermophilus*. J Biol Chem 286:24434–24442.

49. McCallum M, Tammam S, Little DJ, Robinson H, Koo J, Shah M, Calmettes C, Moraes TF, Burrows LL, Howell PL. 2016. PilN binding modulates the structure and binding partners of the *Pseudomonas aeruginosa* type IVa pilus protein PilM. J Biol Chem 291:11003–11015.

50. Sampaleanu LM, Bonanno JB, Ayers M, Koo J, Tammam S, Burley SK, Almo SC, Burrows LL, Howell PL. 2009. Periplasmic Domains of *Pseudomonas aeruginosa* PilN and PilO Form a Stable Heterodimeric Complex. J Mol Biol 394:143–159.

51. Leighton TL, Yong DH, Howell PL, Burrows LL. 2016. Type IV Pilus Alignment Subcomplex Proteins PilN and PilO Form Homo- and Heterodimers *in vivo*. J Biol Chem 291:19923–19938.

52. Leighton TL, Mok MC, Junop MS, Howell PL, Burrows LL. 2018. Conserved, unstructured regions in *Pseudomonas aeruginosa* PilO are important for type IVa pilus function. Sci Rep 8.

53. Tammam S, Sampaleanu LM, Koo J, Sundaram P, Ayers M, Andrew Chong P, Forman-Kay JD, Burrows LL, Howell PL. 2011. Characterization of the PilN, PilO and PilP type IVa pilus

subcomplex. Mol Microbiol 82:1496–1514.

54. Tammam S, Sampaleanu LM, Koo J, Manoharan K, Daubaras M, Burrows LL, Howell PL. 2013. PilMNOPQ from the *Pseudomonas aeruginosa* type IV pilus system form a transenvelope protein interaction network that interacts with PilA. J Bacteriol 195:2126–2135.

55. Koo J, Tammam S, Ku SY, Sampaleanu LM, Burrows LL, Howell PL. 2008. PilF is an outer membrane lipoprotein required for multimerization and localization of the *Pseudomonas aeruginosa* type IV pilus secretin. J Bacteriol 190:6961–6969.

56. Watson AA, Alm RA, Mattick JS. 1996. Identification of a gene, *pilF*, required for type 4 fimbrial biogenesis and twitching motility in *Pseudomonas aeruginosa*. Gene 180:49–56.

57. Koo J, Lamers RP, Rubinstein JL, Burrows LL, Howell PL. 2016. Structure of the *Pseudomonas aeruginosa* Type IVa Pilus Secretin at 7.4 Å. Structure 24:1778–1787.

58. McCallum M, Tammam S, Rubinstein JL, Burrows LL, Howell PL. 2021. CryoEM map of *Pseudomonas aeruginosa* PilQ enables structural characterization of TsaP. Structure 29:457-466.e4.

59. Takhar HK, Kemp K, Kim M, Howell PL, Burrows LL. 2013. The platform protein is essential for type IV pilus biogenesis. J Biol Chem 288:9721–9728.

60. Bischof LF, Friedrich C, Harms A, Søgaard-Andersen L, Van Der Does C. 2016. The Type IV pilus assembly ATPase PilB of *Myxococcus xanthus* interacts with the inner membrane platform protein PilC and the nucleotide-binding protein PilM. J Biol Chem 291:6946–6957.

61. Burrows LL. 2012. *Pseudomonas aeruginosa* Twitching Motility: Type IV Pili in Action. Annu Rev Microbiol 66:493–520.

62. Merz AJ, So M, Sheetz MP. 2000. Pilus retraction powers bacterial twitching motility. Nature 407:98–102.

63. Mancl JM, Black WP, Robinson H, Yang Z, Schubot FD. 2016. Crystal Structure of a Type IV Pilus Assembly ATPase: Insights into the Molecular Mechanism of PilB from *Thermus thermophilus*. Structure 24:1886–1897.

64. Skerker JM, Berg HC. 2001. Direct observation of extension and retraction of type IV pili. Proc Natl Acad Sci U S A 98:6901–6904.

65. McCallum M, Benlekbir S, Nguyen S, Tammam S, Rubinstein JL, Burrows LL, Howell PL. 2019. Multiple conformations facilitate PilT function in the type IV pilus. Nat Commun 10:5198.

66. McCallum M, Tammam S, Khan A, Burrows LL, Howell PL. 2017. The molecular mechanism of the type IVa pilus motors. Nat Commun 8:15091.

67. Ellison CK, Kan J, Dillard RS, Kysela DT, Ducret A, Berne C, Hampton CM, Ke Z, Wright ER, Biais N, Dalia AB, Brun Y V. 2017. Obstruction of pilus retraction stimulates bacterial surface sensing. Science (80-) 358:535–538.

68. Ellison CK, Dalia TN, Vidal Ceballos A, Wang JCY, Biais N, Brun Y V., Dalia AB. 2018. Retraction of DNA-bound type IV competence pili initiates DNA uptake during natural transformation in *Vibrio cholerae*. Nat Microbiol 3:773–780.

69. Ng D, Harn T, Altindal T, Kolappan S, Marles JM, Lala R, Spielman I, Gao Y, Hauke CA, Kovacikova G, Verjee Z, Taylor RK, Biais N, Craig L. 2016. The *Vibrio cholerae* Minor Pilin TcpB Initiates Assembly and Retraction of the Toxin-Coregulated Pilus. PLoS Pathog 12.

70. Giltner CL, van Schaik EJ, Audette GF, Kao D, Hodges RS, Hassett DJ, Irvin RT. 2006. The *Pseudomonas aeruginosa* type IV pilin receptor binding domain functions as an adhesin for both biotic and abiotic surfaces. Mol Microbiol 59:1083–1096.

71. Harvey H, Bondy-Denomy J, Marquis H, Sztanko KM, Davidson AR, Burrows LL. 2018. *Pseudomonas aeruginosa* defends against phages through type IV pilus glycosylation. Nat Microbiol 3:47–52.

72. Kim S, Rahman M, Seol SY, Yoon SS, Kim J. 2012. *Pseudomonas aeruginosa* Bacteriophage PA1Ø Requires Type IV Pili for Infection and Shows Broad Bactericidal and Biofilm Removal Activities. Appl Environ Microbiol 78:6380–6385.

73. Chen I, Dubnau D. 2003. DNA Transport During Transformation. Front Biosci 8:544–556.

74. Leong CG, Bloomfield RA, Boyd CA, Dornbusch AJ, Lieber L, Liu F,

Owen A, Slay E, Lang KM, Lostroh CP. 2017. The role of core and accessory type IV pilus genes in natural transformation and twitching motility in the bacterium *Acinetobacter baylyi*. PLoS One 12:e0182139.

75. Reguera G, McCarthy KD, Mehta T, Nicoll JS, Tuominen MT, Lovley DR. 2005. Extracellular electron transfer via microbial nanowires. Nature 435:1098–1101.

76. Kehl-Fie TE, Miller SE, St. Geme JW. 2008. *Kingella kingae* expresses type IV pili that mediate adherence to respiratory epithelial and synovial cells. J Bacteriol 190:7157–7163.

77. Bahar O, Goffer T, Burdman S. 2009. Type IV Pili Are Required for Virulence, Twitching Motility, and Biofilm Formation of *Acidovorax avenae subsp. citrulli* . Mol Plant-Microbe Interact 22:909–920.

78. Essex-Lopresti AE, Boddey JA, Thomas † Richard, Smith MP, Gill Hartley M, Atkins T, Brown NF, Chuk ‡, Tsang H, Peak IRA, Hill J, Beacham IR, Titball RW. 2005. A Type IV Pilin, PilA, Contributes to Adherence of *Burkholderia pseudomallei* and Virulence In Vivo. Infect Immun 73:1260–1264.

79. Hoppe J, Ünal CM, Thiem S, Grimpe L, Goldmann T, Gaßler N, Richter M, Shevchuk O, Steinert M. 2017. PilY1 promotes *Legionella pneumophila* infection of human lung tissue explants and contributes to bacterial adhesion, host cell invasion, and twitching motility. Front Cell Infect Microbiol 7.

80. Heiniger RW, Winther-Larsen HC, Pickles RJ, Koomey M, Wolfgang MC. 2010. Infection of human mucosal tissue by *Pseudomonas aeruginosa* requires sequential and mutually dependent virulence factors and a novel pilus-associated adhesin. Cell Microbiol 12:1158–1173.

81. Hahn HP. 1997. The type-4 pilus is the major virulence-associated adhesin of *Pseudomonas aeruginosa* - A review, p. 99–108. *In* Gene.

82. Nieto V, Kroken AR, Grosser MR, Smith BE, Metruccio MME, Hagan P, Hallsten ME, Evans DJ, Fleiszig SMJ. 2019. Type IV Pili Can Mediate Bacterial Motility within Epithelial Cells. MBio 10:e02880-18.

83. Marko VA, Kilmury SLN, MacNeil LT, Burrows LL. 2018. *Pseudomonas aeruginosa* type IV minor pilins and PilY1 regulate

virulence by modulating FimS-AlgR activity. PLoS Pathog 14.

84. Bradley DE. 1980. A function of *Pseudomonas aeruginosa* PAO polar pili: Twitching motility. Can J Microbiol 26:146–154.

85. Maier B, Potter L, So M, Seifert HS, Sheetz MP. 2002. Single pilus motor forces exceed 100 pN. Proc Natl Acad Sci U S A 99:16012–16017.

86. Adams DW, Pereira JM, Stoudmann C, Stutzmann S, Blokesch M. 2019. The type IV pilus protein PilU functions as a PilT-dependent retraction ATPase. PLOS Genet 15:e1008393.

87. Talà L, Fineberg A, Kukura P, Persat A. 2019. *Pseudomonas aeruginosa* orchestrates twitching motility by sequential control of type IV pili movements. Nat Microbiol. Nature Publishing Group.

88. Comolli JC, Hauser AR, Waite L, Whitchurch CB, Mattick JS, Engel JN. 1999. *Pseudomonas aeruginosa* gene products PilT and PilU are required for cytotoxicity in vitro and virulence in a mouse model of acute pneumonia. Infect Immun 67:3625–3630.

89. Merz AJ, Enns CA, So M. 1999. Type IV pili of pathogenic *Neisseriae elicit* cortical plaque formation in epithelial cells. Mol Microbiol 32:1316–1332.

90. Han X, Kennan RM, Davies JK, Reddacliff LA, Dhungyel OP, Whittington RJ, Turnbull L, Whitchurch CB, Rood JI. 2008. Twitching motility is essential for virulence in *Dichelobacter nodosus*. J Bacteriol 190:3323–3335.

91. Galán JE, Collmer A. 1999. Type III secretion machines: Bacterial devices for protein delivery into host cells. Science (80-).

92. Alsharif G, Ahmad S, Islam MS, Shah R, Busby SJ, Krachler AM. 2015. Host attachment and fluid shear are integrated into a mechanical signal regulating virulence in *Escherichia coli* O157:H7. Proc Natl Acad Sci U S A 112:5503–5508.

93. Siryaporn A, Kuchma SL, O'Toole GA, Gitai Z, Ausubel FM. 2014. Surface attachment induces *Pseudomonas aeruginosa* virulence. Proc Natl Acad Sci U S A 111:16860–16865.

94. Rahme LG, Stevens EJ, Wolfort SF, Shao J, Tompkins RG, Ausubel FM. 1995. Common virulence factors for bacterial pathogenicity in

plants and animals. Science (80-) 268:1899–1902.

95. Colombatti A, Bonaldo P, Doliana R. 1993. Type A Modules: Interacting Domains Found in Several Non-Fibrillar Collagens and in Other Extracellular Matrix Proteins. Matrix 13:297–306.

96. Kuchma SL, Ballok AE, Merritt JH, Hammond JH, Lu W, Rabinowitz JD, O'Toole GA. 2010. Cyclic-di-GMP-mediated repression of swarming motility by *Pseudomonas aeruginosa*: The *pilY1* gene and its impact on surface-associated behaviors. J Bacteriol 192:2950–2964.

97. Konto-Ghiorghi Y, Mairey E, Mallet A, Duménil G, Caliot E, Trieu-Cuot P, Dramsi S. 2009. Dual Role for Pilus in Adherence to Epithelial Cells and Biofilm Formation in *Streptococcus agalactiae*. PLoS Pathog 5:e1000422.

98. Laventie BJ, Sangermani M, Estermann F, Manfredi P, Planes R, Hug I, Jaeger T, Meunier E, Broz P, Jenal U. 2019. A Surface-Induced Asymmetric Program Promotes Tissue Colonization by *Pseudomonas aeruginosa*. Cell Host Microbe 25:140-152.e6.

99. Luo Y, Zhao K, Baker AE, Kuchma SL, Coggan KA, Wolfgang MC, Wong GCL, O'Toole GA. 2015. A hierarchical cascade of second messengers regulates *Pseudomonas aeruginosa* Surface Behaviors. MBio 6:1–11.

100. Rodesney CA, Roman B, Dhamani N, Cooley BJ, Katira P, Touhami A, Gordon VD. 2017. Mechanosensing of shear by *Pseudomonas aeruginosa* leads to increased levels of the cyclic-di-GMP signal initiating biofilm development. Proc Natl Acad Sci U S A 114:5906–5911.

101. Kuchma SL, Griffin EF, O'Toole GA. 2012. Minor pilins of the type IV pilus system participate in the negative regulation of swarming motility. J Bacteriol 194:5388–5403.

102. Okkotsu Y, Little AS, Schurr MJ. 2014. The *Pseudomonas aeruginosa* AlgZR two-component system coordinates multiple phenotypes. Front Cell Infect Microbiol 0:82.

103. Kohler T, Curty LK, Barja F, Van Delden C, Pechere JC. 2000. Swarming of *Pseudomonas aeruginosa* is dependent on cell-to-cell signaling and requires flagella and pili. J Bacteriol 182:5990–5996.

104. Chuang SK, Vrla GD, Fröhlich KS, Gitai Z. 2019. Surface association sensitizes *Pseudomonas aeruginosa* to quorum sensing. Nat Commun 10.

105. Gupta K, Liao J, Petrova OE, Cherny KE, Sauer K. 2014. Elevated levels of the second messenger c-di-GMP contribute to antimicrobial resistance of *Pseudomonas aeruginosa*. Mol Microbiol 92:488–506.

106. Almblad H, Harrison JJ, Rybtke M, Groizeleau J, Givskov M, Parsek MR, Tolker-Nielsen T. 2015. The cyclic AMP-Vfr signaling pathway in *Pseudomonas aeruginosa* is inhibited by cyclic Di-GMP. J Bacteriol 197:2190–2200.

107. West AH, Stock AM. 2001. Histidine kinases and response regulator proteins in two-component signaling systems. Trends Biochem Sci.

108. Parkinson JS, Kofoid EC. 1992. Communication Modules in Bacterial Signaling Proteins. Annu Rev Genet 26:71–112.

109. Stock JB, Ninfa AJ, Stock AM. 1989. Protein phosphorylation and regulation of adaptive responses in bacteria. Microbiol Rev.

110. Grebe TW, Stock JB. 1999. The histidine protein kinase superfamily. Adv Microb Physiol. Academic Press.

111. Rodrigue A, Quentin Y, Lazdunski A, Méjean V, Foglino M. 2000. Two-component systems in *Pseudomonas aeruginosa*: Why so many? Trends Microbiol.

112. Broder UN, Jaeger T, Jenal U. 2017. LadS is a calcium-responsive kinase that induces acute-to-chronic virulence switch in *Pseudomonas aeruginosa*. Nat Microbiol 2:16184.

113. Kulasekara HD, Ventre I, Kulasekara BR, Lazdunski A, Filloux A, Lory S. 2004. A novel two-component system controls the expression of *Pseudomonas aeruginosa* fimbrial cup genes. Mol Microbiol 55:368–380.

114. Hobbs M, Mattick JS. 1993. Common components in the assembly of type 4 fimbriae, DNA transfer systems, filamentous phage and protein-secretion apparatus: a general system for the formation of surface-associated protein complexes. Mol Microbiol 10:233–243.

115. Craig L, Forest KT, Maier B. 2019. Type IV pili: dynamics, biophysics and functional consequences. Nat Rev Microbiol. Nature

Publishing Group.

116. Kilmury SLN, Burrows LL. 2016. Type IV pilins regulate their own expression via direct intramembrane interactions with the sensor kinase PilS. Proc Natl Acad Sci U S A 113:6017–6022.

117. Giltner CL, Nguyen Y, Burrows LL. 2012. Type IV Pilin Proteins: Versatile Molecular Modules. Microbiol Mol Biol Rev 76:740–772.

118. Smith DR, Chapman MR. 2010. Economical Evolution: Microbes Reduce the Synthetic Cost of Extracellular Proteins. MBio 1:28–32.

119. Hobbs M, Collie ESR, Free PD, Livingston SP, Mattick JS. 1993. PilS and PilR, a two-component transcriptional regulatory system controlling expression of type 4 fimbriae in *Pseudomonas aeruginosa*. Mol Microbiol 7:669–682.

120. Boyd JM, Koga T, Lory S. 1994. Identification and characterization of PilS, an essential regulator of pilin expression in *Pseudomonas aeruginosa*. MGG Mol Gen Genet 243:565–574.

121. Ishimoto KS, Lory S. 1992. Identification of *pilR*, which encodes a transcriptional activator of the *Pseudomonas aeruginosa* pilin gene. J Bacteriol 174:3514–3521.

122. Boyd JM, Lory S. 1996. Dual function of PilS during transcriptional activation of the *Pseudomonas aeruginosa* pilin subunit gene. J Bacteriol 178:831–839.

123. Ishimoto KS, Lory S. 1989. Formation of pilin in *Pseudomonas aeruginosa* requires the alternative σ factor (RpoN) of RNA polymerase. Proc Natl Acad Sci U S A 86:1954–1957.

124. Jin S, Ishimoto KS, Lory S. 1994. PilR, a transcriptional regulator of piliation in *Pseudomonas aeruginosa*, binds to a cis-acting sequence upstream of the pilin gene promoter. Mol Microbiol 14:1049–1057.

125. Ronson CW, Nixon T, Ausubel FM. 1987. Conserved Domains in Bacterial Regulatory Proteins That Respond to Environmental Stimuli MinireviewCell.

126. Taylor M, Butler R, Chambers S, Casimiro M, Badii F, Merrick M. 1996. The RpoN-box motif of the RNA polymerase sigma factor N plays a role in promoter recognition. Mol Microbiol 22:1045–1054.

127. Aiba H, Nakasai F, Mizushima S, Mizuno T. 1989. Phosphorylation of a bacterial activator protein, OmpR, by a protein kinase, EnvZ, results in stimulation of its DNA-binding ability. J Biochem 106:5–7.

128. Forst SA, Delgado J, Inouye M. 1989. DNA-binding properties of the transcription activator (OmpR) for the upstream sequences of ompF in *Escherichia coli* are altered by envZ mutations and medium osmolarity. J Bacteriol 171:2949–2955.

129. Parker D, Kennan RM, Myers GS, Paulsen IT, Songer JG, Rood JI. 2006. Regulation of type IV fimbrial biogenesis in *Dichelobacter nodosus*. J Bacteriol 188:4801–4811.

130. Kehl-Fie TE, Porsch EA, Miller SE, St Geme III JW. 2009. Expression of *Kingella kingae* Type IV Pili Is Regulated by Sigma-54, PilS, and PilR. J Bacteriol 191:4976–4986.

131. Wu SS, Kaiser D. 1997. Regulation of Expression of the *pilA* Gene in *Myxococcus xanthus*Journal of Bacteriology.

132. Hernández-Eligio A, Andrade Á, Soto L, Morett E, Juárez K. 2017. The unphosphorylated form of the PilR two-component system regulates pilA gene expression in *Geobacter sulfurreducens*. Environ Sci Pollut Res 24:25693–25701.

133. Rendón MA, Hockenberry AM, McManus SA, So M. 2013. Sigma factor RpoN (σ54) regulates *pilE* transcription in commensal *Neisseria elongata*. Mol Microbiol 90:103–113.

134. Rendón MA, Lona B, Ma M, So M. 2019. RpoN and the Nps and Npa two-component regulatory system control pilE transcription in commensal *Neisseria*. Microbiologyopen 8:1–11.

135. Ethier J, Boyd JM. 2000. Topological analysis and role of the transmembrane domain in polar targeting of PilS, a *Pseudomonas aeruginosa* sensor kinase. Mol Microbiol 38:891–903.

136. Boyd JM. 2000. Localization of the histidine kinase PilS to the poles of *Pseudomonas aeruginosa* and identification of a localization domain. Mol Microbiol 36:153–162.

137. Buensuceso RNC, Nguyen Y, Zhang K, Daniel-Ivad M, Sugiman-Marangos SN, Fleetwood AD, Zhulin IB, Junop MS, Lynne Howell P, Burrows LL. 2016. The conserved tetratricopeptide repeat-containing C-Terminal domain of *Pseudomonas aeruginosa* FimV is

required for its cyclic AMP-dependent and -independent functions. J Bacteriol 198:2263–2274.

138. Buensuceso RNC, Daniel-Ivad M, Kilmury SLN, Leighton TL, Harvey H, Howell PL, Burrows LL. 2017. Cyclic AMP-Independent Control of Twitching Motility in *Pseudomonas aeruginosa*. J Bacteriol 199:1–14.

139. LaBaer J, Qiu QQ, Anumanthan A, Mar W, Zuo D, Murthy TVS, Taycher H, Halleck A, Hainsworth E, Lory S, Brizuela L. 2004. The *Pseudomonas aeruginosa* PAO1 gene collection. Genome Res 14:2190–2200.

140. Petrova OE, Sauer K. 2011. SagS Contributes to the Motile-Sessile Switch and Acts in Concert with BfiSR To Enable *Pseudomonas aeruginosa* Biofilm Formation. J Bacteriol 193:6614–6628.

141. Petrova OE, Cherny KE, Sauer K. 2014. The *Pseudomonas aeruginosa* Diguanylate Cyclase GcbA, a Homolog of P. fluorescens GcbA, Promotes Initial Attachment to Surfaces, but Not Biofilm Formation, via Regulation of Motility. J Bacteriol 196:2827–2841.

142. North AK, Klose KE, Stedman KM, Kustu S. 1993. Prokaryotic Enhancer-Binding Proteins Reflect Eukaryote-Like Modularity: the Puzzle of Nitrogen Regulatory Protein CJournal of Bacteriology.

143. Popham DL, Szeto D, Keener J, Kustu S. 1989. Function of a bacterial activator protein that binds to transcriptional enhancers. Science (80-) 243:629–635.

144. Weiss DS, Batut J, Klose KE, Keener J, Kustu S. 1991. The phosphorylated form of the enhancer-binding protein NTRC has an ATPase activity that is essential for activation of transcription. Cell 67:155–167.

145. Juárez K, Kim B-C, Nevin K, Olvera L, Reguera G, Lovley DR, Methé BA. 2009. PilR, a Transcriptional Regulator for Pilin and Other Genes Required for Fe(III) Reduction in *Geobacter sulfurreducens*. J Mol Microbiol Biotechnol 16:146–158.

146. Krushkal J, Juárez K, Barbe JF, Qu Y, Andrade A, Puljic M, Adkins RM, Lovley DR, Ueki T. 2010. Genome-wide survey for PilR recognition sites of the metal-reducing prokaryote *Geobacter sulfurreducens*. Gene 469:31–44.

147. Chen Y, Xia J, Su Z, Xu G, Gomelsky M, Qian G, Liu F. 2017. Lysobacter PilR, the Regulator of Type IV Pilus Synthesis, Controls Antifungal Antibiotic Production via a Cyclic di-GMP Pathway. Appl Environ Microbiol 83:1–19.

148. Kilmury SLN, Burrows LL. 2018. The *Pseudomonas aeruginosa* PILSR two-component system regulates both twitching and swimming motilities. MBio 9:e01310-18.

149. Wolfgang MC, Lee VT, Gilmore ME, Lory S. 2003. Coordinate regulation of bacterial virulence genes by a novel adenylate cyclase-dependent signaling pathway. Dev Cell 4:253–263.

150. Ritchings BW, Almira EC, Lory S, Ramphal R. 1995. Cloning and phenotypic characterization of fleS and fleR, new response regulators of *Pseudomonas aeruginosa* which regulate motility and adhesion to mucin. Infect Immun 63:4868–76.

151. Dasgupta N, Wolfgang MC, Goodman AL, Arora SK, Jyot J, Lory S, Ramphal R. 2003. A four-tiered transcriptional regulatory circuit controls flagellar biogenesis in *Pseudomonas aeruginosa*. Mol Microbiol 50:809–824.

152. Arora SK, Ritchings BW, Almira EC, Lory S, Ramphal R. 1997. A transcriptional activator, FleQ, regulates mucin adhesion and flagellar gene expression in *Pseudomonas aeruginosa* in a cascade manner. J Bacteriol 179:5574–5581.

153. Liberati NT, Urbach JM, Miyata S, Lee DG, Drenkard E, Wu G, Villanueva J, Wei T, Ausubel FM. 2006. An ordered, nonredundant library of *Pseudomonas aeruginosa* strain PA14 transposon insertion mutants. Proc Natl Acad Sci U S A 103:2833–2838.

154. Lyczak JB, Cannon CL, Pier GB. 2000. Establishment of *Pseudomonas aeruginosa* infection: Lessons from a versatile opportunist. Microbes Infect. Elsevier Masson SAS.

155. Pier GB. 2007. *Pseudomonas aeruginosa* lipopolysaccharide: A major virulence factor, initiator of inflammation and target for effective immunity. Int J Med Microbiol. Elsevier GmbH.

156. Lee DG, Urbach JM, Wu G, Liberati NT, Feinbaum RL, Miyata S, Diggins LT, He J, Saucier M, Déziel E, Friedman L, Li L, Grills G, Montgomery K, Kucherlapati R, Rahme LG, Ausubel FM. 2006. Genomic analysis reveals that *Pseudomonas aeruginosa* virulence

is combinatorial. Genome Biol 7.

157. Heiniger RW, Winther-Larsen HC, Pickles RJ, Koomey M, Wolfgang MC. 2010. Infection of human mucosal tissue by *Pseudomonas aeruginosa* requires sequential and mutually dependent virulence factors and a novel pilus-associated adhesin. Cell Microbiol 12:1158–1173.

158. Zolfaghar I, Evans DJ, Fleiszig SMJ. 2003. Twitching motility contributes to the role of pili in corneal infection caused by *Pseudomonas aeruginosa*. Infect Immun 71:5389–93.

159. Biais N, Ladoux B, Higashi D, So M, Sheetz M. 2008. Cooperative Retraction of Bundled Type IV Pili Enables Nanonewton Force Generation. PLoS Biol 6:e87.

160. Herrero M, Lorenzo V de, Timmis KN. 1990. Transposon vectors containing non-antibiotic resistance selection markers for cloning and stable chromosomal insertion of foreign genes in gram-negative bacteria. J Bacteriol 172:6557.

161. Bondy-Denomy J, Qian J, Westra ER, Buckling A, Guttman DS, Davidson AR, Maxwell KL. 2016. Prophages mediate defense against phage infection through diverse mechanisms. ISME J 10:2854–2866.

162. Zegans ME, Wagner JC, Cady KC, Murphy DM, Hammond JH, O'Toole GA. 2009. Interaction between bacteriophage DMS3 and host CRISPR region inhibits group behaviors of *Pseudomonas aeruginosa*. J Bacteriol 91:210–219.

163. YJ H, IY C, KB C, GW L, YH C. 2007. Genome sequence comparison and superinfection between two related *Pseudomonas aeruginosa* phages, D3112 and MP22. Microbiology 153:2885–2895.

164. Persat A, Inclan YF, Engel JN, Stone HA, Gitai Z. 2015. Type IV pili mechanochemically regulate virulence factors in *Pseudomonas aeruginosa*. Proc Natl Acad Sci U S A 112:7563–7568.

165. Ho SN, Hunt HD, Horton RM, Pullen JK, Pease LR. 1989. Site-directed mutagenesis by overlap extension using the polymerase chain reaction. Gene 77:51–59.

166. Hmelo LR, Borlee BR, Almblad H, Love ME, Randall TE, Tseng BS,

Lin C, Irie Y, Storek KM, Yang JJ, Siehnel RJ, Howell PL, Singh PK, Tolker-Nielsen T, Parsek MR, Schweizer HP, Harrison JJ. 2015. Precision-engineering the *Pseudomonas aeruginosa* genome with two-step allelic exchange. Nat Protoc 10:1820–1841.

167. Kus J V., Tullis E, Cvitkovitch DG, Burrows LL. 2004. Significant differences in type IV pilin allele distribution among *Pseudomonas aeruginosa* isolates from cystic fibrosis (CF) versus non-CF patients. Microbiology 150:1315–1326.

168. Tan MW, Mahajan-Miklos S, Ausubel FM. 1999. Killing of *Caenorhabditis elegans* by *Pseudomonas aeruginosa* used to model mammalian bacterial pathogenesis. Proc Natl Acad Sci U S A 96:715–720.

169. McClure R, Balasubramanian D, Sun Y, Bobrovskyy M, Sumby P, Genco CA, Vanderpool CK, Tjaden B. 2013. Computational analysis of bacterial RNA-Seq data. Nucleic Acids Res 41.

170. Ellison CK, Dalia TN, Dalia AB, Brun Y V. 2019. Real-time microscopy and physical perturbation of bacterial pili using maleimide-conjugated molecules. Nat Protoc 14:1803–1819.

171. Huynh TAN, Noriega CE, Stewart V. 2010. Conserved mechanism for sensor phosphatase control of two-component signaling revealed in the nitrate sensor NarX. Proc Natl Acad Sci U S A 107:21140–21145.

172. Klose KE, Weiss DS, Kustu S. 1993. Glutamate at the site of phosphorylation of nitrogen-regulatory protein NtrC mimics aspartyl-phosphate and activates the protein. J Mol Biol 232:67–78.

173. Moore JB, Shiau SP, Reitzer LJ. 1993. Alterations of highly conserved residues in the regulatory domain of nitrogen regulator I (NtrC) of *Escherichia coli*. J Bacteriol 175:2692.

174. Mattick JS. 2002. Type IV Pili and Twitching Motility. Annu Rev Microbiol 56:289–314.

175. Leighton TL, Dayalani N, Sampaleanu LM, Howell PL, Burrows LL. 2015. Novel role for PilNO in type IV pilus retraction revealed by alignment subcomplex mutations. J Bacteriol 197:2229–2238.

176. Ellison CK, Dalia TN, Klancher CA, Shaevitz JW, Gitai Z, Dalia AB. 2021. *Acinetobacter baylyi* regulates type IV pilus synthesis by

employing two extension motors and a motor protein inhibitor. Nat Commun 2021 121 12:1–9.

177. Bertrand JJ, West JT, Engel JN. 2010. Genetic analysis of the regulation of type IV pilus function by the Chp chemosensory system of *Pseudomonas aeruginosa*. J Bacteriol 192:994–1010.

178. Hauser AR. 2009. The type III secretion system of *Pseudomonas aeruginosa*: Infection by injection. Nat Rev Microbiol.

179. Wareham D, Papakonstantinopoulou A, Curtis M. 2005. The Pseudomonas aeruginosa PA14 type III secretion system is expressed but not essential to virulence in the Caenorhabditis elegans-P. aeruginosa pathogenicity model. FEMS Microbiol Lett 242:209–216.

180. Lewenza S, Charron-Mazenod L, Giroux L, Zamponi AD. 2014. Feeding behaviour of *Caenorhabditis elegans* is an indicator of *Pseudomonas aeruginosa* PAO1 virulence. PeerJ 2.

181. Blaylock B, Riordan R, Missiakas D, Schneewind O. 2006. Characterization of the Yersinia enterocolitica type III secretion ATPase YscN and its regulator, YscL. J Bacteriol 188:3525–3534.

182. Akeda Y, Galán J. 2004. Genetic analysis of the Salmonella enterica type III secretion-associated ATPase InvC defines discrete functional domains. J Bacteriol 186:2402–2412.

183. Burgess JL, Case HB, Burgess RA, Dickenson NE. 2020. Dominant negative effects by inactive Spa47 mutants inhibit T3SS function and *Shigella* virulence. PLoS One 15:e0228227.

184. Gauthier A, Puente JL, Finlay BB. 2003. Secretin of the Enteropathogenic *Escherichia coli* Type III Secretion System Requires Components of the Type III Apparatus for Assembly and Localization. Infect Immun 71:3310.

185. Halder PK, Roy C, Datta S. 2019. Structural and functional characterization of type three secretion system ATPase PscN and its regulator PscL from *Pseudomonas aeruginosa*. Proteins Struct Funct Bioinforma 87:276–288.

186. Bergeron JRC, Fernández L, Wasney GA, Vuckovic M, Reffuveille F, Hancock REW, Strynadka NCJ. 2016. The Structure of a type 3 secretion system (T3SS) ruler protein suggests a molecular

mechanism for needle length sensing. J Biol Chem 291:1676–1691.

187. Journet L, Agrain C, Broz P, Cornelis GR. 2003. The Needle Length of Bacterial Injectisomes Is Determined by a Molecular Ruler. Science (80-) 302:1757–1760.

188. Mavrodi D V., Bonsall RF, Delaney SM, Soule MJ, Phillips G, Thomashow LS. 2001. Functional analysis of genes for biosynthesis of pyocyanin and phenazine-1-carboxamide from *Pseudomonas aeruginosa* PAO1. J Bacteriol 183:6454–6465.

189. Cezairliyan B, Vinayavekhin N, Grenfell-Lee D, Yuen GJ, Saghatelian A, Ausubel FM. 2013. Identification of *Pseudomonas aeruginosa* Phenazines that Kill *Caenorhabditis elegans*. PLoS Pathog 9:e1003101.

190. Bezirtzoglou EEV. 2012. Intestinal cytochromes P450 regulating the intestinal microbiota and its probiotic profile. Microb Ecol Heal Dis 23:18370.

191. Ochsner UA, Fiechter A, Reiser J. 1994. Isolation, characterization, and expression in *Escherichia coli* of the *Pseudomonas aeruginosa rhlAB* genes encoding a rhamnosyltransferase involved in rhamnolipid biosurfactant synthesis. J Biol Chem 269:19787–19795.

192. Zhu K, Rock CO. 2008. RhlA converts β-hydroxyacyl-acyl carrier protein intermediates in fatty acid synthesis to the β-hydroxydecanoyl-β-hydroxydecanoate component of rhamnolipids in *Pseudomonas aeruginosa*. J Bacteriol 190:3147–3154.

193. Hall BM, Breidenstein EBM, de la Fuente-Núñez C, Reffuveille F, Mawla GD, Hancock REW, Baker TA. 2017. Two isoforms of Clp peptidase in *Pseudomonas aeruginosa* control distinct aspects of cellular physiology. J Bacteriol 199.

194. Wagner VE, Bushnell D, Passador L, Brooks AI, Iglewski BH. 2003. Microarray analysis of *Pseudomonas aeruginosa* quorum-sensing regulons: Effects of growth phase and environment. J Bacteriol 185:2080–2095.

195. Chattopadhyay A, Förster-Fromme K, Jendrossek D. 2010. PQQ-Dependent Alcohol Dehydrogenase (QEDH) of *Pseudomonas aeruginosa* is involved in catabolism of acyclic terpenes. J Basic Microbiol 50:119–124.

196. Schobert M, Görisch H. 1999. Cytochrome c550 is an essential component of the quinoprotein ethanol oxidation system in *Pseudomonas aeruginosa*: Cloning and sequencing of the genes encoding cytochrome c550 and an adjacent acetaldehyde dehydrogenase. Microbiology 145:471–481.

197. Mern DS, Ha SW, Khodaverdi V, Gliese N, Görisch H. 2010. A complex regulatory network controls aerobic ethanol oxidation in *Pseudomonas aeruginosa*: Indication of four levels of sensor kinases and response regulators. Microbiology 156:1505–1516.

198. Elfarash A, Wei Q, Cornelis P. 2012. The soluble pyocins S2 and S4 from *Pseudomonas aeruginosa* bind to the same FpvAI receptor. Microbiologyopen 1:268–275.

199. Petersen B, Petersen TN, Andersen P, Nielsen M, Lundegaard C. 2009. A generic method for assignment of reliability scores applied to solvent accessibility predictions. BMC Struct Biol 2009 91 9:1–10.

200. Dunger G, Guzzo C, Andrade M, Jones J, Farah C. 2014. Xanthomonas citri subsp. citri type IV Pilus is required for twitching motility, biofilm development, and adherence. Mol Plant Microbe Interact 27:1132–1147.

201. Meng Y, Li Y, Galvani C, Hao G, Turner J, Burr T, Hoch H. 2005. Upstream migration of Xylella fastidiosa via pilus-driven twitching motility. J Bacteriol 187:5560–5567.

202. Takahashi H, Yanagisawa T, Kim T, Yokoyama S, Ohnishi M. 2012. Meningococcal PilV potentiates Neisseria meningitidis type IV pilus-mediated internalization into human endothelial and epithelial cells. Infect Immun 80:4154–4166.

203. Hockenberry A, Hutchens D, Agellon A, So M. 2016. Attenuation of the Type IV Pilus Retraction Motor Influences Neisseria gonorrhoeae Social and Infection Behavior. MBio 7.

204. Weller-Stuart T, Toth I, De Maayer P, Coutinho T. 2017. Swimming and twitching motility are essential for attachment and virulence of Pantoea ananatis in onion seedlings. Mol Plant Pathol 18:734–745.

205. Eriksson J, Eriksson O, Jonsson A. 2012. Loss of meningococcal PilU delays microcolony formation and attenuates virulence *in vivo*. Infect Immun 80:2538–2547.

206. Inclan YF, Persat A, Greninger A, Dollen J Von, Johnson J, Krogan N, Gitai Z, Engel JN. 2016. A scaffold protein connects type IV pili with the Chp chemosensory system to mediate activation of virulence signaling in *Pseudomonas aeruginosa*. Mol Microbiol 101:590.

207. DeLange PA, Collins TL, Pierce GE, Robinson JB. 2007. PilJ Localizes to Cell Poles and Is Required for Type IV Pilus Extension in *Pseudomonas aeruginosa*. Curr Microbiol 2007 555 55:389–395.

208. Hayashi N, Nishizawa H, Kitao S, Deguchi S, Nakamura T, Fujimoto A, Shikata M, Gotoh N. 2015. Pseudomonas aeruginosa injects type III effector ExoS into epithelial cells through the function of type IV pili. FEBS Lett 589:890–896.

209. Shikata M, Hayashi N, Fujimoto A, Nakamura T, Matsui N, Ishiyama A, Maekawa Y, Gotoh N. 2016. The pilT gene contributes to type III ExoS effector injection into epithelial cells in Pseudomonas aeruginosa. J Infect Chemother 22:216–220.

210. Whitchurch CB, Beatson SA, Comolli JC, Jakobsen T, Sargent JL, Bertrand JJ, West J, Klausen M, Waite LL, Kang PJ, Tolker-Nielsen T, Mattick JS, Engel JN. 2005. *Pseudomonas aeruginosa fimL* regulates multiple virulence functions by intersecting with Vfr-modulated pathways. Mol Microbiol 55:1357–1378.

211. Brutinel ED, Vakulskas CA, Brady KM, Yahr TL. 2008. Characterization of ExsA and of ExsA-dependent promoters required for expression of the *Pseudomonas aeruginosa* type III secretion system. Mol Microbiol 68:657–671.

212. Feinbaum R, Urbach J, Liberati N, Djonovic S, Adonizio A, Carvunis A, Ausubel F. 2012. Genome-wide identification of Pseudomonas aeruginosa virulence-related genes using a Caenorhabditis elegans infection model. PLoS Pathog 8:11.

213. Feltman H, Schulert G, Khan S, Jain M, Peterson L, Hauser A. 2001. Prevalence of type III secretion genes in clinical and environmental isolates of Pseudomonas aeruginosa. Microbiology 147:2659–2669.

214. Jin Y, Zhang M, Zhu F, Peng Q, Weng Y, Zhao Q, Liu C, Bai F, Cheng Z, Jin S, Wu W. 2019. NrtR Regulates the Type III Secretion System Through cAMP/Vfr Pathway in Pseudomonas aeruginosa. Front Microbiol 10.

215. Whitchurch CB, Leech AJ, Young MD, Kennedy D, Sargent JL, Bertrand JJ, Semmler ABT, Mellick AS, Martin PR, Alm RA, Hobbs M, Beatson SA, Huang B, Nguyen L, Commolli JC, Engel JN, Darzins A, Mattick JS. 2004. Characterization of a complex chemosensory signal transduction system which controls twitching motility in *Pseudomonas aeruginosa*. Mol Microbiol 52:873–893.

216. Fulcher NB, Holliday PM, Klem E, Cann MJ, Wolfgang MC. 2010. The *Pseudomonas aeruginosa* Chp chemosensory system regulates intracellular cAMP levels by modulating adenylate cyclase activity. Mol Microbiol 76:889–904.

217. Marsden AE, Intile PJ, Schulmeyer KH, Simmons-Patterson ER, Urbanowski ML, Wolfgang MC, Yahr TL. 2016. Vfr directly activates *exsA* transcription to regulate expression of the *Pseudomonas aeruginosa* type III secretion system. J Bacteriol 198:1442–1450.

218. Pujol C, Eugène E, Marceau M, Nassif X. 1999. The meningococcal PilT protein is required for induction of intimate attachment to epithelial cells following pilus-mediated adhesion. Proc Natl Acad Sci 96:4017–4022.

219. Price-Whelan A, Dietrich LEP, Newman DK. 2006. Rethinking “secondary” metabolism: Physiological roles for phenazine antibiotics. Nat Chem Biol. Nature Publishing Group.

220. Bru JL, Rawson B, Trinh C, Whiteson K, Høyland-Kroghsbo NM, Siryaporn A. 2019. PQS produced by the *Pseudomonas aeruginosa* stress response repels swarms away from bacteriophage and antibiotics. J Bacteriol 201.

221. Beebout CJ, Eberly AR, Werby SH, Reasoner SA, Brannon JR, De S, Fitzgerald MJ, Huggins MM, Clayton DB, Cegelski L, Hadjifrangiskou M. 2019. Respiratory heterogeneity shapes biofilm formation and host colonization in uropathogenic *Escherichia coli*. MBio 10.

222. Juhas M, Wiehlmann L, Salunkhe P, Lauber J, Buer J, TÃ¼mmler B. 2005. GeneChip expression analysis of the VqsR regulon of *Pseudomonas aeruginosa* TB. FEMS Microbiol Lett 242:287–295.

223. Hentzer M, Wu H, Andersen JB, Riedel K, Rasmussen TB, Bagge N, Kumar N, Schembri MA, Song Z, Kristoffersen P, Manefield M, Costerton JW, Molin S, Eberl L, Steinberg P, Kjelleberg S, Høiby N, Givskov M. 2003. Attenuation of *Pseudomonas aeruginosa* virulence

by quorum sensing inhibitors. EMBO J 22:3803–3815.

224. Romero IG, Pai AA, Tung J, Gilad Y. 2014. RNA-seq: impact of RNA degradation on transcript quantification. BMC Biol 12:42.

225. Rosqvist R, Magnusson KE, Wolf-Watz H. 1994. Target cell contact triggers expression and polarized transfer of *Yersinia* YopE cytotoxin into mammalian cells. EMBO J 13:964.

226. B C, E C. 2018. Antibacterial Weapons: Targeted Destruction in the Microbiota. Trends Microbiol 26:329–338.

227. Ruhe Z, Subramanian P, Song K, Nguyen J, Stevens T, Low D, Jensen G, Hayes C. 2018. Programmed Secretion Arrest and Receptor-Triggered Toxin Export during Antibacterial Contact-Dependent Growth Inhibition. Cell 175:921-933.e14.

228. Ruhe ZC, Townsley L, Wallace AB, King A, Woude MW Van der, Low DA, Yildiz FH, Hayes CS. 2015. CdiA promotes receptor-independent intercellular adhesion. Mol Microbiol 98:175–192.

229. Allen JP, Hauser AR. 2019. Diversity of Contact-Dependent Growth Inhibition Systems of *Pseudomonas aeruginosa*. J Bacteriol 201.

230. Pastor A, Chabert J, Louwagie M, Garin J, Attree I. 2005. PscF is a major component of the *Pseudomonas aeruginosa* type III secretion needle. FEMS Microbiol Lett 253:95–101.

231. Winsor GL, Griffiths EJ, Lo R, Dhillon BK, Shay JA, Brinkman FSL. 2016. Enhanced annotations and features for comparing thousands of *Pseudomonas* genomes in the *Pseudomonas* genome database. Nucleic Acids Res 44:D646–D653.

232. Palmer AD, Kim K, Slauch JM. 2019. PhoP-mediated repression of the SPI1 type 3 secretion system in *Salmonella enterica* Serovar Typhimurium. J Bacteriol 201.

233. Gellatly SL, Needham B, Madera L, Trent MS, Hancock REW. 2012. The *Pseudomonas aeruginosa* PhoP-PhoQ Two-Component Regulatory System Is Induced upon Interaction with Epithelial Cells and Controls Cytotoxicity and Inflammation. Infect Immun 80:3122.

234. Rietsch A, Vallet-Gely I, Dove SL, Mekalanos JJ. 2005. ExsE, a secreted regulator of type III secretion genes in *Pseudomonas aeruginosa*. Proc Natl Acad Sci 102:8006–8011.

235. Zheng Z, Chen G, Joshi S, Brutinel ED, Yahr TL, Chen L. 2007. Biochemical Characterization of a Regulatory Cascade Controlling Transcription of the *Pseudomonas aeruginosa* Type III Secretion System. J Biol Chem 282:6136–6142.

236. Armentrout EI, Kundracik EC, Rietsch A. 2021. Cell-type-specific hypertranslocation of effectors by the *Pseudomonas aeruginosa* type III secretion system. Mol Microbiol 115:305–319.

237. Eriksson J, Eriksson OS, Maudsdotter L, Palm O, Engman J, Sarkissian T, Aro H, Wallin M, Jonsson A-B. 2015. Characterization of motility and piliation in pathogenic *Neisseria*. BMC Microbiol 15.

238. Marathe R, Meel C, Schmidt NC, Dewenter L, Kurre R, Greune L, Schmidt MA, Müller MJI, Lipowsky R, Maier B, Klumpp S. 2014. Bacterial twitching motility is coordinated by a two-dimensional tug-of-war with directional memory. Nat Commun 2014 51 5:1–10.

239. Yaeger LN, Coles VE, Chan DCK, Burrows LL. 2021. How to kill *Pseudomonas*—emerging therapies for a challenging pathogen. Ann N Y Acad Sci 1496:59–81.